Polymersomes for biomedical applications: surface functionalization of silicone-based polymer vesicles

Inauguraldissertation

zur

Erlangung der Würde eines Doktors der Philosophie

vorgelegt der

Philosophisch-Naturwissenschaftlichen Fakultät

der Universität Basel

von

Stefan Egli

aus Wald (ZH)

Basel 2011

UNI
BASEL

Genehmigt von der Philosophisch-Naturwissenschaftlichen Fakultät der Universität Basel auf Antrag von

Prof. Dr. Wolfgang P. Meier

und

Prof. Dr. Thomas Pfohl

Basel, den 24. Mai 2011

Prof. Dr. Martin Spiess

Dekan

„Natürlicher Verstand kann fast jeden Grad von Bildung ersetzen, aber keine Bildung den natürlichen Verstand.“

Arthur Schopenhauer (1788 – 1860)

Acknowledgments

First of all I want to thank *Prof. Wolfgang Meier* for giving me the opportunity to perform my PhD thesis in his research group. I admire his patience and the trust he gave me to work on my project as well as his cordiality.

Also I thank *Prof. Thomas Pfohl* for his interest in my research work and for examining my doctoral thesis. *Prof. Stefan Willitsch* is kindly acknowledged for chairing the exam.

Furthermore I thank our research group leaders, all our present and former Post-Doc group members. In this respect, my special thanks go to: *PD Dr. Cornelia Palivan* for her competent inputs, fruitful collaboration and for leading the group when times were difficult, *Dr. Nico Bruns* for fruitful collaboration and especially for being the greatest Queen fan ever! I also want to thank *Dr. Ozana Onaca* for her motivating attitude and the unfailing believe in and fight for a clean biolab, *Dr. Katarzyna Kita* for providing me precious advice with scientific issues. Great thanks to *Dr. Per Rigler* for introducing me in FCS and in the rules of publishing scientific articles.

During my PhD, I supervised two master students, Martin Nussbaumer and Adrian Najer. They are motivated, intelligent and handsome scientists who did (and I am sure they still do) excellent work and I wish them all the best for their future career.

This work would never be possible without the support of numerous collaborators outside our research group. In this respect I am thankful to *Dr. Daniel Häussinger* and *Adnan Ganic* (Organic Chemistry, Basel), *Dr. Mohamed Chami* (C-CINA, Basel), *Dr. Barbara Fischer, Sonja Hartmann* and *Prof. Patrick Hunziker* (University Hospital Basel), *Ursula Sanders* and *Vesna Oliveri* (ZMB), *PD Dr. Helmut Schlaad* (Max Planck Institute of Colloids and Interfaces), *Karmena Jaskiewicz* and *Dr. Ingo Lieberwirth* (Max Planck

Institute for Polymer Research), *Dr. Tina Stölzle* and *Prof. Nancy Hynes* (Friedrich Miescher Institute). Dr. Charl F. J. Faul (School of Chemistry, University of Bristol) I want to acknowledge for his support in designing and writing a SNF post-doc proposal. Unfortunately, the proposal was not accepted, but therefore I learned a lot about ionic self-assembly and got interesting results which are presented in this thesis.

Many thanks go to *Mark Inglin* for asking lots of tricky questions and for being always helpful and interested in discussions. He edited most of my manuscripts and thus added substantial value to their quality.

From our research group I especially want to acknowledge *Gabrielle Persy* for numberous GPC measurements, *Vimalkumar Balasubramanian* and *Pascal Tanner* for fruitful co-author collaboration, *Dr. Mariusz Grzelakowski* for introducing me in CROP and all other group members for their precious help. Also I will always remember the great activities like after work beers, Christmas parties, hiking tour and ski weekends we spend together.

I also want to thank *Dr. Dirk de Bruyn*, *Philipp Graf*, *Dr. Serena Belegrinou*, *Dr. Diana Sebök*, *Dr. Etienne Cabane*, *Dr. Thomas Schuster* and *Sven Kasper* for spending a lot of their free-time with me, for being good friends and for having lots of fun.

Besides all my friends from Basel, Dietlikon and other places I finally thank my *family* and *Lena*, who provided support and mental backup whenever it was needed.

Abstract

Polymersomes prepared from amphiphilic block copolymers are of great interest for applications in diagnostic and therapeutic medicine. In drug delivery, for instance, cargo-carrying polymersomes that can target and attach to specific cell receptors will lead to greater drug efficacy and to fewer side effects. A key aspect considering such applications is to direct the polymersomes to a specific site *in vivo*, which requires the conjugation of targeting ligands to the surface of the polymeric self-assemblies. Such conjugation chemistry has in turn to fulfill several aspects comprising reaction selectivity and efficiency, stability of the resulting bond, biocompatibility and traceability.

In this thesis, we present different chemical approaches of surface modification of silicone-based block copolymer vesicles. In a first trial, the covalent attachment of oligonucleotides was performed by specific alkyne-azide click-chemistry conjugation. In a second trial, we introduced a new conjugation chemistry that achieves the criteria mentioned before by simple conjugation of 4-formylbenzoate (4FB) functionalized polymersomes with 6-hydrazinonicotinate acetone hydrazine functionalized proteins and antibodies in aqueous buffer. To prove attachment of biomolecules to polymersomes, HyNic functionalized enhanced yellow fluorescent protein (eYFP) was attached to 4FB functionalized polymersomes, resulting in an average number of 5 eYFP molecules per polymersome. Two different polymersome–antibody conjugates were produced using either antibiotin IgG or trastuzumab. They showed specific targeting toward biotin-patterned surfaces and breast cancer cells.

In addition, a new cationic silicone was synthesized, which assembles in certain aqueous salt solutions exclusively in vesicle structures. Because they form complexes with fluorescently labeled siRNA, such cationic silicone vesicles might be useful transfection agents.

In summary, this thesis might impact the future generations and design of modern drug delivery systems.

Abbreviations

ABTS	2,2'-azinobis(3-ethylbenzothiazoline-6-sulfonic acid)
AFM	atomic force microscopy
ATRP	atom transfer radical polymerization
BPhT	bathophenantroline disulfonate
BSA	bovine serum albumin
CalB	candida antarctica lipase B
(C)LSM	(confocal) laser scanning microscope
C(R)OP	cationic (ring) opening polymerization
D	diffusion coefficient
DIPEA	N-ethyldiisopropylamine
DLS	dynamic light scattering
DMF	dimethylformamide
DMSO	dimethyl sulfoxide
DNA	deoxyribonucleic acid
eGFP	enhanced green fluorescent protein
ELISA	enzyme-linked immunosorbent assay
eYFP	enhanced yellow fluorescent protein
FACS	fluorescence-activated cell sorting
4FB	4-formyl benzoate
F(C)CS	fluorescence (cross) correlation spectroscopy
GOx	glucose oxidase
GPC	gel permeation chromatography
GTP	group transfer polymerization
GUV	giant unilamellar vesicle
NMR	nuclear magnetic resonance
HER2	human epidermal growth factor receptor 2
HRP	horseradish peroxidase
HyNic	6-hydrazinonicotinate
ICAM	inter-cellular adhesion molecule 1
IgG	immunoglobulin G
ITC	isothermal titration calorimetry
k	rate constant
K_D	dissociation constant

MALDI-TOF-MS	matrix assisted laser desorption/ionization - time of flight – mass spectroscopy
M_n	number weighted molecular weight
M_w	mass weighted molecular weight
MTS	3-(4,5-dimethylthiazol-2-yl)-5-(3-carboxymethoxyphenyl)-2-(4-sulfophenly)-2H-tetrazolium
NHS	N-hydroxysuccinimide
NTA	nitrilotriacetic acid
PAA	poly(acrylic acid)
PBD	poly(butadiene)
PBS	phosphate buffered saline
P(M)CL	poly((methyl)caprolactone)
PDI	polydispersity index
PDMS	poly(dimethylsiloxane)
PEE	poly(ethylethylene)
PEG	poly(ethylenglycol)
PEI	poly(ether imide)
PI	poly(isoprene)
PIAT	poly(1-isocyanoalanine(2-thiophen-3-yl-ethyl)amid)
PLA	poly(lactide)
PMOXA	poly(2-methyloxazoline)
poly(G)	poly(guanylic acid)
PS	poly(styrene)
RFP	red fluorescent protein
R_g	radius of gyration
R_h	hydrodynamic radius
(si)RNA	(short interfering) ribonucleic acid
SLS	static light scattering
SRA1	scavenger receptor A1
SRB	sulforhodamine B
TBTA	tris-(benzyltriazolylmethyl)amine
TEM	transmission electron microscopy
TFA	trifluoroacetic acid
THF	tetrahydrofuran
x_n	mole percentage
β-CD	β-cyclodextrin
τ_D	diffusion time

Table of contents

1. Introduction

1.1. Vesicles based on amphiphilic block copolymers – promising candidates for biomedical applications

Evolution has provided Nature with numerous sophisticated materials and strategies to confer viability to living organisms, even under the most extreme of conditions. If we consider the building blocks of a human body, which mainly consists of water but also lipids, peptides, nucleotides, salts and carbohydrates, it becomes obvious that such compounds need to be connected or to interact in specific ways to ensure viability. Supramolecular structures such as cell membranes, polymer materials such as proteins or nucleic acids and composite materials that include bones or teeth are good examples of how the combination of simple building blocks leads to special properties and functionality.

Well inspired by Nature, scientists attempt to mimic known supramolecular structures, polymers and composites. New, artificial materials are being developed to repair or replace parts of the human body or to afford faster convalescence. Moreover, such novel materials are also intended to make various therapies more efficient. Examples include new biomineralization strategies that make use of polymeric materials in bone-tissue engineering,[1] scaffolds for skin wound healing,[2] the reconstitution of channel proteins in block copolymer membranes,[3] and intelligent drug delivery carriers based on polymers.[4] In this work we focus on vesicles formed by amphiphilic block copolymers for applications in the field of biomedicine and nanotechnology.

Self-assembly of amphiphilic molecules to liquid crystal-like structures such as membranes is driven by thermodynamic forces and influenced by the molecule architecture.[5] In this respect, the ratio of hydrophilic to hydrophobic blocks and their volume ratio are crucial factors to control whether bilayers, cylindrical or spherical morphologies are obtained.[6] Upon vesicle formation in aqueous solution, the polymer is diluted continuously and an evolution from the bulk solid to lyotropic liquid (low molecular weight copolymers) or directly to the lamellar phase (high molecular weight copolymers) is observed (Figure 1).[7]

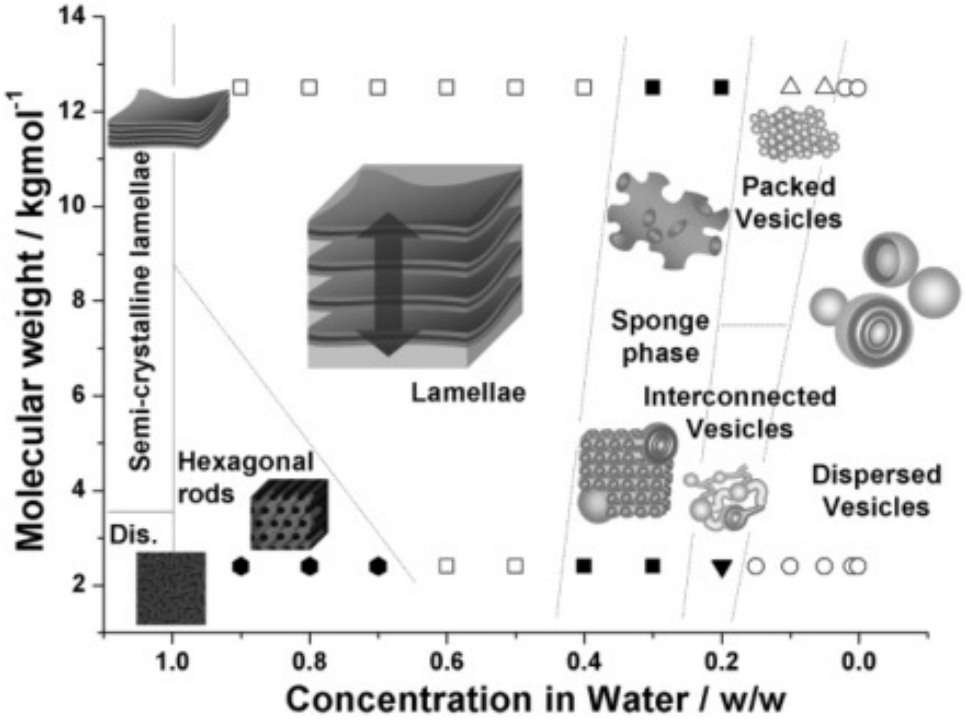

Figure 1. Isothermal illustration of molecular weight vs concentration phase diagram of poly(ethylene oxide)-*co*-poly(butyl oxide) and water. Reproduced by permission of the American Chemical Society.[8]

Via sponge phases and possibly vesicular gel clusters, dispersed vesicles are formed at sufficiently high dilution. From the thermodynamic point of view, the free energy depends on the interfacial energy of the hydrophilic-hydrophobic boundary layer, which is influenced by the nature of the solvent and as a consequence by the hydration of the hydrophilic part. This interfacial energy is aimed to compensate the loss of entropy which occurs when amphiphilic molecules such as block copolymers aggregate to well-ordered microdomains.[6] Other factors such as π-stacking between aromatic building blocks or intermolecular hydrogen bonds in the hydrophilic part of the membrane can contribute to the minimization of free energy. Soft and flexible polymer chains help to accelerate such a process, whereas rigid and stiff polymers need longer time to equilibrate.

The first noteworthy attempts to deliver drugs using lipid based vesicles, so called liposomes, were made as early as the 1950s.[9] Over years those systems improved e.g. by modifying the liposomes with poly(ethyleneglycol) (PEG) in order to prolong the circulation time in blood and to escape destruction by the reticuloendothelial system.[10] Additionally, cationic lipids that complex deoxyribonucleic acid (DNA) were used for gene

delivery.[11] However, while liposome-based drug and gene delivery systems appear to be promising for therapeutic applications, they lack stability and exhibit uncontrolled release of the hydrophilic cargo.[12] Furthermore, lipids are relatively small molecules that allow very limited chemical modification and functionalization.

In contrast to liposomes, vesicles made of amphiphilic block copolymers, so called polymersomes, lend themselves to construct vesicles by a huge variety of hydrophobic and hydrophilic building blocks,[13] allowing for the control of membrane thickness and thus of membrane stability and permeability.[14] The diversity of building blocks can also be used to impart properties such as responsiveness to external or internal stimuli that enable the release or the activation of cargo in a controlled manner. Stimuli-triggered polymersomes are sensitive to parameters such as pH, temperature, light, oxidative stress, magnetic fields or ultrasound.[15] In particular in drug delivery, such smart stimuli-responsive systems are a prerequisite for the release of a drug at a certain location and at a certain time. To guide the drug-loaded polymersome to the region of interest, to diseased tissue in the body in the case of a drug delivery system, the vesicle outer surface needs to feature ligands that specifically interact with receptors present on the membrane of the diseased cell.[16] The range of possibilities and challenges presented by polymersome surface functionalization is subject of this thesis, with a state of the art overview on this topic presented in Chapter 1.3 of this work.
In addition to functional and stimuli-responsive properties, the block copolymer should also be non-toxic (biocompatible) and, ideally, biodegradable.[17] The fate and behavior of the polymer in the human body after delivery of a drug is the final and crucial point determining whether the polymer can be used for therapeutic applications.

It is now the challenge of the chemists to design and develop polymers that fulfill the prerequisites mentioned above and to combine the best systems to a multifunctional and complete product. The following section provides an overview of the most common synthetic routes to synthesize amphiphilic block copolymers.

1.2. Synthetic routes to create amphiphilic block copolymers

1.2.1. Atom transfer radical polymerization

Popular and simple methods to synthesize polymers with controlled molecular weights and narrow polydispersities are controlled radical polymerizations (CRP). The most often used type of CRP is the atom transfer radical polymerizations (ATRP), which is known to give a high control over the reaction. Well known polymers synthesized by ATRP are polyacrylates, polymethacrylates, polystyrenes, acrylonitriles and many others. The components needed for ATRP are 1) initiatior molecules such as mono- and multifunctional alkane-halides (R-X), where the halide is usually bromide or chloride. An important requirement is the presence of substituents around the atom containing halogen that are able to stabilize the initiating radicals (R•). 2) Transition metal complexes such as iron, ruthenium, nickel, molybdenum, etc. were applied as catalyst systems in ATRP. Copper is the most commonly used for polymerization reactions. 3) A variety of ligands has been developed in order to improve the solubility, selectivity and reactivity of those catalysts. Ligands such as bipyridines, aliphatic amines or phosphines have lone electron pairs that coordinate to the transition metal and help to form strong and stable complexes (M_t^n-Y / Ligand).[18]

The mechanism of ATRP, where a reversible halogen atom transfer reaction between a transition metal complex and a dormant chain occurs, is depicted in Scheme 1.

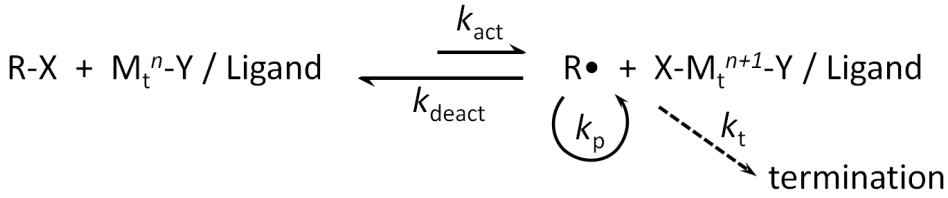

Scheme 1. Mechanism of the transition-metal catalyzed ATRP.[19] Reaction rates: k_{act} (activation), k_{deact} (deactivation), k_p (propagation), k_t (termination)

Methacrylate-based amphiphilic di- and triblock copolymers having different block length were synthesized by ATRP and their self-organization behavior in aqueous solution was investigated.[20] They were found to self-assemble in micelles, compound micelles and vesicular structures. The same and similar methycrylate-based block copolymer systems were used to generate solid-supported membranes by “grafting to” and “grafting

from"[21] approaches as well as by the interfacial adsorption of charged polymersome.[22]

1.2.2. Group transfer polymerization

More than 30 years ago, group transfer polymerization (GTP) was discovered at DuPont.[23] It is a method for the polymerization of acrylic monomers and allows one to synthesize different polymer chain architectures. It is a sequential Micheael addition of organosilicone compounds to α,β-unsaturated esters, ketones, nitriles and carboxamides.[24] This straightforward reaction is not sensitive to air, can be carried out at ambient temperatures or above, enables excellent control over polydispersities and over the polymer molecular weight simply through the ratio of initiator to monomer.[25] Also, the reaction is tolerant towards different functionalities, such as vinyl groups that would otherwise undergo polymerization during radical polymerization.[18] The most common catalysts used for GTP are oxyanion and bifluoride.[26] GTP has been applied for the synthesis of amphiphilic end-linked conetworks[27] as well as for the synthesis of water soluble diblock copolymers that form micellar structures in deionized water.[28]

1.2.3. Anionic polymerization

In anionic polymerizations, monomer molecules are added stepwise to a negatively charged center, where the charge is transferred to the new end. Monomers suitable for anionic polymerization should have electrophile groups being able to stabilize the charge by resonance, e.g. esters and nitriles of acrylic acids, methacrylic acids or vinyl ketones.[29] We differentiate between two mechanisms for the initiaton of the anionic polymerization (Scheme 2).

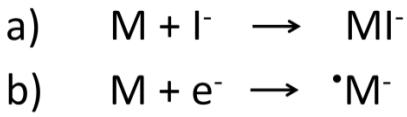

Scheme 2. Mechanisms for the initiation of anionic polymerization. Monomer species (M), ionic or ionogenic species (I^-) and electron (e^-).

In a), the carbanion is formed by adding the anion of an ionic or ionogenic species to the

vinyl double bond. Commonly used initiators for this kind of initiation are KNH_2, *n*-butyl lithium and Grignard reagents.[24] Mechanism b) describes the direct transfer of an electron from a donor, such as alkali metals, to the monomer to form a radical anion.[24] The anionic centers at the polymers stay reactive, even when all monomer is depleted, and can be quenched by terminating agents having certain functionalities. By quenching the reaction one can induce certain functionalities, e.g. with carbon dioxide, the polymer has a carboxylic acid end group, by using ethylene oxide one obtains an alcohol.[30]

Anionic polymerization is one of the preferred methods to synthesize silicone polymers, which are of special interest in this work. Its main advantage, compared to e.g. the acid catalyzed polycondensation,[3b] is the narrow molecular weight distribution of the product and better control over reaction. There are several sources reporting the anionic polymerization of silicone polymers.[31] An attractive route for the synthesis of monofunctional poly(dimethylsiloxane) (PDMS) is described by Kazama et al.[31c] They used *n*-butyllithium to initiate the anionic ring opening polymerization of hexamethylcyclotrisiloxane, which was finally quenched using dimethylchlorosilane. The resulting silane-terminated PDMS could be easily funtionalized by the hydrosilation reaction with allyl-functional molecules, comprising different functionalities, in the presence of platinum catalyst. Due to its low molecular weight distribution, the commercial PDMS we used in this work was probably synthesized by anionic polymerization.

1.2.4. Polycondensation

Polycondensation is a typical step-growth polymerization reaction. In a stepwise reaction of monomers small molecules such as water, or in the case of the acid-catalyzed synthesis of PDMS, methanol are eliminated.[24] Some examples of polymers synthesized by step-growth polymerization are polyesters, polyamides, polyurethanes, polyanhydrides and, mostly important for us, polysiloxanes. In this work we made use of the acid-catalyzed polycondensation reaction to obtain bifunctional PDMS polymer. This reaction, which was traditionally used for the synthesis of amphiphilic, PDMS-based block copolymers in our group,[3b] is not sensitive to moisture and therefore easy to

handle. In comparison to the anionic polymerization, a dramatic drawback is the rather poor molecular weight distribution of the resulting polymer.

1.2.5. Cationic polymerization

Compared to other polymerization techniques, the cationic polymerization is rarely used for technical applications.[24] The main advantage is the control of its reactivity by the solvent. Disadvantages are its sensitivity towards traces of water and impurities, what makes the use of Schlenk techniques to carry out the polymerization reaction indispensable. Additionally, low temperatures are required to obtain polymers with high molecular weights.

The initiation of cationic polymerization can be classed in three groups: a) carbenium ion salts; b) common protonic acids such as HCl, H_2SO_4 and $HClO_4$; c) Friedel-Crafts catalysts or Lewis acids such as BF_3, $AlCl_3$, $TiCl_4$ and $SnCl_4$.[24] Besides the variation of initators, there are also different monomers being capable for cationic polymerization. In this regard, electron-rich alkene derivatives having electron donor substituents, heteronuclear double and triple bonds as well as heteroatomic cyclic molecules should be mentioned.

In this work we pay special attention to the cationic ring opening polymerization (CROP), which makes use of the ring strain as driving force to react. Linear polymers can be formed from monomers such as lactones, lactams, cyclic amines and cyclic ethers after initiation with a cationic species.[24] The CROP reaction mechanism and kinetics of cyclic imino ethers were studied extensively during the last four decades.[32] It was shown that solvent polarity and composition as well as substituents of the oxazoline affect the polymerization reaction.[33] In Chapters 2 and 3 we use the CROP of the cyclic imino ether 2-methyl-2-oxazoline to polymerize a hydrophilic tail to the hydrophobic PDMS block, which finally results in amphiphilic block copolymer product. The CROP reaction mechanism of 2-methyl-2-oxazoline is shown in Scheme 3.

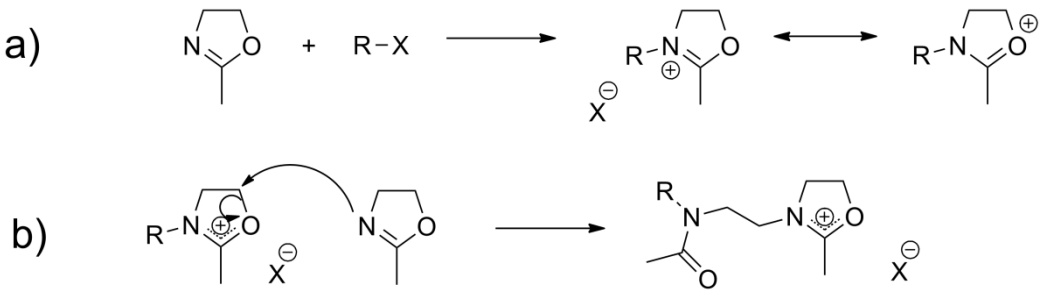

Scheme 3. Mechanism of the polymerization of 2-methyl-2-oxazoline: a) initiation of the reaction by a species R (e.g. PDMS) activated with a leaving group X (e.g. triflate or tosylate). b) propagation of the polymerization reaction. After all the monomer is converted, the reaction is quenched by a nucleophile (e.g. hydroxyl anion or secondary amines).

1.3. Functionalization of block copolymer vesicle surfaces

Polymersomes that have assembled from amphiphilic block copolymers have proven to be useful tools as drug delivery systems,[4d, 17a, 34] nanoreactors and sensors.[3c, 35] The attachment of targeting ligands or enzymes to the polymersomes, as well as the immobilization of polymer vesicles on surfaces, is of crucial importance in most of the previously mentioned applications. In this chapter, we will review the chemical methods that have been used for conjugation of a variety of ligands to the membrane surfaces of preformed polymersomes. The main requirements of such conjugation chemistries are their viability in an aqueous environment, the need to avoid cross-linking between polymersomes and between ligands, as well as stability and irreversibility of the resulting bond. Furthermore, it is desirable that the bonds are detectable and quantifiable in a simple, non-destructive manner. The state of the art in terms of common conjugation chemistry that fulfills all or some of these requirements is summarized in Table 1.

The first method that was used to attach ligands to the surface of preformed polymersomes was the biotin-streptavidin conjugation approach,[36] which allows an arbitrary variation of ligands bearing biotin groups.[3c, 4d, 37] Ligands are bound indirectly by biotin-streptavidin-biotin interactions to the polymersome surface. The modification of block copolymers with biotin has been performed either by N,N'-dicyclohexylcarbodiimide/4-(dimethylamino)pyridine-activated esterification[3c, 4d, 37] or by preactivation of the terminal hydroxyl functionality by tresyl chloride[38] or 4-fluoro-3-nitrobenzoic acid[39] and subsequent reaction with biocytin.[36, 39a] Both the esterification and the tresylation method resulted in a good yield of biotin modified polymer, which is essential for streptavidin and thus ligand binding after self-assembly of the polymersome.

Table 1. Overview of methods used to conjugate ligands and other functional entities to preformed block copolymer vesicles.

Polymersome functional group	Ligand / substrate functional group	Resulting bond	Block copolymer	Ligand / substrate
Alkyne	Azide	1,4-disubstituted 1,2,3-triazole	PS_{40}-*b*-$PIAT_{50}$, or mixture of PS_{40}-*b*-$PIAT_{50}$ with PS_{40}-*b*-PEG_{68}[35e,55]	Horseradish peroxidase[35e] and an azidofunctionalized *Candida antarctica* Lipase B[55]
Azide	Alkyne	1,4-disubstituted 1,2,3-triazole	PBD-*b*-PEG[56], PS-*b*-PAA[54]	Mannose functional polyester Dendron[56], dansyl probe[54], biotin[54], eGFP[54]
Biotin	Streptavidin	Biotin-Streptavidin interaction	PBD-*b*-PEG and PEG-*b*-PEE[36], PMOXA-*b*-PDMS-*b*-PMOXA[3c,4d,37a+b]	Superavidin-coated microspheres[36], antibody[39], polyguanylic acid[4d,37a], streptavidin-modified glass surface[3c], fluorescently labeled avidin[36,37b]
Ni^{2+}-nitrilotriacetic acid (Ni^{2+}-NTA)	Oligohistidine sequence	Complexation	PDB-*b*-PEG[45a+b]	Fluorescein labeled maltose binding protein[45a], eGFP[45a+b], RFP[45b]
Cyclodextrin (CD)	Adamantane	Hydrophobic interactions	PS-CD[49], CD-PEI-CD[50]	HRP[49], PEG[50]
N-hydroxysuccinimidyl ester	Thiol	C-S bond	PCL-*b*-PEG[60]	Antibody OX26[60]
Vinyl sulfone	Thiol	C-S bond	PEG-*b*-PMCL[61]	Cysteine-RGD peptide[61]
Aldehyde	Amine	Imine	PCL-*b*-PEG, PLA-*b*-PEG and PI-*b*-PEG[62]	Aminated glass surface[62]

Enhanced green fluorescent protein (eGFP), horseradish peroxidase (HRP), , poly(butadiene) (PBD), poly(caprolactone) (PCL), poly(dimethylsiloxane) (PDMS), poly(ethylethylene) (PEE), poly(ethylene glycol) (PEG), poly(ether imide) (PEI), poly(l-isocyanoalanine(2-thiophen-3-yl-ethyl)amide) (PIAT), poly(isoprene) (PI), poly(lactide) (PLA), poly(γ-methyl-ε-caprolactone) (PMCL), poly(2-methyl-2-oxazoline) (PMOXA), polystyrene (PS), red fluorescent protein (RFP).

In order to obtain polymersomes that interact with biotin-modified ligands, biotin-modified block copolymers (Figure 2a) were hydrated in aqueous solution to form polymersomes that were then incubated in an excess of streptavidin (Figure 2b). The optimal concentrations of polymersomes and streptavidin need to be determined experimentally in order to avoid undesired cross-linking reactions. If the ratio of streptavidin to biotinylated polymersomes is too low, the probability of cross-linking between polymersomes increases. Once the surface of the biotin modified polymersome had been saturated with streptavidin, biotin modified ligands were then attached.

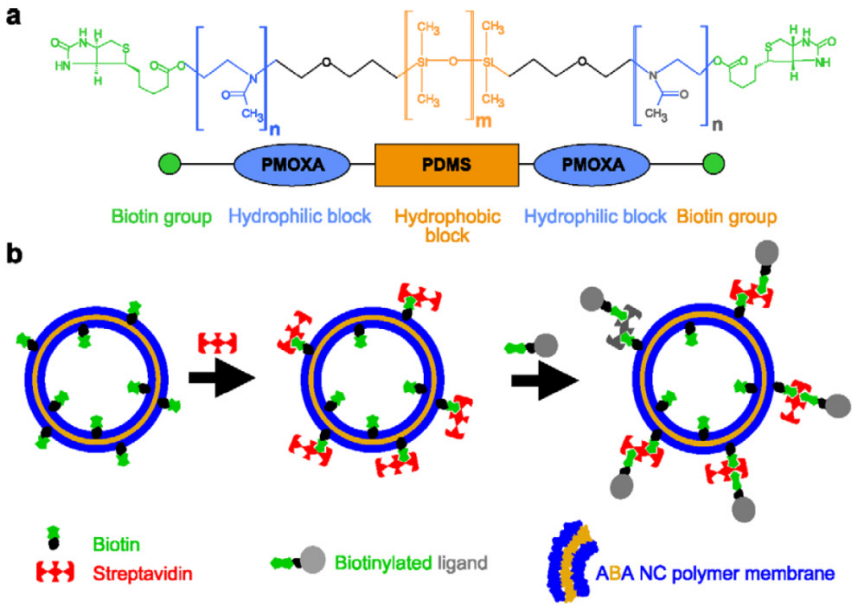

Figure 2. Surface-modification of polymersomes exploiting biotin-streptavidin binding. a) Biotin-functionalized poly(2-methyl-2-oxazoline)-*block*-poly(dimethylsiloxane)-*block*-poly(2-methyl-2-oxazoline) (PMOXA-*b*-PDMS-*b*-PMOXA). This was synthesized from the unmodified block copolymer by an esterification. b) Attachment of biotinylated ligands to the self-assembled polymersomes by a biotin-streptavidin binding approach. Reproduced by permission of Elsevier.[4d]

The modification strategy has some possible disadvantages. Although biotin and streptavidin form one of the strongest non-covalent interactions known (with dissociation constant around 10^{-15} M),[40] it is not a covalent bond. After binding, there is thus the possibility of ligand exchange with other biotinylated molecules in response to a change of ionic strength and/or temperature.[41] Furthermore, streptavidin is a macromolecule of considerable size (52.8 kDa). Therefore, when small ligands are intended for attachment to polymersomes via this strategy, the atom efficiency is not very favorable and steric problems might occur.

The binding of fluorescent dye-modified streptavidin to biotin modified polymersomes, with diameters between 140 and 172 nm, was demonstrated by fluorescence imaging,[36] fluorescence correlation spectroscopy (FCS), as well as fluorescence cross-correlation spectroscopy (FCCS).[37b] A model system, investigated by FCS and FCCS and comprising rhodamine-green-biotin modified polymersomes and cyanin5-labeled streptavidin, was utilized in order to determine the number of binding sites and the dissociation constant, K_D, of the receptor interaction between biotin-modified polymersomes and streptavidin.[37b] An average number of 1921 ± 357 streptavidin-Cy5 per polymersome and an intrinsic K_D of $(1.7 \pm 0.4) \times 10^{-8}$ M were determined.[37b] The latter differs from the value of 10^{-15} M given in the literature for the biotin-streptavidin interaction, which was explained by entropic and steric effects.

The biotin-streptavidin binding approach was used to modify polymersomes with the oligonucleotide polyguanylic acid (polyG), which specifically targets the macrophage A1 scavenger receptor.[4d] Moreover, the decorated polymersome has also proven to be suitable to target tumor cell lines.[37a] The receptor-specific binding of these polymersomes in human and transgenic cell lines and in mixed cultures was followed by vesicular uptake. A major improvement in biologic efficacy was obtained for polymersomes (containing pravastatin) compared to free drug, whereas no increased cytotoxic effect was observed in muscle tissue.[37a]

The group of Hammer has conducted extensive work on the surface-modification of polybutadiene-block-poly(ethylene glycol) (PBD-*b*-PEG) polymersomes via biotin-avidin interactions with the aim of creating and investigating vesicles that stick to biological surfaces under flow conditions, thus mimicking the adhesive properties of leucocites (Figure 3). The first papers in this series investigated the adhesion of biotin-decorated vesicles to avidin-coated surfaces.[36, 42] To this end, PBD-*b*-PEG conjugated to biotin-lysin (biocytin) was synthesized. The functionalized copolymer formed vesicles on its own, or when mixed with unmodified block copolymers. Two different unfunctionalized block copolmers were mixed with the biotinylated block copolymer. One was shorter, the other was the same length as the functionalized polymer. Micropipette aspiration allowed measurement of the critical tension required to peel the membrane away from a bead covered with avidin as a function of biotin surface density and of the length-ratio between unmodified and modified block copolymers. When biocytin was conjugated to a PEG block

that was longer than the surrounding unmodified PEG blocks, the critical tension reached a maximum at a content of 55% functionalized blockcopolymer. However, when both copolymers were of the same length, the critical tension was maximal at 10%, after which it increased only marginally. Thus, the biotin end groups need to be accessible at the surface, while they tend to be buried in the hydrophilic polymer layer at higher concentrations.

Biotinylated vesicles were coated with neutravidin, by means of which various biotin-labeled ligands were able to be conjugated to the surface, these include Alexa Fluor 488-biocytin, biotinylated adhesion molecule-1 antibody (anti-ICAM-1) and biotin-sialyl Lewis^x (sLe^x; a selectin ligand) (Figure 3a).[39a] The surface density of the antibody was tuned by varying the ratio of anti-ICAM-1 to sLe^x during the conjugation. The adhesiveness was measured between the decorated vesicles and ICAM-1-coated beads. In contrast to previous studies, the adhesion strength did not depend on the amount of biotinylated block copolymer, but rather increased linearly with the surface-density of the binding ligand, because the flexible polymer chains are buried underneath the coat of neutravidin (Figure 3b+c). Under physiological flow rates, such decorated vesicles do adhere to surfaces coated with inflammatory adhesion molecules P-selectin (to which sLe^x binds) and ICAM-1,[39b, 43] as well as to inflamed endothelium,[43] indicating possible applications as a targeted drug-delivery system.

Although cell-specific targeting *in vitro* was shown with polymersomes that were surface-modified by a biotin-streptavidin approach,[4d, 37a] such polymersomes would not be of use *in vivo* studies because streptavidin is known to block essential immune reactions in the human body.[44]

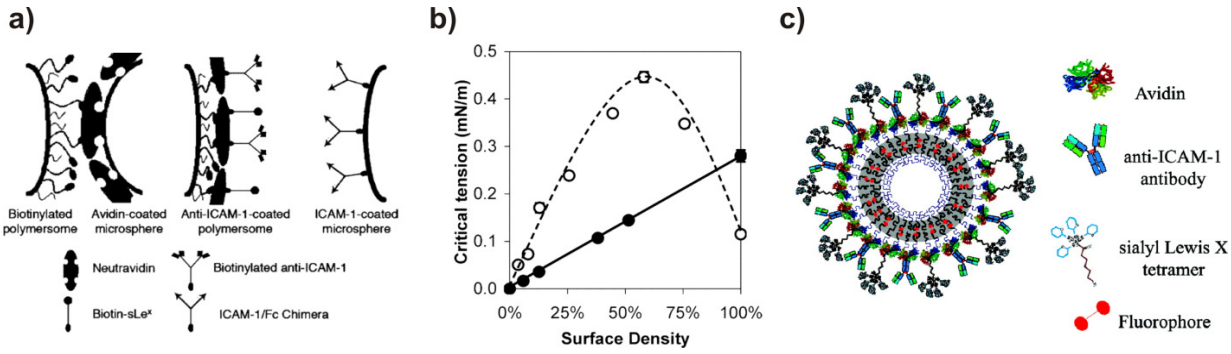

Figure 3. a) Schematic illustration of biotin-coated polymersome and anti-ICAM-1-coated polymersome. This system was used to compare the critical tension behavior of biotinylated polymersomes to avidin-coated microspheres and anti-ICAM-1-coated polymersomes to ICAM-1-coated microspheres, respectively. b) Comparison of the critical tension of those two different receptor-ligand pairs: biotin-avidin (open circle, dashed line) and anti-ICAM-1-ICAM-1 (closed circle, solid line). The divergence between the two critical tension curves is due to the variable manner by which the adhesion molecules were presented. c) Schematic illustration of a leukocyte-mimicking polymersome. In order to mediate adhesion, biotinylated sialyl-Lewis X or biotinylated anti-ICAM-1, or both simultaneously, was (were) attached to the polymersome surface. Reproduced by permission of the American Chemical Society.[39a, 43]

Another method of non-covalent but selective attachment of ligands to polymersomes and solid supported membranes was described by Nehring et al.[45] Polymersomes were synthesized based on PBD-*b*-PEG diblock copolymer comprising carboxylic acid or lysine-nitrilotriacetic acid (NTA) functional end groups. No disturbance of self-assembly behavior was observed upon mixing these two polymers. After vesicle formation, the peripheral NTA groups were able to form complexes with Ni^{2+} or Cu^{2+} ions. NTA-metal complexes are well known to selectively bind to oligohistidine sequences of proteins. Thus, maltose binding protein labeled with fluoresceine (His_{10}-MBP-FITC),[45a] as well as His-tagged enhanced green fluorescent protein (His_6-eGFP)[45] and red fluorescent protein (His_6-RFP),[45b] were able to be conjugated to the vesicle surface. After confirmation of the polymer-metal complex by UV-Vis spectroscopy and electron paramagnetic resonance (EPR), dissociation constants K_D of the different His-modified proteins to the Ni^{2+}-NTA functionalized polymersome were determined by FCS. A K_D of 7.0 ± 1.2 µM was measured for His_{10}-MBP-FITC, 12.3 ± 1.2 µM for His_6-eGFP and 1.99 ± 0.42 µM for His_6-RFP.[45a] These values are the same order of magnitude as the K_D values obtained with Ni^{2+}-NTA-modified liposomes (K_D = 4.3 µM)[46] and Cu^{2+}-NTA complexes.[47]

Solid supported monolayers of the same block copolymers were prepared by Langmuir-Schaefer transfer and incubated with a His-tagged protein, with the aim of investigating protein binding to metal ion-complexing polymer surfaces. Atomic force microscopy (AFM) revealed structural details of the protein-decorated membranes, indicating that polymer

monolayers may induce the formation of highly ordered protein arrays. Thus, the immobilization of densely packed proteins to such planar surfaces is a key step for 2D protein crystallization.[48]

A further type of non-covalent interaction, the binding of adamantane in the cavity of cyclodextrins, can be exploited to functionalize polymersome surfaces. PS homopolymer terminated with a permethylated β-cyclodextrin (β-CD) group,[49] as well as polyether imide (PEI) terminated at both chain ends with β-CDs[50] self-assembled into polymersomes, due to the hydrophilicity of the carbohydrate headgroups and the hydrophobicity of the polymer. The surface of these vesicles is a corona of β-CDs, which allowed the conjugation of adamantane-tagged horse radish peroxidase[49] and adamantane-terminated PEG.[50] Isothermal titration calorimetry (ITC) and static light scattering (SLS) revealed that both the inner and the outer polymersome surfaces were modified with the PEG. The enzyme-coated polymersomes were subjected to multiple washing steps. The amount of enzyme on the vesicles was found to decrease, indicating that the non-covalent interaction between β-CD and adamantane is too weak to withstand the washing procedure.[49]

A much more efficient and – in contrast to the biotin-streptavidin, Ni-NTA-His-tag, and β-CD-adamantane interactions – covalent conjugation method is the Huisgen 1,3-dipolar cycloaddition of azides and alkynes, promoted by Sharpless and co-workers as a reaction that fulfills the criteria of click chemistry.[51] This reaction is usually carried out in a variety of organic solvents such as DMF, DMSO, THF, halogenated solvents,[52] or in water-alcohol mixtures or pure water.[53] It is driven by heat or a catalytic amount of Cu(I). Because most polymersomes are destabilized in the presence of organic solvents, it is a prerequisite to perform this click chemistry conjugation reaction in aqueous media. Click chemistry with polymersomes in aqueous solution was introduced by van Hest and co-workers using poly(styrene)-*block*-poly(acrylic acid) (PS-*b*-PAA) diblock copolymers with terminal azide groups (Figure 4).[54] Different ligands, such as an alkyne bearing fluorescent dansyl probe, biotin and eGFP, have been conjugated to preformed polymersomes.

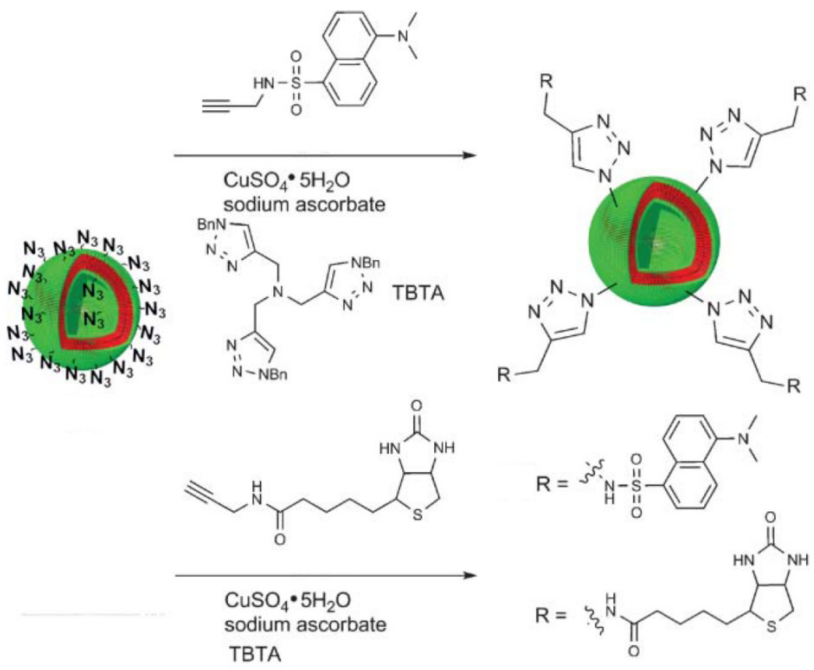

Figure 4. Modification of the outer polymersome surface by click chemistry. Alkyne bearing fluorescent dansyl probe and biotin were attached to azide functionalized polymersomes. Reproduced by permission of the Royal Society of Chemistry.[54]

The Cu(I) species that is used to catalyze this click reaction is usually formed *in situ* by mixing sodium ascorbate with a copper sulfate solution. In order to reach high conversion, the reduced Cu(I) species should be kept active for about 24 hours. For this purpose, the Cu(I) was stabilized by tris-(benzyltriazolylmethyl)amine (TBTA) or sodium bathophenantroline disulfonate (BPhT). The degree of functionalization was investigated by measuring the fluorescence intensity of the alkyne bearing fluorescent dansyl probe "clicked" to azide functionalized polymersomes. In order to find optimal reaction conditions and to improve the degree of functionalization of the polymersome surface, different parameters, such as the Cu(I) stabilizing ligands TBTA and BPhT, the copper concentration, the reaction temperature, and the pH of the reaction buffer, were varied. Degrees of functionalization between 24% and 26% were found under all conditions tested, which did not indicate a significant influence by the changed parameters. However, the relatively low degree of functionalization might be explained by functional group availability on the polymersome surface, with the majority of functional groups being buried in the hydrophilic layer of the block copolymer membrane. In addition to azide-functional polymersomes, van Hest and co-workers also introduced polymersomes based on alkyne-functionalized PS-*b*-PEG mixed with a high ratio of poly(styrene)-*block*-poly(l-isocyanoalanine(2-thiophen-3-yl-ethyl)amide) (PS-*b*-PIAT).[55]

An approach used to increase the number of surface-accessible functional groups on polymersomes was shown by Gillies and co-workers. By click chemistry, they attached dendritic and nondendritic displays of mannose, bearing alkyne functionality, to azide functional polymersomes and compared their binding to the mannose binding protein, concanavalin A, by using a hemagglutination assay.[56] As shown in Figure 5, membranes functionalized with dendritic displays are expected to show a higher availability of the mannose ligands than the nondendritic ones. In fact, this hypothesis was verified by experiments that showed that the binding of polymersomes functionalized with dendritic mannose displays was increased by 1-2 orders of magnitude relative to the nondendritic polymersomes.

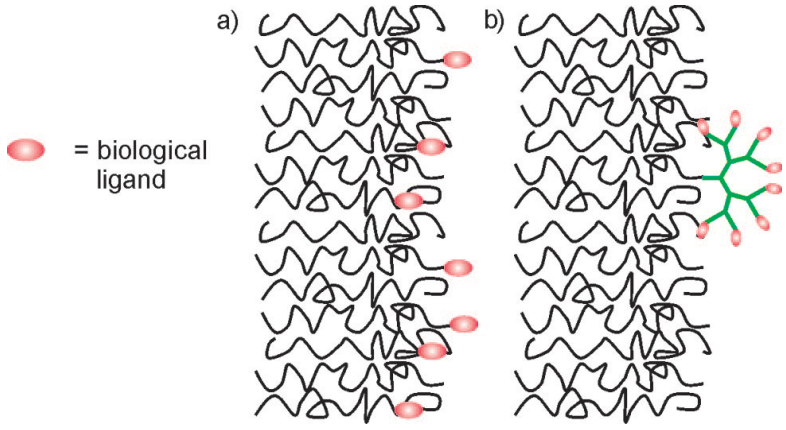

Figure 5. Schematic illustration of preformed polymersome membranes functionalized with (a) nondendritic and (b) dendritic biological ligand displays. Reproduced by permission of the American Chemical Society.[56]

Polymersome-enzyme conjugates made by azide-alkyne click chemistry have been applied as nanoreactors for enzymatic cascade reactions.[35e] Glucose oxidase (GOx) was encapsulated in the interior of these polymersomes and Candida antarctica lipase B (CalB) was incorporated into the vesicle bilayer membranes. Horseradish peroxidase (HRP) was reacted with imidazole-1-sulfonyl azide hydrochloride to introduce azide functionalities to this enzyme.[57] The HRP was then conjugated to the outer surface of the polymersomes via click-chemistry. The resulting construct had the three different enzymes partitioned in three different, well-defined local environments and was able to catalyze a three-step enzymatic reaction cascade, thus mimicking the confinement of individual reaction steps in compartments of living cells. Monoacetylated glucose was deprotected by CalB while diffusing from the bulk solution through the membrane into the cavity of the polymersome. In the cavity, the glucose was oxidized by GOx to gluconolactone and hydrogen peroxide. This small molecule was able to diffuse out of the nanoreactor through the membrane and was utilized by HRP to convert 2,2‘-azinobis(3-

ethylbenzothiazoline-6-sulfonic acid) (ABTS) to $ABTS^{\bullet+}$. In order to determine the enzyme encapsulation and conjugation efficiencies, the enzymes were decorated with a ruthenium complex and the biohybrid polymersomes were analyzed by inductively coupled plasma mass spectrometry. More than 90% (a remarkably high percentage) of available alkyne functionalities on the polymersome surface were thus found to be occupied by HRP enzymes. This example again shows the high efficiency of the azide-alkyne click reaction in aqueous media.

Reactions well-known in the field of protein conjugation chemistry, such as the reactions of maleimide functions with thiol groups,[58] or N-hydroxy succinimidyl esters with the amine groups of lysins,[59] can be applied to modify polymersomes bearing suitable functional groups on their surfaces. An example is the conjugation of the monoclonal antibody OX26 to poly(caprolactone)-*block*-poly(ethylene glycol) (PCL-*b*-PEG) polymersomes by reacting cysteine residues of the antibody with maleimido end groups of the PEG block present on the polymersome surface.[60] These decorated polymersomes were investigated as possible vessels for the delivery of peptides to the brain, as the antibody binds to a receptor that can initiate transcytosis of particles across the blood-brain barrier. A quantity of 34 OX26 antibodies on the surface of a polymersome was found to result in the greatest blood-brain barrier permeability.

Another example of a mild conjugation reaction known in biochemistry is the addition of thiols to vinyl groups. This reaction was exploited to link cysteine-containing peptides to vesicles with a reactive surface.[61] Poly(ethylene oxide)-*block*-poly(γ-methyl-*ε*-caprolactone) (PEG-*b*-PMCL) was functionalized at its hydrophilic terminus with a vinyl sulfone group. These block copolymers formed vesicles in aqueous solution that displayed vinyl sulfone groups on their surface. Short targeting peptides containing thiol groups did bind to the vesicles, while similar peptides lacking cysteine did not adhere. As this work was only recently published, future experiments are needed to show the efficiency of these peptide-labeled polymersomes in targeted drug-delivery.

Foster and co-workers reported the immobilization of polymersomes composed of PCL-*b*-PEG, poly(lactide)-*block*-poly(ethylene glycol) (PLA-*b*-PEG), and poly(isoprene)-*block*-poly(ethylene glycol) (PI-*b*-PEG), each polymer with aldehyde end groups, to aminated glass surfaces, resulting in a covalent imine bond (Figure 6).[62] Depending on the different bilayer

stiffnesses, the three different species of polymersomes showed different footprint areas upon immobilization.

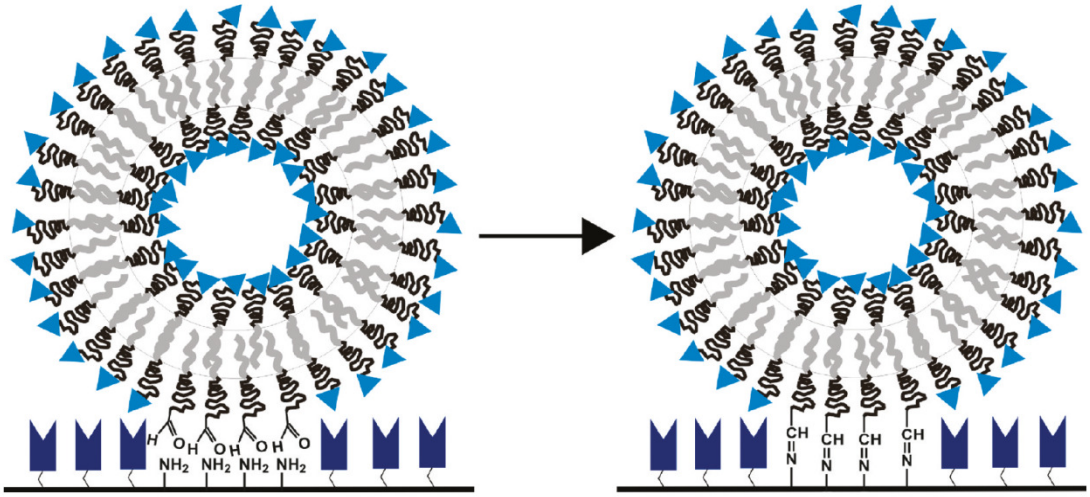

Figure 6. Covalent immobilization of aldehyde modified polymersomes on an aminated glass surface. Reproduced by permission of the American Chemical Society.[62]

An extension of this concept would involve the conjugation of proteins to the aldehyde decorated polymersome surface, as proteins generally display a multitude of amine groups on their surfaces. However, this approach is unfavorable because cross-linking of polymersomes by proteins could occur, which would lead to large aggregates. Moreover, this approach would not be suitable for the formation of permanent covalent bonds in aqueous environments, because aliphatic imines are known to be unstable and to hydrolyze into their original amine and aldehyde functionalities.

In this section we have reviewed a variety of synthetic routes to modify polymersome surfaces with moieties such as biomolecules. These methods differ by their binding specificities and efficiencies, by their biocompatibilities, as well as by their binding strengths. Non-covalent (e.g., biotin-streptavidin) and covalent binding strategies (e.g., Cu-catalyzed alkyne-azide click chemistry) are possible. An advantage of non-covalent binding may be that a higher density of functional ligands can be achieved, due to rearrangement of ligands and functional anchor groups. Benefits of covalent binding strategies include improved site-specificity and reproducibility, as well as increased binding stability. The copper catalyzed azide-alkyne click chemistry has proven itself to be applicable to the conjugation of different species such as proteins, enzymes or dendrons to the polymersome surface. The use of

copper as a catalyst, as well as the redox conditions while reducing Cu(II) to Cu(I), are unfavorable for biological and pharmaceutical applications.

Specific reactions to form bonds between block copolymer membranes and biological ligands, as well as the stability, and biocompatibility of the resulting bonds and linkers, are not the only points of interest when surface modified polymersomes are produced. Further investigations on the control of binding site availability, as well as membrane stability following a high degree of modification, will have to be carried out in the future.

1.4. Motivation and concept

In the context of designing, preparing and evaluating chemically "smart" nanomaterials for targeted drug delivery, block copolymer-based vesicles have shown to be promising candidates.[4d, 15, 63] The possibility to introduce miscellaneous functionalities and triggers and also their stability makes them favourable compared to lipid-based systems. Despite remarkable advances in the development of polymersomes for targeting purposes, no adequate chemical method to attach biomolecules in a specific, biocompatible, stable and simple way to their outer surface has been reported to date. Moreover, no detailed investigation on the stability of the self-assembly upon ligand attachment has been done.

In this respect, we aim to develop a new generation of surface functionalized vesicles, which are based on amphiphilic block copolymers. The major advantages that our system should offer compared to well-known lipid and also polymer-based drug delivery systems are:

- *(i)* Functionality on the hydrophilic end of the block copolymer that enables simple, versatile modification after vesicle formation in aqueous solution
- *(ii)* a specific conjugation chemistry that enables specific, biocompatible, covalent attachment of biomolecules to the polymersome surface
- *(iii)* Reproducible, predictable and exclusive self-assembly followed by extrusion to uniform, nanosized vesicle morphologies
- *(iv)* Mechanical and chemical membrane stability as well as impermeability towards hydrophilic payload

In order to realize these objectives, silicone-based di- and triblock copolymers with poly(2-methyloxazoline) as hydrophilic part were prepared. Polymersomes assembled from PMOXA-*b*-PDMS-*b*-PMOXA triblock copolymers were previously shown to be – due to their stability and non-toxicity – adequate drug delivery vehicles.[4d, 37a] Furthermore they have proven to be impermeable to hydrophilic cargo[64] and to act as nanoreactors.[35f]

In this work, two established conjugation approaches being well known for their

specificity, efficiency and stability were used for the polymersome-ligand conjugation: the copper catalyzed alkyne-azide click chemistry that was introduced by Sharpless[51] and applied to polymersomes by van Hest[54] and a benzaldehyde-hydrazinonicotinamide conjugation chemistry.[65] New synthesized block copolymers as well as their self-assembled structures in aqueous solution were characterizded by spectroscopic and chromatographic methods. Successful ligand conjugation to polymersomes was demonstrated by fluorescence correlation spectroscopy. Finally, the specific targeting to functional surfaces or to certain receptors, expressed by cancer cell lines, was visualized by fluorescence imaging and verified by cell sorting experiments.

1.5. References

[1] I. B. Leonor, S. Gomes, P. C. Bessa, J. F. Mano, R. L. Reis and M. Casal, *Nat.-Polym. Biomed. Appl.* **2008**, 193-230.
[2] G. E. J. Poinern, D. Fawcett, Y. J. Ng, N. Ali, R. K. Brundavanam and Z. T. Jiang, *J. Biomed. Nanotechnol.* **2010**, *6*, 497-510.
[3] a) W. Meier, C. Nardin and M. Winterhalter, *Angew. Chem., Int. Ed.* **2000**, *39*, 4599-4602; b) M. Kumar, M. Grzelakowski, J. Zilles, M. Clark and W. Meier, *Proc. Natl. Acad. Sci. U. S. A.* **2007**, *104*, 20719-20724; c) M. Grzelakowski, O. Onaca, P. Rigler, M. Kumar and W. Meier, *Small* **2009**, *5*, 2545-2548.
[4] a) E. R. Gillies and J. M. J. Frechet, *Chem. Commun. (Cambridge, U. K.)* **2003**, 1640-1641; b) E. R. Gillies and J. M. J. Frechet, *Drug Discovery Today* **2005**, *10*, 35-43; c) M. Sauer and W. Meier, *ACS Symp. Ser.* **2004**, *879*, 224-237; d) P. Broz, S. M. Benito, C. Saw, P. Burger, H. Heider, M. Pfisterer, S. Marsch, W. Meier and P. Hunziker, *J. Controlled Release* **2005**, *102*, 475-488.
[5] D. E. Discher and A. Eisenberg, *Science (Washington, DC, U. S.)* **2002**, *297*, 967-973.
[6] M. Antonietti and S. Foerster, *Adv. Mater. (Weinheim, Ger.)* **2003**, *15*, 1323-1333.
[7] G. Battaglia and A. J. Ryan, *J. Phys. Chem. B* **2006**, *110*, 10272.
[8] G. Battaglia and A. J. Ryan, *Macromolecules* **2006**, *39*, 798-805.
[9] G. Gregoriadis, *J. Drug Targeting* **2008**, *16*, 520-524.
[10] Y. Sadzuka, I. Sugiyama, T. Tsuruda and T. Sonobe, *Int. J. Pharm.* **2006**, *312*, 83-89.
[11] a) I. Koltover, T. Salditt, J. O. Radler and C. R. Safinya, *Science (Washington, D. C.)* **1998**, *281*, 78-81; b) P. L. Felgner and G. Rhodes, *Nature* **1991**, *349*, 351-352.
[12] V. Balasubramanian, O. Onaca, R. Enea, D. W. Hughes and C. G. Palivan, *Expert Opin. Drug Delivery* **2010**, *7*, 63-78.
[13] B. M. Discher, Y.-Y. Won, D. S. Ege, J. C. M. Lee, F. S. Bates, D. E. Discher and D. A. Hammer, *Science (Washington, D. C.)* **1999**, *284*, 1143-1146.
[14] K. P. Davis, T. P. Lodge and F. S. Bates, *Macromolecules (Washington, DC, U. S.)* **2008**, *41*, 8289-8291.

[15] O. Onaca, R. Enea, D. W. Hughes and W. Meier, *Macromol. Biosci.* **2009**, *9*, 129-139.
[16] S. Egli, H. Schlaad, N. Bruns and W. Meier, *Polymers (Basel, Switz.)* **2011**, *3*, 252-280.
[17] a) F. Ahmed, R. I. Pakunlu, A. Brannan, F. Bates, T. Minko and D. E. Discher, *J. Controlled Release* **2006**, *116*, 150-158; b) A. Wittemann, T. Azzam and A. Eisenberg, *Langmuir* **2007**, *23*, 2224-2230; c) C. Sanson, C. Schatz, J.-F. Le Meins, A. Brulet, A. Soum and S. Lecommandoux, *Langmuir* **2010**, *26*, 2751-2760.
[18] E. Rakhmatullina in *Methacrylate-based amphiphilic block copolymers in solution and at surfaces : synthesis, characterization and self-assembly*, *Vol. Doctor* University of Basel, Basel, **2008**.
[19] K. Matyjaszewski and J. Xia, *Chem. Rev. (Washington, D. C.)* **2001**, *101*, 2921-2990.
[20] E. Rakhmatullina, T. Braun, M. Chami, V. Malinova and W. Meier, *Langmuir* **2007**, *23*, 12371-12379.
[21] a) E. Rakhmatullina, A. Mantion, T. Burgi, V. Malinova and W. Meier, *J. Polym. Sci., Part A Polym. Chem.* **2008**, *47*, 1-13; b) E. Rakhmatullina, T. Braun, T. Kaufmann, H. Spillmann, V. Malinova and W. Meier, *Macromol. Chem. Phys.* **2007**, *208*, 1283-1293.
[22] E. Rakhmatullina and W. Meier, *Langmuir* **2008**, *24*, 6254-6261.
[23] O. W. Webster, *J. Polym. Sci., Part A Polym. Chem.* **2000**, *38*, 2855-2860.
[24] J. M. G. Cowie, *Polymers: Chemistry & Physics of Modern Materials*, Nelson Thornes Ltd., Cheltenham, **2001**, p.
[25] O. W. Webster, W. R. Hertler, D. Y. Sogah, W. B. Farnham and T. V. RajanBabu, *J. Am. Chem. Soc.* **1983**, *105*, 5706-5708.
[26] A. H. Gabor and C. K. Ober, *Chem. Mater.* **1996**, *8*, 2272-2281.
[27] G. Kali, T. K. Georgiou, B. Ivan and C. S. Patrickios, *J. Polym. Sci., Part A Polym. Chem.* **2009**, *47*, 4289-4301.
[28] F. L. Baines, N. C. Billingham and S. P. Armes, *Macromolecules* **1996**, *29*, 3416-3420.
[29] R. Hanselmann in *Anionische Polymerisation*, *Vol. 3.11* Georg Thieme Verlag, Stuttgart, **2005**.
[30] J. Jagur-Grodzinski, *J. Polym. Sci., Part A Polym. Chem.* **2002**, *40*, 2116-2133.
[31] a) V. Bellas, H. Iatrou and N. Hadjichristidis, *Macromolecules* **2000**, *33*, 6993-6997; b) C. L. Elkins and T. E. Long, *Macromolecules* **2004**, *37*, 6657-6659; c) H. Kazama, Y. Tezuka and K. Imai, *Polym. J. (Tokyo)* **1987**, *19*, 1091-1100; d) R. Stoenescu, A. Graff and W. Meier, *Macromol. Biosci.* **2004**, *4*, 930-935; e) R. Stoenescu in *Asymmetric amphiphilic triblock copolymers*, *Vol. PhD* University of Basel, Basel, **2004**.
[32] a) S. Kobayashi, T. Tokuzawa and T. Saegusa, *Macromolecules* **1982**, *15*, 707-710; b) S. Kobayashi, S. Iijima, T. Igarashi and T. Saegusa, *Macromolecules* **1987**, *20*, 1729-1734; c) T. Saegusa, H. Ikeda and H. Fujii, *Macromolecules* **1972**, *5*, 359-362; d) S. Kobayashi and H. Uyama, *J. Polym. Sci., Part A Polym. Chem.* **2001**, *40*, 192-209.
[33] K. Kempe, M. Lobert, R. Hoogenboom and U. S. Schubert, *J. Comb. Chem.* **2009**, *11*, 274-280.
[34] a) I. F. Uchegbu, *Expert Opin. Drug Delivery* **2006**, *3*, 629-640; b) K. K. Upadhyay, A. N. Bhatt, A. K. Mishra, B. S. Dwarakanath, S. Jain, C. Schatz, J.-F. Le Meins, A. Farooque, G. Chandraiah, A. K. Jain, A. Misra and S. Lecommandoux, *Biomaterials* **2010**, *31*, 2882-2892.
[35] a) K. Renggli, P. Baumann, K. Langowska, O. Onaca, N. Bruns and W. Meier, *Adv. Funct. Mater.* **2011**, *accepted*; b) C. Nardin, S. Thoeni, J. Widmer, M. Winterhalter and W. Meier, *Chem. Commun. (Cambridge)* **2000**, 1433-1434; c) F. Axthelm, O. Casse, W. H. Koppenol, T. Nauser, W. Meier and C. G. Palivan, *J. Phys. Chem. B* **2008**, *112*, 8211-8217; d) C. De Vocht, A. Ranquin, R. Willaert, J. A. Van Ginderachter, T. Vanhaecke, V. Rogiers,

W. Versees, P. Van Gelder and J. Steyaert, *J. Controlled Release* **2009**, *137*, 246-254; e) S. F. M. van Dongen, M. Nallani, J. J. L. M. Cornelissen, R. J. M. Nolte and J. C. M. van Hest, *Chem.--Eur. J.* **2009**, *15*, 1107-1114; f) O. Onaca, D. W. Hughes, V. Balasubramanian, M. Grzelakowski, W. Meier and C. G. Palivan, *Macromol. Biosci.* **2010**, *10*, 531-538; g) P. Broz, S. Driamov, J. Ziegler, N. Ben-Haim, S. Marsch, W. Meier and P. Hunziker, *Nano Lett.* **2006**, *6*, 2349-2353.
[36] J. J. Lin, J. A. Silas, H. Bermudez, V. T. Milam, F. S. Bates and D. A. Hammer, *Langmuir* **2004**, *20*, 5493-5500.
[37] a) P. Broz, N. Ben-Haim, M. Grzelakowski, S. Marsch, W. Meier and P. Hunziker, *J. Cardiovasc. Pharmacol.* **2008**, *51*, 246-252; b) P. Rigler and W. Meier, *J. Am. Chem. Soc.* **2006**, *128*, 367-373.
[38] K. Nilsson and K. Mosbach, *Methods Enzymol.* **1984**, *104*, 56-69.
[39] a) J. J. Lin, P. P. Ghoroghchian, Y. Zhang and D. A. Hammer, *Langmuir* **2006**, *22*, 3975-3979; b) D. A. Hammer, G. P. Robbins, J. B. Haun, J. J. Lin, W. Qi, L. A. Smith, P. Peter Ghoroghchian, M. J. Therien and F. S. Bates, *Faraday Discuss.* **2008**, *139*, 129-141.
[40] P. C. Weber, D. H. Ohlendorf, J. J. Wendoloski and F. R. Salemme, *Science (Washington, D. C., 1883-)* **1989**, *243*, 85-88.
[41] A. Holmberg, A. Blomstergren, O. Nord, M. Lukacs, J. Lundeberg and M. Uhlen, *Electrophoresis* **2005**, *26*, 501-510.
[42] J. J. Lin, F. S. Bates, D. A. Hammer and J. A. Silas, *Phys. Rev. Lett.* **2005**, *95*, 026101/026101-026101/026104.
[43] G. P. Robbins, R. L. Saunders, J. B. Haun, J. Rawson, M. J. Therien and D. A. Hammer, *Langmuir* **2010**, *26*, 14089-14096.
[44] R. Alon, R. Hershkoviz, E. A. Bayer, M. Wilchek and O. Lider, *Eur. J. Immunol.* **1993**, *23*, 893-898.
[45] a) R. Nehring, C. G. Palivan, O. Casse, P. Tanner, J. Tuxen and W. Meier, *Langmuir* **2009**, *25*, 1122-1130; b) R. Nehring, C. G. Palivan, S. Moreno-Flores, A. Mantion, P. Tanner, J. L. Toca-Herrera, A. Thuenemann and W. Meier, *Soft Matter* **2010**, *6*, 2815-2824.
[46] I. T. Dorn, K. R. Neumaier and R. Tampe, *J. Am. Chem. Soc.* **1998**, *120*, 2753-2763.
[47] Y. Rahimi, S. Shrestha, T. Banerjee and S. K. Deo, *Anal. Biochem.* **2007**, *370*, 60-67.
[48] R. D. Kornberg and S. A. Darst, *Curr. Opin. Struct. Biol.* **1991**, *1*, 642-646.
[49] M. Felici, M. Marza-Perez, N. S. Hatzakis, R. J. M. Nolte and M. C. Feiters, *Chem.--Eur. J.* **2008**, *14*, 9914-9920.
[50] M. Guo, M. Jiang and G. Zhang, *Langmuir* **2008**, *24*, 10583-10586.
[51] V. V. Rostovtsev, L. G. Green, V. V. Fokin and K. B. Sharpless, *Angew. Chem., Int. Ed.* **2002**, *41*, 2596-2599.
[52] W. H. Binder and R. Sachsenhofer, *Macromol. Rapid Commun.* **2007**, *28*, 15-54.
[53] C. E. Evans and P. A. Lovell, *Chem. Commun. (Cambridge, U. K.)* **2009**, 2305-2307.
[54] J. A. Opsteen, R. P. Brinkhuis, R. L. M. Teeuwen, D. W. P. M. Loewik and J. C. M. van Hest, *Chem. Commun. (Cambridge, U. K.)* **2007**, 3136-3138.
[55] S. F. M. van Dongen, M. Nallani, S. Schoffelen, J. J. L. M. Cornelissen, R. J. M. Nolte and J. C. M. van Hest, *Macromol. Rapid Commun.* **2008**, *29*, 321-325.
[56] A. L. Martin, B. Li and E. R. Gillies, *J. Am. Chem. Soc.* **2009**, *131*, 734-741.
[57] a) E. D. Goddard-Borger and R. V. Stick, *Org. Lett.* **2007**, *9*, 3797-3800; b) S. F. M. van Dongen, R. L. M. Teeuwen, M. Nallani, S. S. van Berkel, J. J. L. M. Cornelissen, R. J. M. Nolte and J. C. M. van Hest, *Bioconjugate Chem.* **2009**, *20*, 20-23.
[58] a) S. S. Ghosh, P. M. Kao, A. W. McCue and H. L. Chappelle, *Bioconjugate Chem.*

1990, *1*, 71-76; b) K. Velonia, A. E. Rowan and R. J. M. Nolte, *J. Am. Chem. Soc.* **2002**, *124*, 4224-4225.
[59] H. Xu, J. L. Kaar, A. J. Russell and W. R. Wagner, *Biomaterials* **2006**, *27*, 3125-3135.
[60] Z. Pang, W. Lu, H. Gao, K. Hu, J. Chen, C. Zhang, X. Gao, X. Jiang and C. Zhu, *J. Controlled Release* **2008**, *128*, 120-127.
[61] M. A. Petersen, L. Yin, E. Kokkoli and M. A. Hillmyer, *Polym. Chem.* **2010**, *1*, 1281-1290.
[62] S. Domes, V. Filiz, J. Nitsche, A. Fromsdorf and S. Forster, *Langmuir* **2010**, *26*, 6927-6931.
[63] a) D. E. Discher, P. Photos, F. Ahmed, R. Parthasrathy and F. S. Bates, *Biomedical Aspects of Drug Targeting* **2002**, pp. 459-471; b) M. M. J. Kamphuis, A. P. R. Johnston, G. K. Such, H. H. Dam, R. A. Evans, A. M. Scott, E. C. Nice, J. K. Heath and F. Caruso, *J. Am. Chem. Soc.* **2010**, *132*, 15881-15883.
[64] S. Litvinchuk, Z. Lu, P. Rigler, T. D. Hirt and W. Meier, *Pharm. Res.* **2009**, *26*, 1711-1717.
[65] N. Bruns, K. Pustelny, L. M. Bergeron, T. A. Whitehead and D. S. Clark, *Angew. Chem., Int. Ed.* **2009**, *48*, 5666-5669, S5666/5661-S5666/5617.

2. Covalent attachment of poly-G ligands to polymersomes by azide-alkyne click chemistry

Stefan Egli[1], Barbara Fischer[2], Sonja Hartmann[2], Patrick Hunziker[2], Wolfgang Meier[1], Per Rigler[1]

[1]Department of Chemistry, University of Basel, Klingelbergstrasse 80, 4056 Basel, Switzerland

[2]Medical Intensive Care Unit, University Hospital Basel, Petersgraben 4, 4031 Basel, Switzerland

Adaptd with permission from *Macromolecular Symposia* **2010,** 29*6* (1), 278

Article online via: http://onlinelibrary.wiley.com/doi/10.1002/masy.201051039/abstract

2.1. Introduction

Previously, we established methods to produce functional nanocontainers based on amphiphilic block copolymers with ideal properties for drug delivery applications.[1] Here, we present a new strategy for specific cellular targeting by applying click chemistry in order to covalently attach oligonucleotides to polymeric nanocontainers comprising the amphiphilic block copolymer poly(2-methyloxazoline)-*block*-poly(dimethylsiloxane)-*block*-poly(2-methyloxazoline) (PMOXA-*b*-PDMS-*b*-PMOXA). The goal of this work was to create a versatile drug delivery vehicle that not only shows specific targeting towards diseased cells, but also fluorescent properties for imaging purposes. To achieve our goal, we synthesized triblock copolymers with hydroxyl, alkyne or sulforhodamine B (SRB) functionalities at the hydrophilic terminus. These triblock copolymers were used to form polymersomes with surface-exposed alkyne groups. In aqueous solution, the alkyne group can react specifically with azide-modified molecules by the copper(I)-catalyzed Huisgen 1,3-dipolar cycloaddition, as shown previously.[2]

Macrophages play an important role in a wide range of disease states such as autoimmune diseases, infections, cancer or atherosclerosis. It has been shown that nanocontainers, functionalized with the 23 nucleotide-long polyguanosine (poly$(G)_{23}$), were taken up by the human monocytic cell line, THP-1 macrophages, that overexpressed the scavenger receptor A1 (SRA1) in a specific manner.[1a] However, the binding of the ligands to the nanocontainers was performed via biotin-streptavidin conjugation, which is known to be stable, but not irreversible and not covalent. Furthermore, streptavidin is known to block essential immune reactions in the human body and would thus not be of use in *in vivo* applications.[3] Therefore, the cycloaddition of alkynes and azides to produce a stable triazole bond is a promising method to covalently attach biological ligands to polymer self-assemblies.

2.2. Results and discussion

2.2.1. Synthesis of triblock copolymers

The synthesis of the hydrophobic PDMS and the amphiphilic block copolymer PDMS-*b*-PMOXA-*b*-PDMS was described previously by our group.[4] In a first step, the hydroxyl bifunctional PDMS was synthesized by an acid-catalyzed polycondensation reaction. In a second step, the PDMS was reacted with trifluoromethanesulfonic anhydride and this preactivated species was reacted in a cationic ring opening polymerization with 2-methyl-2-oxazoline. Finally, the polymerization reaction was quenched using a KOH solution in methanol, resulting in a hydroxyl-terminated triblock copolymer (ABA-1). We obtained an alkyne-terminated triblock copolymer (ABA-2) using N-methylpropargylamine instead of KOH as the nucleophile to quench the reaction. The third polymer, comprising SRB as the terminal functionality (ABA-SRB), was synthesized by an esterification reaction according to a procedure described previously.[5] The structures of the three different polymers are shown in Scheme 4.

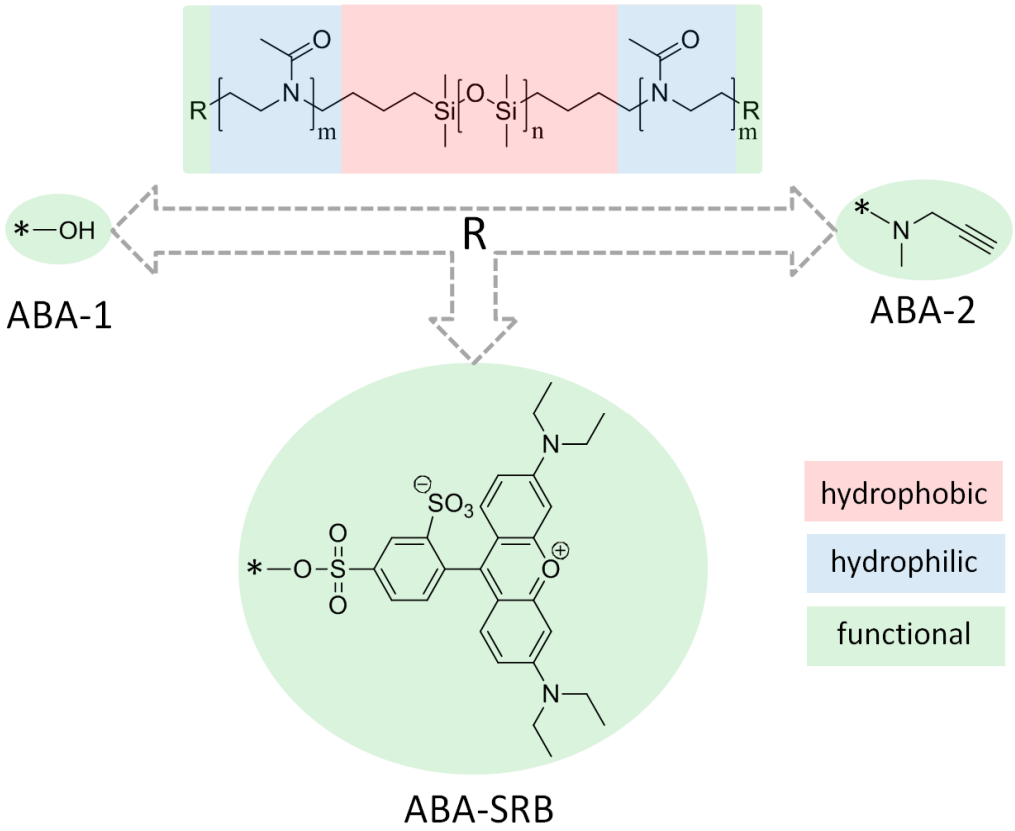

Scheme 4. PMOXA-*b*-PDMS-*b*-PMOXA triblock copolymers comprising different functionalities: ABA-1 having a hydroxyl group, ABA-2 having a N-methylpropargyl (alkyne) group and ABA-SRB having a SRB group at its hydrophilic end.

2.2.2. Characterization of the block copolymers

The block length of the ABA polymers was characterized by ^{1}H NMR using a 400 MHz Bruker spectrometer. Spectra of those polymers are shown in Figures 36 and 37. From the integral values we calculated a composition of $A_{10}B_{87}A_{10}$ for the ABA-1 polymer, $A_7B_{86}A_7$ for the ABA-2 polymer and $A_{10}B_{85}A_{10}$ for the ABA-SRB polymer.

The conjugation of SRB to the polymer was confirmed by pulsed field gradient spin echo ^{1}H-NMR experiments (PFGSE), as shown in Table 2. The diffusion coefficient of the SRB-labeled polymer (signal at 6.80 ppm) was determined as $2.41*10^{-10}$ m^2 s^{-1}. For the diffusion coefficient of free SRB acid chloride in $CDCl_3$ (7.16 ppm), we obtained $6.04*10^{-10}$ m^2 s^{-1}. Using the Stokes-Einstein equation and assuming that the molecular weight is proportional to a spherical volume, we calculated the molecular weight of the SRB-labeled polymer based on the molecular weight of SRB acid chloride (577.11 g mol^{-1}) and the two measured diffusion coefficients. We obtained an average polymer molecular

weight of 9085 g mol^{-1}, which is in good agreement with the molecular weight calculated from ^{1}H-NMR integrals (8756 g mol^{-1}).

Table 2. ^{1}H NMR Chemical shifts of different functional building blocks of the block copolymer and SRB dye. Diffusion coefficients were measured at * and # labeled chemical shifts.

Component	$\delta_{CH3\text{-}Si}$	$\delta_{CH3CON<}$	$\delta_{>N\text{-}CH2\text{-}CH2\text{-}N<}$	$\delta_{aromatic}$	D [m^2 s^{-1}] 10^{-10}
ABA-OH	0.1	2.0 – 2.2	3.3 – 3.5	-	-
ABA-SRB	0.1$^{\#}$	2.0 – 2.2	3.3 – 3.5	6.7 – 8.7*	2.36$^{\#}$ / 2.41*
SRB	-	-	-	6.7 – 8.7*	6.04*

A different approach to determine whether the fluorescent dye is conjugated covalently to the block copolymer was the measurement of its diffusion time by fluorescence correlation spectroscopy (FCS) in ethanol solution. At an excitation wavelength λ_{ex} of 514 nm, the diffusion time of solutions with a polymer concentration of 1.9 μg mL was measured. The data we obtained for free SRB (50 nM), for ABA-SRB and for ABA-1 in a solution of 50 nM SRB are presented in Table 3.

Table 3. Parameters obtained by FCS of free SRB, ABA-SRB and mixed free SRB and ABA-1 in ethanol

Sample	Count rate [kHz]	N^a	τ_1 [μs]^b	F_1 [%]^c	τ_2 [μs]^b	F_2 [%]^c
SRB	36.5	23.5	51	100	-	-
ABA-SRB	25.6	28.5	51	0.8	124	99.2
SRB + ABA-1	36.7	23.9	51	6.9	53	93.1

[a] **Number of molecules**
[b] **Diffusion time of molecular species**
[c] **Fraction of molecules with certain diffusion times**

The free SRB in ethanol shows a diffusion time τ that is twice that of the diffusion time of free SRB in aqueous solution.[6] This could be explained by the different solubility of SRB in ethanol as compared to water, but also the solvent viscosity ($\eta_{water,\ 291\ K}$ = 1.06; $\eta_{ethanol,\ 291\ K}$ = 1.22) could have a minor effect on the mobility of the dye. The ABA-SRB solution contained mainly species with a high diffusion time of 124 μs and only an insignificant fraction of 0.8% of free dye. In contrast, the sample of ABA-1 mixed with SRB showed two fractions with almost identical τ of 51 μs and 53 μs. The latter τ, which differs slightly from the diffusion time of free SRB, can be explained by the influence of the ABA-1 on the viscosity of the solution. However, there is a significant difference

between the τ of ABA-SRB and that of the mixed solution of ABA-1 and SRB, which is additional proof that SRB is covalently bound to ABA-SRB.

2.2.3. Preparation and characterization of polymersomes

Polymeric nanocontainers were prepared by mixing the three different ABA polymers in the following weight ratio: ABA-1/ABA-2/ABA-SRB 16.0/3.7/1.0. This mixture was dissolved in ethanol, the solvent was evaporated under vacuum and bidistilled water was added to yield a total polymer concentration of 4 mg mL^{-1}. After two days hydration, the polymersome solution was extruded through a polycarbonate filter (0.2 μm pore size) and characterized by transmission electron microscopy (TEM, Figure 7), Fluorescence correlation spectroscopy (FCS, Figure 8), confocal laser scanning microscopy (CLSM, Figure 9) and by light scattering.

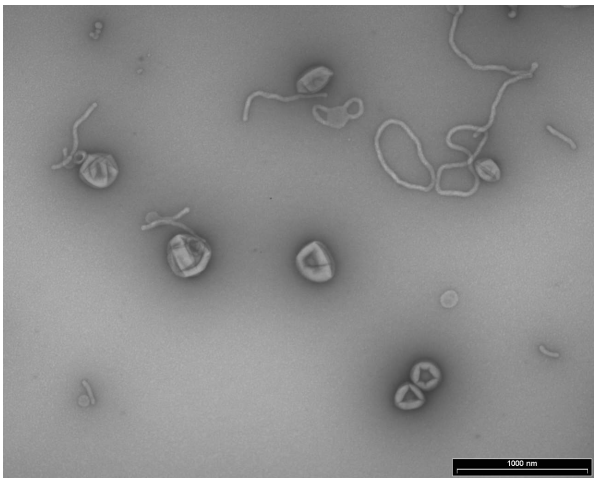

Figure 7. Transmission electron micrographs of polymersomes consisting of ABA-1, ABA-2 and ABA-SRB, stained with 2% uranylacetate solution. The scale bar represents 1 μm.

We obtained information on the morphology of our self-assemblies using dynamic (DLS) and static (SLS) light scattering. DLS showed a hydrodynamic radius (R_h) of 126.9 nm and SLS a radius of gyration (R_g) of 107 nm (Guinier-plot in Figure 35). From these values, we obtained the ρ-value given as $\rho = R_g/R_h$, which provides information on the internal structure of our particles in solution.[7] A ρ-value of 0.84 indicates that amongst vesicles, there are other morphologies present in our sample. The TEM image (Figure 7) shows collapsed vesicles, but also wormlike micelles. This indicates that the rather low ρ-value could be a combination of both vesicles and micelles.

FCS autocorrelation curves (Figure 8) clearly show the difference between freely diffusing SRB dye (τ_D = 28 μs) and the polymersomes (τ_D = 7.5 ms) containing ABA-SRB. The values for τ_D were found to be in an expectable range.[6] By CLSM (Figure 9) we confirmed the absence of big aggregates. However, the optical resolution of the confocal microscope is not sufficient to distinguish single vesicles by CLSM. What is shown are individual fluorescent spots corresponding to single vesicles.

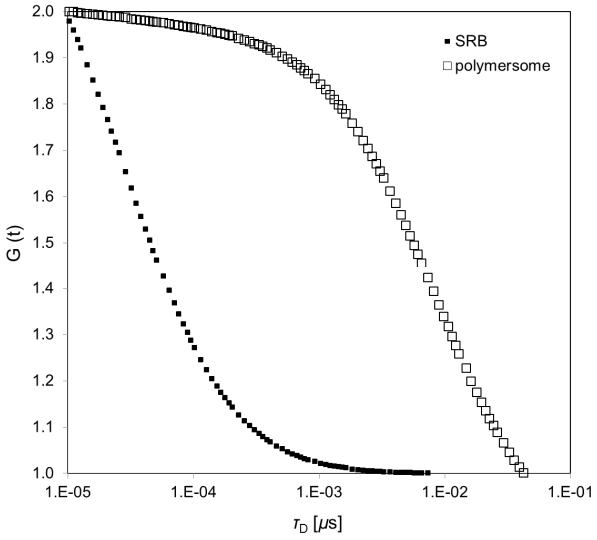

Figure 8. FCS autocorrelation curves of 50 nM SRB and of a 0.5 mg mL^{-1} polymersome solution consisting of ABA-1, ABA-2 and ABA-SRB in bidistilled water. The applied laser excitation wavelength was 543 nm.

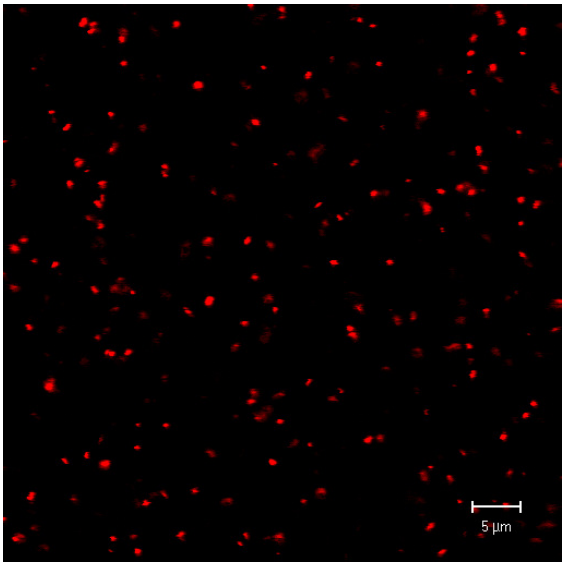

Figure 9. Confocal laser scanning micrograph of a 0.5 mg mL^{-1} polymersome solution consisting of ABA-1, ABA-2 and ABA-SRB in bidistilled water. The scale bar represents 5 μm.

2.2.4. Specific uptake of poly(G)$_{23}$-modified polymersomes by THP-1 cells

In order to verify the specific cellular uptake we used the human monocytic cell line THP–1. Previous studies have shown the feasibility of specific uptake of poly(G)$_{23}$ modified polymeric nanocontainers by THP-1 cells using the biotin-streptavidin interaction as a link for the ligand.[1] Although modular and of high affinity, biotin-streptavidin interactions have the drawback that the number of binding sites of the nanocontainer has to be precisely determined in order to prevent excess free ligand reducing uptake significantly, and that streptavidin might lead to adverse immunogenicity. Therefore, we made use of azide-alkyne click chemistry to conjugate the poly(G)$_{23}$ ligands to the polymersome surface by following a protocol from van Hest and co-workers.[2] It was not possible to prove and quantify the conjugation of azide-functionalized poly(G)$_{23}$ ligands to alkyne-functional polymersomes by spectroscopic methods. A possible explanation for this is the poor solubility of oligonucleotides in chloroform, which is the standard ^{1}H NMR solvent for our polymers, as well as the low concentration of poly(G)$_{23}$, which makes IR and UV-Vis spectroscopy impossible. The only proof presented here is the specific and enhanced uptake of fluorescent vesicle-poly(G)$_{23}$ conjugates by THP-1 cells.

Two days prior to imaging, THP-1 cells were activated with phorbol-12-myristate-13-acetate (PMA, 100 nM) to differentiate the monocytes into macrophages and approximately 500 000 cells mL^{-1} were seeded into each well of the tissue culture slide (Lab-tek, NUNC). Both poly(G)$_{23}$ modified nanocontainers and control ABA nanocontainers lacking the ligand were added to the activated cells and incubated (37°C, 5% CO_2) for 4 and 24 hours, respectively. Confocal fluorescence imaging using the 543 nm laser line of a ZEISS LSM 510 microscope was used to determine the extent of specific cellular uptake (Figure 10).

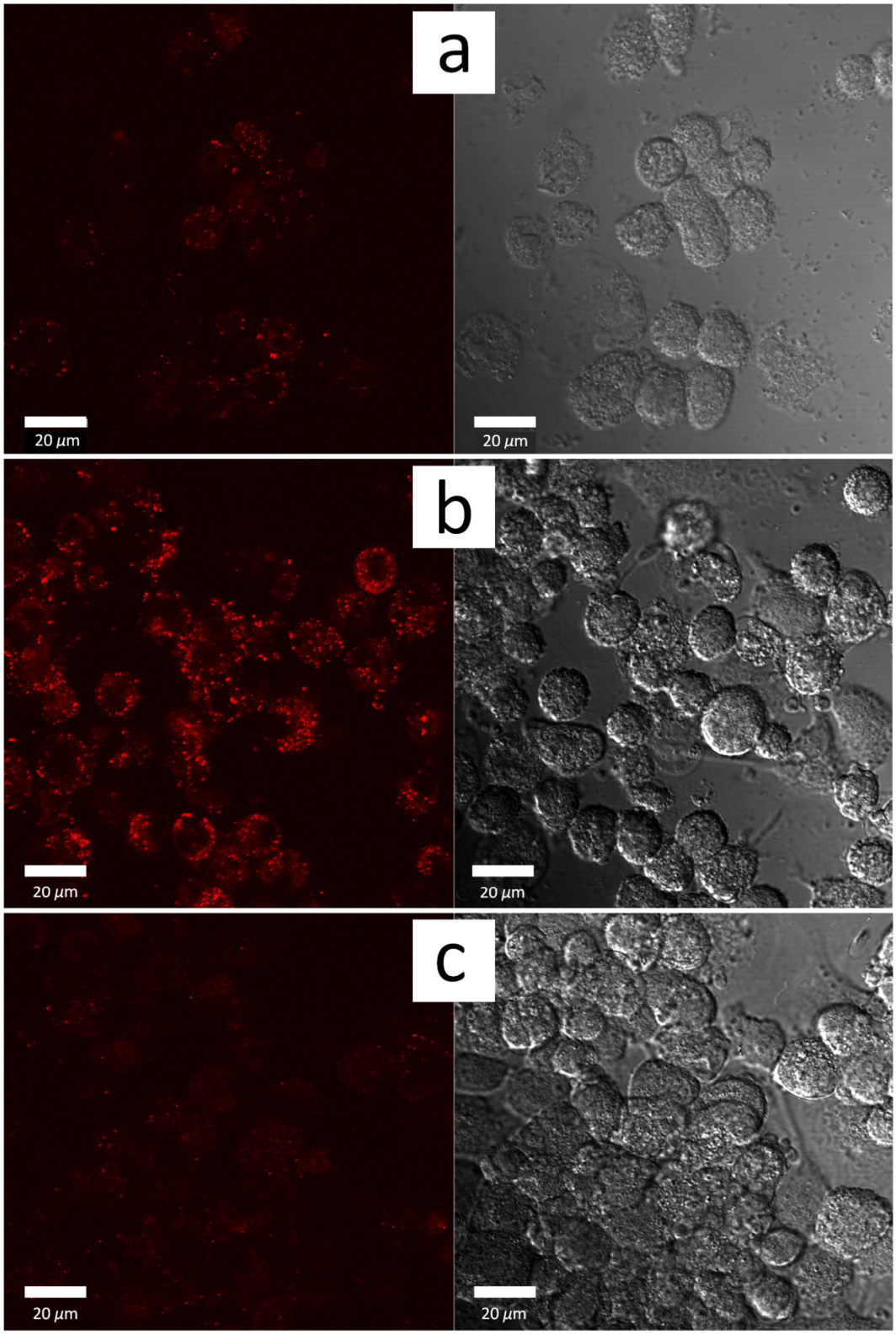

Figure 10. Confocal laser scanning micrographs (CLSM, left) and differential interference image (DIC, right) images of THP-1 macrophages. a) after 4 h and b) after 24 h incubation with polymersomes consisting of ABA-1, ABA-SRB and ABA-2 after click-conjugation with polyG_{23}-azide. c) after 24 h incubation with polymersomes consisting of ABA-1, ABA-SRB and ABA-2; without polyG_{23}-azide. All cell samples were washed with PBS before imaging.

Significantly higher relative fluorescence intensity was found in THP-1 samples incubated with poly$(G)_{23}$-modified polymersomes (Figure 10a+b) in contrast to THP-1 cells incubated with polymersomes lacking the poly$(G)_{23}$ ligand (Figure 10c). By comparing Figure 10a and 10b, it is obvious that, after 24 h incubation time, the cells were full of polymersomes, whereas after 4 h incubation time there was only little fluorescence in the cells. This shows that the uptake is, to a certain extent, time-dependent. However, from Figure 10c it is clear that there is some unspecific uptake of polymersomes after 24 h incubation time as well. The ABA-SRB, which exhibits charged, hydrophilic SRB groups at its hydrophilic end, might also have an effect on the polymersome uptake. Since both the poly$(G)_{23}$-labeled and the control polymersomes contain ABA-SRB, this effect should be about the same for both samples.

2.2.5. Scission of biological ligands under click-conditions

When we tried to conjugate antibodies and bovine serum albumin (BSA) to polymersomes by click chemistry, we obtained results that indicated no binding of the ligands to the polymersomes (measured by FCS, data not shown). This lets us assume that reactions other than the click conjugation can occur in our system. It has been shown that ascorbate redox systems are able to form OH-radicals in the presence of copper and O_2 under physiological conditions.[8] Such radicals are considered to be responsible e.g. for the scission of polysaccharides[9], peptides[10], proteins[11] and nucleic acids[12]. This makes clear that the conjugation of biomolecules under click chemistry conditions in aqueous solution is unfavorable for pharmaceutical and biomedical applications.

2.3. Conclusion

Here, we have presented the functionalization of polymersomes by linking poly$(G)_{23}$ ligands to the outer vesicle membrane by the copper catalyzed azide-alkyne click chemistry approach. To determine whether this system is viable for targeting specific cells, poly$(G)_{23}$ modified polymersomes were incubated with activated macrophages, resulting in specific cellular uptake. Even though THP-1 cell uptake results look promising, we were not able to show direct evidence of click conjugation of the ligands to the polymersomes. Furthermore it is questionable whether the use of copper as a catalytic agent is an appropriate option for applications such as drug delivery. In addition, the redox reaction of copper and ascorbate, which is unavoidable for "clicking" the ligands to the polymersomes, induces unwanted cleavage or scission of different biomolecules.

The fluorescently labeled ABA-SRB was characterized in detail by a combined analytic approach using both ^{1}H-NMR and FCS. Both of these methods indicated successful conjugation of SRB acid chloride to ABA-1 polymer by esterification reaction. Such labeled polymers are interesting materials to study the fate of polymersome drug delivery systems *in vivo*, but also e.g. the mixing behavior of different species of amphiphilic molecules in membranes.[13] Further studies are necessary to optimize the covalent modification of ligands to the polymersomes, other promising receptor-ligand interactions have to be screened for optimal uptake and specificity, and ultimately release of biological active molecules has to be accomplished in order to develop a successful polymeric platform for targeted drug delivery.

2.4. References

[1] a) P. Broz, S. M. Benito, C. Saw, P. Burger, H. Heider, M. Pfisterer, S. Marsch, W. Meier and P. Hunziker, *J. Controlled Release* **2005**, *102*, 475-488; b) P. Broz, N. Ben-Haim, M. Grzelakowski, S. Marsch, W. Meier and P. Hunziker, *J. Cardiovasc. Pharmacol.* **2008**, *51*, 246-252; c) N. Ben-Haim, P. Broz, S. Marsch, W. Meier and P. Hunziker, *Nano Lett.* **2008**, *8*, 1368-1373.
[2] J. A. Opsteen, R. P. Brinkhuis, R. L. M. Teeuwen, D. W. P. M. Loewik and J. C. M. van Hest, *Chem. Commun. (Cambridge, U. K.)* **2007**, 3136-3138.
[3] R. Alon, R. Hershkoviz, E. A. Bayer, M. Wilchek and O. Lider, *Eur. J. Immunol.* **1993**, *23*, 893-898.
[4] a) C. Nardin, T. Hirt, J. Leukel and W. Meier, *Langmuir* **2000**, *16*, 1035-1041; b) M. Kumar, M. Grzelakowski, J. Zilles, M. Clark and W. Meier, *Proc. Natl. Acad. Sci. U. S. A.* **2007**, *104*, 20719-20724.
[5] S. Hornig, C. Biskup, A. Graefe, J. Wotschadlo, T. Liebert, G. J. Mohr and T. Heinze, *Soft Matter* **2008**, *4*, 1169-1172.
[6] P. Rigler and W. Meier, *J. Am. Chem. Soc.* **2006**, *128*, 367-373.
[7] O. Stauch, R. Schubert, G. Savin and W. Burchard, *Biomacromolecules* **2002**, *3*, 565-578.
[8] B. Halliwell and J. M. C. Gutteridge, *Methods Enzymol.* **1990**, *186*, 1-85.
[9] S. C. Fry, *Biochem. J.* **1998**, *332*, 507-515.
[10] H. Inoue and M. Hirobe, *Chem. Pharm. Bull.* **1986**, *34*, 1075-1079.
[11] a) T. Miura, S. Muraoka and T. Ogiso, *Chem.-Biol. Interact.* **1992**, *85*, 243-254; b) J. Sereikaite, J. Jachno, R. Santockyte, P. Chmielevski, V.-A. Bumelis and G. Dienys, *Protein J.* **2006**, *25*, 369-378.
[12] S. H. Chiou, *J. Biochem.* **1983**, *94*, 1259-1267.
[13] K. Kita-Tokarczyk, F. Itel, M. Grzelakowski, S. Egli, P. Rossbach and W. Meier, *Langmuir* **2009**, *25*, 9847-9856.

3. Biocompatible functionalization of polymersome surfaces

Stefan Egli[1], Martin G. Nussbaumer[1], Vimalkumar Balasubramanian[1], Mohamed Chami[2], Nico Bruns[1], Cornelia Palivan[1], Wolfgang Meier[1]

[1]Department of Chemistry, University of Basel, Klingelbergstrasse 80, CH- 4056 Basel, Switzerland

[2]Center for Cellular Imaging and Nano Analytics, Biozentrum, University of Basel, Mattenstrasse 26, CH- 4058 Basel, Switzerland

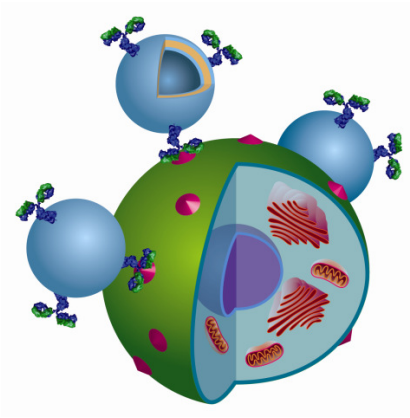

Article online via: http://pubs.acs.org/doi/abs/10.1021/ja110275f

3.1. Introduction

Because of their considerable potential, nanoscale vesicles composed of block copolymers, that is, nanovesicles or polymersomes, continue to draw wide interest in diverse areas of nanotechnology and medical research.[1] In drug delivery, for example, cargo-carrying polymersomes that target and attach to specific cells will lead to greater drug efficacy and to fewer side effects. In the field of biosensing, for example, in ELISA assays, polymersome-antibody conjugates have, due to their high loading capacity, the potential to provide a marked advantage to nanosensor design by providing elevated sensitivities as they report specific attachment to a variety of antigens or to complementary species in general.

To achieve their promised potential in areas such as those indicated above, it is essential that nanovesicles be subject to both precise control of design and functionality, and that they exhibit stability. In drug delivery, nanosize vesicles have been shown to possess far greater load-carrying capacity as compared to simple drug-polymer conjugates for medicinal therapy.[2] This capacity can be used for direct, site-specific transport of hydrophilic drug cargos such as doxorubicin[3] and pravastatin,[4] but also of proteins and nucleic acids.[5] Block copolymer vesicles are leading candidates for such nanosize applications because they feature superior membrane stability, select impermeability, precise chemical control, and a resulting structural versatility that yields a prodigious variety of possible sizes and functionalities.[6] To be effective in drug delivery, nanovesicles must maximize three essential features: (1) membrane impermeability to a hydrophilic cargo to prevent loss of drug;[2] (2) reduced adhesion of protein to the outer surface to avoid elimination by the immune system and thus to increase circulation time in blood;[7] and (3) stable attachment of ligands that specifically target receptors of diseased cells.[8] Polymersomes based on poly-(dimethylsiloxane)-poly(2-methyloxazoline) block copolymers possess these three properties[7, 9] and have therefore been used in ligand-interaction, cell uptake, and nanoreactor studies.[8, 10] To avoid possible interactions between targeting ligands and cargo (drugs, RNA, etc.) and to prevent interference with self-assembly, attachment of ligands must take place on the

outer polymersome surface after vesicle formation. Several approaches to attach ligands have been reported, for example, biotin-streptavidin binding[8, 10a, 11] or azide-alkyne click chemistry.[12] Although these approaches have proven feasible, they exhibit problems in terms of application in therapy, including human intolerance to streptavidin and toxic effects due to possible copper residues used to catalyze the alkyne-azide click reaction. Therefore, the challenge was to devise a biocompatible conjugation chemistry that would lead not only to precise control and stable chemical bonding but also to high selectivity while avoiding disadvantageous reaction additives and catalysts. Various studies have clearly shown that different species such as proteins and nucleic acids can be conjugated to each other by a hydrazinonicotinamide- and a formylbenzamide-counterpart functionality, resulting in a bis-aryl hydrazone bond.[13] This bond is known to be biocompatible,[14] stable and selective,[13a] and thus fulfilled our requirements. The reaction is efficient under mild conditions in aqueous buffer at room temperature.[13a] Moreover, an inherent advantage that follows is the ability to trace and quantify the formation of the covalent link between conjugated species due to the absorbance of the formed bis-aryl hydrazone bond.

To achieve our goal, we synthesized poly(dimethylsiloxane)-*block*-poly(2-methyloxazoline) (PDMS-*b*-PMOXA) diblock copolymers with hydroxyl or piperazyl functionalities at the hydrophilic terminus. The piperazyl group represents a secondary amine, which can react with amine-targeting linkers. These diblock copolymers were used to form polymersomes with surface-exposed amine groups. The number of exposed amines on the surface was controlled by varying the molar percentage of piperazyl functional polymer, as shown by attachment of a succinimidyl ester-activated fluorophore.

We therefore applied this linker chemistry for the first time to form covalent attachment of biological ligands, such as proteins and antibodies, to the surface of polymersomes by means of the bis-aryl hydrazone bond. Using two different polymersome-antibody conjugates, we also demonstrate the specific targeting of biotin-functionalized surfaces as well as *in vitro* targeting of human epidermal growth factor receptor 2 (HER2),[15] which is expressed by SKBR3 human breast cancer cells.

3.2. Results and discussion

3.2.1. Block copolymer synthesis and characterization

We synthesized PDMS-*b*-PMOXA diblock copolymers to provide a polymer with amphiphilic properties suitable for the formation of polymersomes. As compared to the PMOXA-*b*-PDMS-*b*-PMOXA triblock copolymers previously studied by our group,[5c] these diblock copolymers have a more defined composition due to their narrower distribution of molecular weights. Additionally, the unreacted PDMS can be easily separated from the diblock copolymer by centrifugation, which makes purification of the diblock copolymers more efficient.

The polymerization of the hydrophilic PMOXA block from an activated PDMS was carried out as previously reported.[9, 16] In our previous work, the cationic ring-opening polymerization of 2-methyl-2-oxazoline from the preactivated PDMS was ultimately quenched using a KOH solution in methanol, resulting in a hydroxyl-terminated PMOXA block. We obtained a secondary amine-terminated diblock copolymer (AB-NH) using piperazine instead of KOH as the nucleophile to quench the reaction.[17] Additionally, a hydroxyl terminated diblock copolymer (AB-OH) was synthesized. The structures of both are shown in Scheme 5.

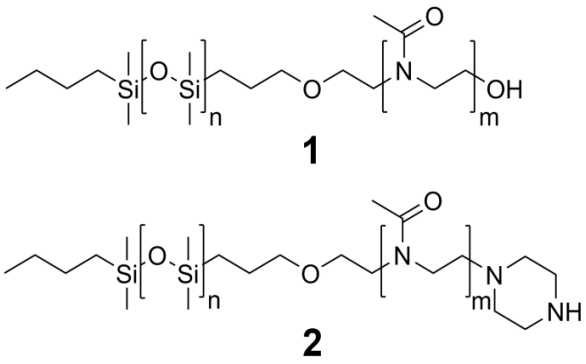

Scheme 5. PDMS-*b*-PMOXA diblock copolymer structures, one having hydroxyl (1, AB-OH) and the other piperazyl functionality (2, AB-NH) at the hydrophilic end

Unreacted piperazine and other low molecular weight impurities were removed by ultrafiltration in ethanol. We calculated the average composition of the block copolymers from ^{1}H NMR integral data, shown in Table 4 and Figures 32-34 (Chapter 8).

Table 4. Specification of the diblock copolymer products. M_w/M_n calculated from M_n^{GPC} and M_w^{GPC}.

Sample	M_n^{GPC} [g mol^{-1}]	M_w^{GPC} [g mol^{-1}]	M_w/M_n [-]	$M_n^{1H\text{-}NMR}$ [g mol^{-1}]	Yield [g; %]
AB-OH	5153	7785	1.51	6139	17.4; 56.7
AB-NH	4518	7506	1.66	6185	8.30; 67.1

Accordingly, the hydroxyl-terminated polymer was shown to be composed of 65 siloxane units and 13 2-methyloxazoline units, and the piperazinyl-terminated polymer is composed of 68 siloxane units and 11 2-methyloxazoline units. The yield of piperazine functional groups was calculated as 82%. These values correspond to a molar mass of 6139 g mol^{-1} for AB-OH and 6185 g mol^{-1} for AB-NH. The polydispersity index M_w/M_n of the polymers was measured by GPC, where calculations were based on polystyrene standards. M_w/M_n of PDMS was found to be 1.10, that of AB-OH was 1.51, and for AB-NH it was 1.66. These values are slightly lower than those of triblock copolymers published previously.[16, 18]

3.2.2. Polymersome formation and characterization

Polymersomes were formed using the film hydration method.[19] We determined the dimensions of the extruded polymersomes by dynamic and static light scattering (DLS, SLS).[20] Corresponding data are shown in Table 5 and as a Guinier plot in Figure 11. From these values, we obtain the ρ-value given as $\rho = R_g/R_h$, which provides information on the internal structure of our particles in solution.[21]

Table 5. Light scattering data of AB-OH and AB-NH in aqueous solution

Polymer	R_h nm	PDI[a]	R_g nm	M_w g mol^{-1}	A_2 mol dm^3 g^{-2}	N_{agg}	ρ-value
AB-OH	96.5	0.12	89.2 ± 0.6	1.66 10^8	5.51 10^{-10}	2.70 10^4	0.92
AB-NH	96.4	0.09	91.6 ± 0.4	6.92 10^7	3.65 10^{-10}	1.12 10^4	0.95

[a]The polydispersity index from lightscattering data represents the error of R_h

Because the ρ-value for an ideal hollow sphere (i.e., vesicle) is 1.0 and for solid spheres is 0.775,[21] the *ρ*-values of our samples, at 0.92 for AB-OH and 0.95 for AB-NH, indicate hollow-sphere morphologies. From the molecular weights of the polymer itself and of its aggregated structures, we calculated the aggregation numbers (N_{agg}) for AB-NH and AB-OH. They agreed well with those of PMOXA-*b*-PMDS-*b*-PMOXA triblock copolymers published previously.[16, 22]

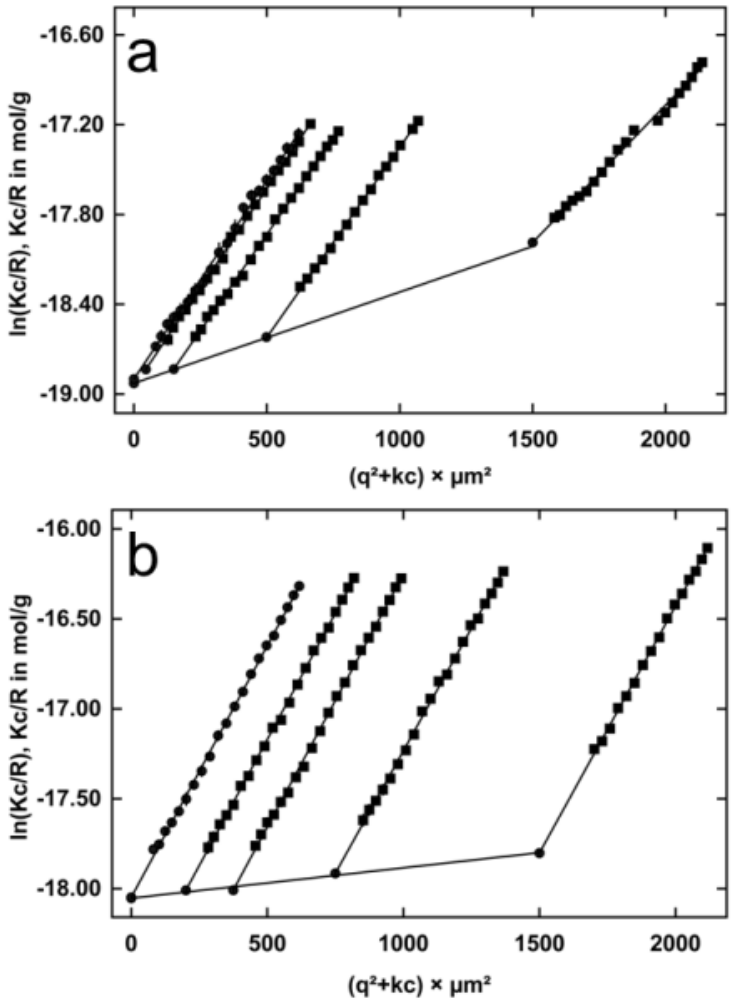

Figure 11. Guinier plots of a) AB-OH and b) AB-NH polymersome solution in water, extrapolated to zero angle and concentration

Transmission electron microscopy (TEM) and cryo-TEM investigations were performed to confirm vesicular structures. Collapsed polymersomes can be seen in the TEM micrograph, and in cryo-TEM images we recognize the polymersome membrane (Figures 12 and 13).

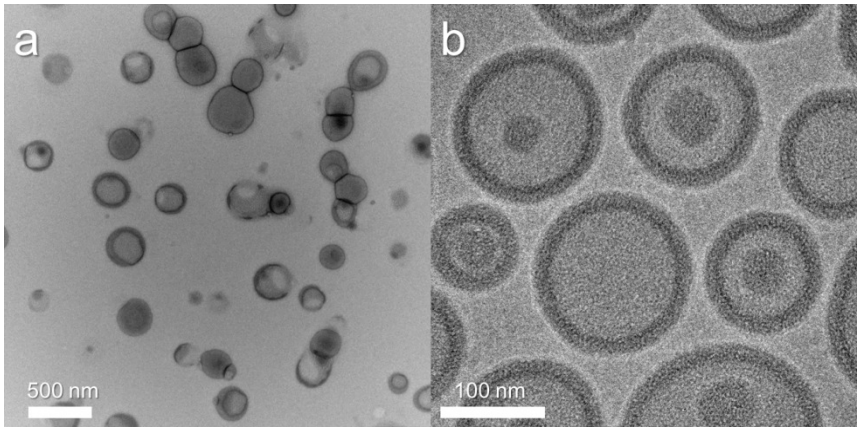

Figure 12. TEM (a) and cryo-TEM (b) micrographs of AB-OH polymersomes after extrusion (0.2 μm) in aqueous solution.

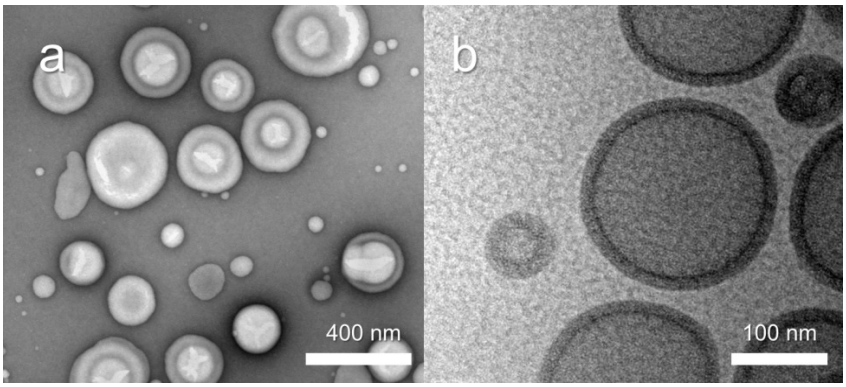

Figure 13. TEM (a) and cryo-TEM (b) micrographs of AB-NH polymersomes after extrusion (0.2 μm) in aqueous solution.

The diameters of polymersomes observed in a cryo-TEM image are, in most cases, smaller than those found in TEM images. The reason for this can be attributed to the preparation of the negative stain TEM sample, which causes drying and thus flattening of the polymersomes, whereas cryo-TEM conserves the native structure because the polymersomes are imaged in the frozen-hydrated state. Inclusions present in some polymersomes are smaller vesicles and micelles. The average membrane thickness of 50 different polymersomes in cryo-TEM images was measured as 15.4 ± 0.7 nm, which is more than 3 times thicker than phospholipid bilayers from liposomes. Thus, we conclude that the relatively thick polymer membrane as well as the inclusions inside the polymersomes (Figure 12b) might explain the small deviation of ρ-values calculated from light scattering data from the ideal ρ-value for vesicles.

3.2.3. Effects on polymersome surface functionalization

Understanding and controlling the binding site density of reactive ligands on polymersome surfaces is of great importance for applications such as targeted drug delivery.[23] To investigate the effects of functional group concentration on polymersome surface modification, we produced different batches of polymersomes consisting of varying molar percentages of the reactive AB-NH and the AB-OH diblock copolymers. Next, a simple fluorescent dye was conjugated to the amine end groups. We decided to use the bright, photostable dye, Alexa Fluor 633 carboxylic acid, activated as succinimidyl ester (A633-NHS), as the ligand for these binding site studies, due to its excellent fluorescence quantum yield and good solubility in aqueous solution. Becausee it was previously shown that such NHS reactive fluorophores bind to secondary amines,[24] we assume that the majority of available AB-NH binding sites are modified after incubation in a large excess of NHS reactive Alexa dye.

Because the NHS group of the fluorophore hydrolyzes quickly in aqueous buffer at higher pH values,[25] an excess of activated dye was required to ensure that accessible amines on the polymersome surface reacted with the ligand within an appropriate time. After complete reaction of polymersomes with A633-NHS, the samples were extensively dialyzed and finally investigated using fluorescence correlation spectroscopy (FCS). In contrast to conventional fluorescence spectroscopy, FCS enables the accurate detection of the diffusion time and brightness of single vesicles.[10a] Diffusion times τ_D = 44 ± 4 μs for freely diffusing A633-NHS and τ_D = 5.7-9.6 ms for polymersome-A633 conjugates were measured. This indicates successful binding of A633-NHS to the polymersomes.

The brightness of the polymersomes, and thus the degree of ligand functionalization on the polymersome surface, was derived from the fluorescence intensity trace. Six samples of each AB-NH mol % were measured to obtain statistical and representative values. By dividing the average polymersome brightness value by the average brightness of a single dye molecule, we obtained the average number of fluorophores per polymersome. In a sample consisting of 100 mol % of AB-OH and 0 mol % of AB-NH polymer, we measured a fluorescence intensity corresponding to 7.6 ± 0.9 fluorophores per polymersome. We

assigned this value to represent unspecific binding of the polyaromatic fluorophore to the polymersome membrane and thus subtracted it from all other values given below. In Figure 14, the interdependence of the average number of fluorophores per polymersome (N_{FP}) and the mole percentage of AB-NH ($x_{n,\ AB\text{-}NH}$) are illustrated.

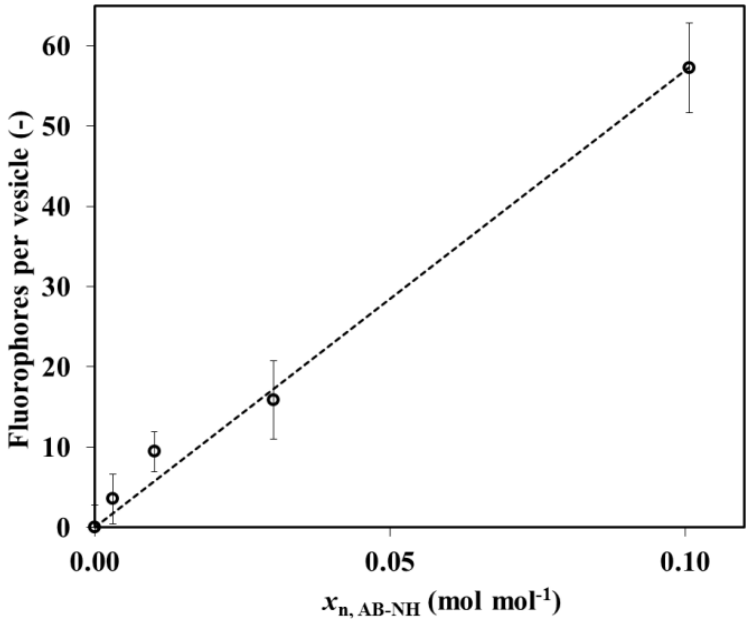

Figure 14. Average number of covalently conjugated fluorophore molecules per polymersome versus the molar percentage of AB-NH. The data were corrected for unspecific adsorption of fluorophores.

Values from 0.3 to 10 mol % AB-NH fit a linear function well, which is shown by NFP = 569.2$x_{n,\ AB\text{-}NH}$ (R^2 = 0.991), quantitatively describing the number of fluorophores per polymersome. The slope in Figure 14 reflects the number of fluorophores per vesicle as a function of the molar ratio of AB-NH in the polymersome composition, but does not contain any information on the variation of the initial fluorophore or polymersome concentration (before conjugation) in solution. Errors in fluorescence intensity (Figure 14) originate basically with polymersome size distribution. A saturation of dye attachment to the polymersome was observed at higher molar percentages of AB-NH, from 10 to 100 mol %. This saturation can be explained by steric hindrance by dye molecules that were already attached to the polymersome surface. Additionally, we assume that at higher $x_{n,\ AB\text{-}NH}$ phase separation of dye-modified and non-modified block copolymers in the membrane occurs,[26] which enhances steric hindrance to further dye conjugation and causes fluorescence quenching.[27] This assumption is supported by the observation of some large aggregates (with diameters up to 10 µm) found in laser

scanning micrographs (Figure 15) and indicates a destabilization and thus aggregation of the original self-assemblies. Because the illuminated sampling volume is rather small, the size-limiting criterion for FCS measurements being less than 1 μm^3,[28] as compared to those aggregates, it was not possible to obtain representative FCS results for samples containing more than 10 mol % AB-NH.

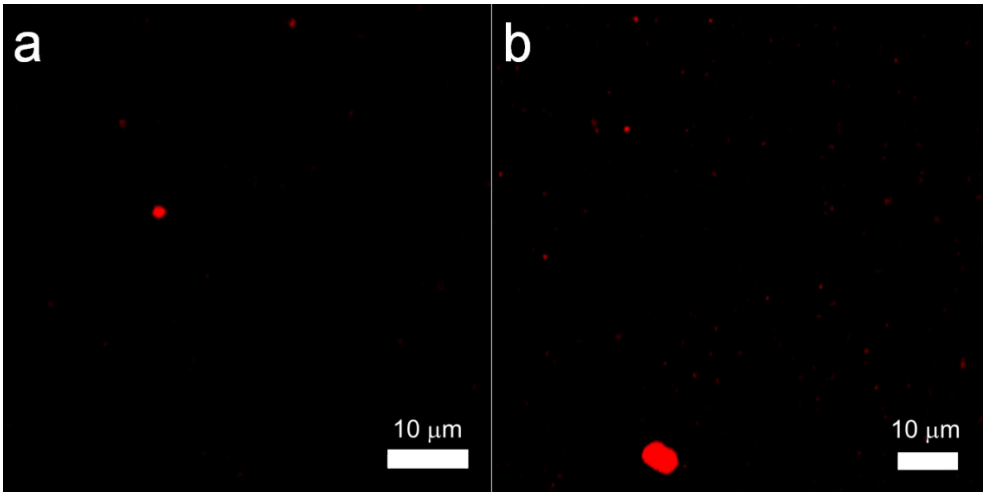

Figure 15. Laser scanning micrograph of polymersomes consisting of (a) 30 mol % and (b) 100 mol % AB-NH, after reaction with Alexa Fluor 633 NHS and dialysis.

The yield of the conjugation reaction can be estimated from the equation above, and the N_{agg} value can be obtained from light scattering data. N_{agg} was measured to be 11200 diblock copolymer molecules per polymersome. Thus, about 5600 of them are in the outer part of the polymersome bilayer membrane. In the linear range up to 10 mol % of AB-NH, the conjugation efficiency is 10%. At first view, this conjugation efficiency might be considered poor. However, by taking into account that a large excess of reagent was used and that some of the functional groups are presumably concealed in the hydrophilic corona of the polymersome, this conjugation efficiency in fact represents the surface-accessible NH-groups.

A further argument in favor of covalent binding of A633-NHS to AB-NH polymer is given by FCS diffusion measurements of polymersomes dried by lyophilization and redissolved in ethanol, in which polymersomes disassemble into individual diblock copolymers. Thus, we determined the τ_D of free A633-NHS and of the AB-NH-A633 conjugates. For A633-NHS (M≈1200 g mol^{-1}, 5.3 nM), we measured a τ_D of 91.8 ± 1.0 μs, and for the AB-NH-A633 conjugate (0.1 μg mL^{-1}), a τ_D of 155.8 ± 2.2 μs was found, which results in a

theoretical molecular weight for the AB-NH-A633 conjugate of 5866 ± 248 g mol^{-1}. This molecular weight agrees well with M_n of AB-NH diblock copolymer obtained from ^{1}H NMR measurements and indicates successful covalent bonding. FCS diffusion measurements of a mixture of A633-NHS (5.3 nM) and AB-OH (0.1 μg mL^{-1}) in ethanol were performed to ensure that the fluorophore was attached exclusively by covalent bonds and not by nonspecific interactions with AB-NH. The resulting τ_D of 104.6 ± 1.4 μs corresponds to a theoretical molecular weight of 1775 ± 71 g mol^{-1}, which allowed us to assume that only a few, nonspecific, noncovalent bindings occurred. These experiments point out that our polymersomes were covalently functionalized with NHS reactive fluorophores in aqueous solution in a controlled, reproducible manner. However, because we assumed that phase separation occurs at a higher molar percentage of modified AB-NH (≥ 10 mol %), we ultimately used polymersomes that contained 3 mol % AB-NH in further conjugation reactions.

3.2.4. Covalent attachment of enhanced yellow fluorescent protein to polymersomes

Simple and efficient attachment of ligands to preformed membranes is of great importance. For drug delivery purposes, not only is the attachment of relatively small sugars and peptides as targeting moieties of interest, but so is the conjugation of large proteins and antibodies to the polymersome surface. We decided to use a conjugation strategy that resulted in a stable and quantifiable bis-aryl hydrazone bond based on two complementary heterobifunctional linkers[13a] (Scheme 6).

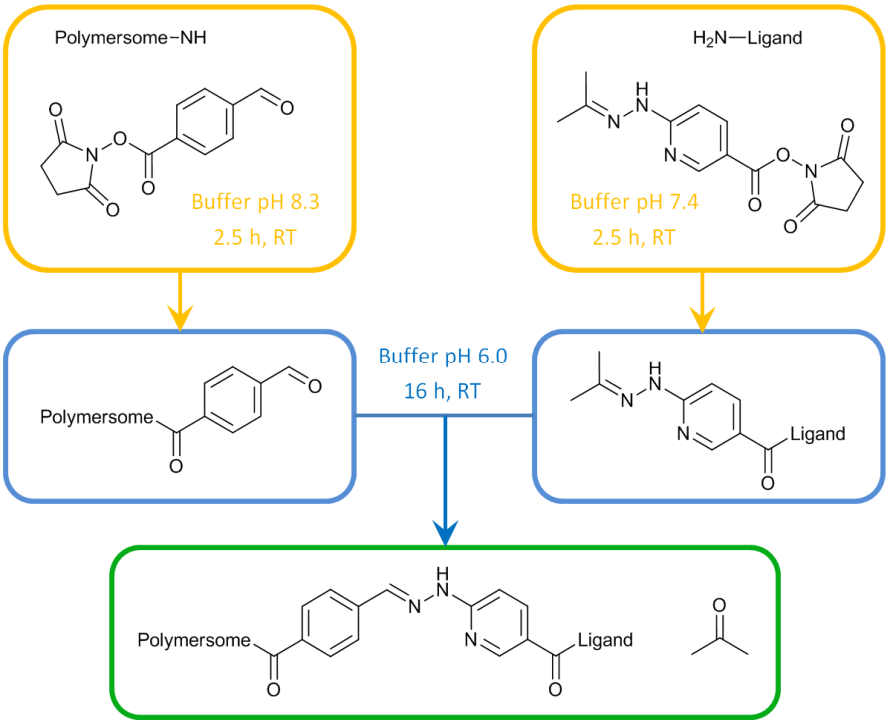

Scheme 6. Modification of polymersome with succinimidyl-4-formyl benzoate (NHS-4FB) and of ligands (e.g., protein or antibody) with succinimidyl-6-hydrazinonicotinate acetone hydrazone (NHS-HyNic). In a final step the 4FB-modified polymersome and the HyNic-modified ligand conjugate specifically and quantitatively resulting in a covalent and stable bis-aryl hydrazone bond.

As compared to other conjugation techniques, this method works under mild conditions in aqueous buffers at pH values between 4.5 and 8.0; more importantly, it does not require the use of toxic catalysts such as, for example, Cu(I), which is required for azide-alkyne click chemistry in aqueous solution.[12, 29] In previous studies, this conjugation chemistry was used to covalently attach biomolecules such as antibodies and oligonucleotides to each other.[13a, 30] However, to our knowledge, it has not been used previously to modify polymeric self-assemblies and, in particular, not for the modification of block copolymer membranes.

Because of its fluorescent properties, eYFP was used as a model protein ligand in our experiment. As outlined in Scheme 6, polymersomes were modified with succinimidyl 4-formylbenzoate (NHS-4FB), and the ligand was modified with succinimidyl 6-hydrazinonicotinate acetone hydrazone (NHS-HyNic). We did not modify the polymers with 4FB before the self-assembly to polymersomes, to avoid possible interactions between the fluorescent dye and the 4FB group. Also, we kept the percentage of reactive AB-NH polymer low, at 3 mol %, to avoid the attachment of more than one polymersome

to eYFP. The 4FB functionalization of polymersomes was confirmed by a colorimetric reaction with 2-hydrazinopyridine and by gel permeation chromatography of the polymer, as shown in Figure 16.

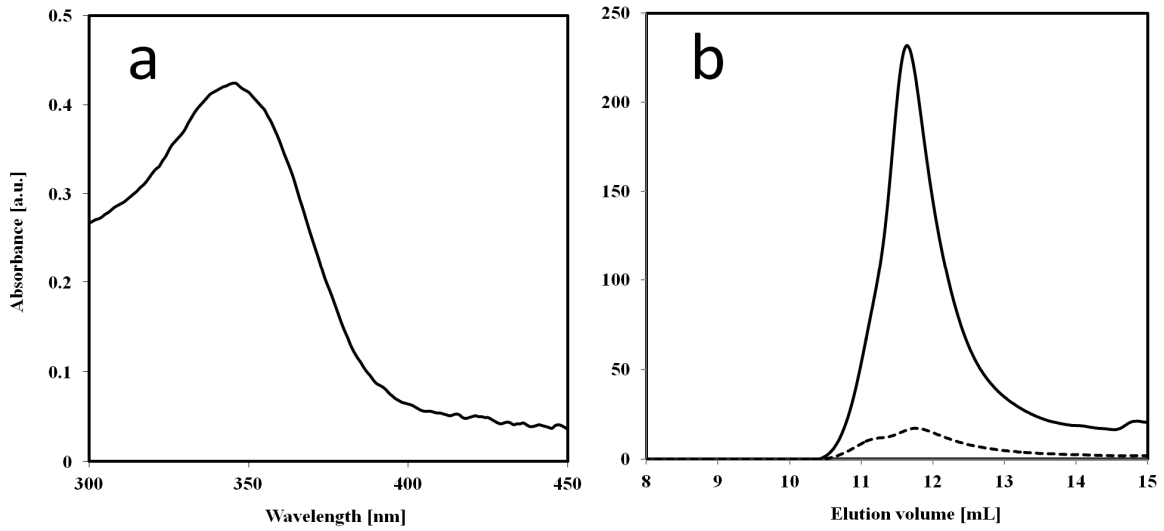

Figure 16. (a) UV-vis spectrograph of 4-formylbenzoate modified polymersomes after dialysis reacted with 4-hydrazinonicotinate acetone hydrazone (λ_{max} 350 nm) (b) Gel permeation chromatogram of AB-NH before (dashed line) and after (solid line) conjugation of 4FB and reaction with 2-hydrazinopyridine (UV detection at 354 nm).

Functional succinimidyl 4-hydrazinonicotinate acetone hydrazone (S-HyNic) groups, being complementary reactive parts to the 4FB-modified polymersomes, were introduced to the eYFP.[13a] The two conjugation partners, the polymersomes and eYFPs, were incubated in phosphate buffer, pH 6.0, for 16 h. The absorption of the resulting bis-aryl hydrazone bond between the polymersome and eYFP was below the detection limit, due to increased scattering of the polymersomes at lower wavelength, and could therefore not be detected via ultraviolet-visible (UV-vis) spectroscopy.

Because eYFP, with its almost perfect cylindrical shape of 42 Å by 24 Å,[31] is smaller by an order of magnitude than polymersomes having an average diameter of 193 nm, we used FCS as a suitable method to investigate the binding of proteins to polymersomes.[10a] The average τ_D for free eYFP in solution was found to be 93 ± 3 μs, and for eYFP-polymersome conjugates it was 3.98 ± 0.57 ms. This difference in τ_D is clearly shown in the shift of the FCS autocorrelation curves (Figure 17).

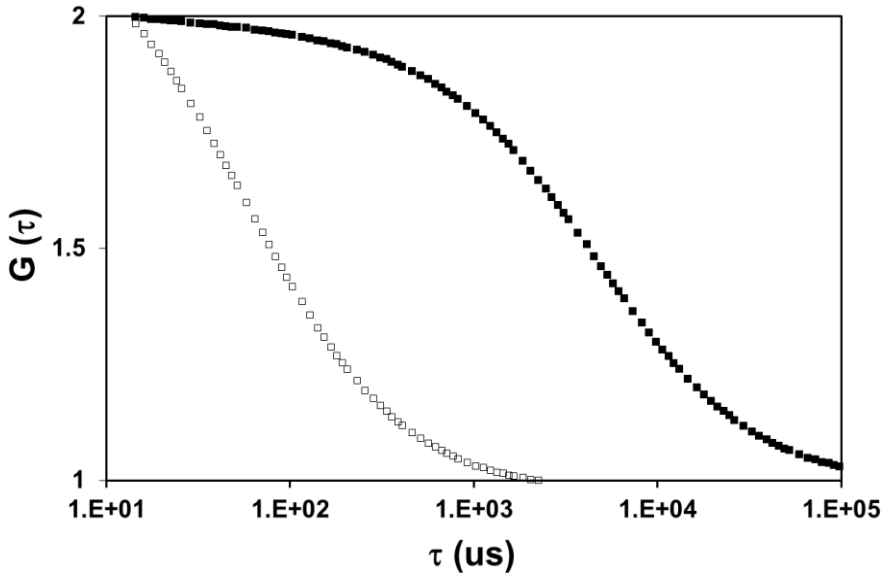

Figure 17. Fitted FCS autocorrelation curve of free eYFP (▫) and polymersome-eYFP conjugate (▪)

The FCS autocorrelation curve of the eYFP-polymersome conjugate was analyzed by a nonlinear least-squares fitting program,[10a] assuming one population of fluorescent species. This indicates binding of eYFP to the polymersome. Using the τ_D for eYFP and for polymersome-eYFP conjugates along with the known diffusion coefficient D of fluorescent GFPs and YFPs,[32] the theoretical R_h of the polymersome-eYFP conjugate was calculated using the relationship between τ_D and D from FCS[10a] and the Stokes-Einstein equation. Assuming, in a first approximation, the eYFP and the polymersomes to be spherical, we calculated an R_h of 2.3 ± 0.1 nm for eYFP, and 98.3 ± 14.1 nm for the eYFP-polymersome conjugate. A diameter of eYFP-polymersome conjugates of approximately 200 nm is further evidence for covalent attachment of eYFP to the polymersomes. Polymersomes without benzaldehyde functional groups on their surfaces did not conjugate to eYFP (τ_D of 93 ± 3 μs). We calculated the average brightness of freely diffusing eYFP and compared it to the brightness of eYFP-polymersome conjugates. An average number of 5 eYFP per polymersome was determined, which is significantly lower than the number of, for example, noncovalently bound streptavidin to biotin-modified polymeric vesicles.[10a] As shown above, A633-NHS-modified polymersomes consisting of the same molar percentage of AB-NH had, on average, 17 covalently attached dye molecules per polymersome. The number of eYFP ligands was found lower by a factor of 3. This could be due to the difference in sizes of the protein and fluorescent dye.

3.2.5. Polymersome-antibody conjugates for specific surface targeting

Because of their specific, strong binding to proteins and haptens, antibodies are ideal candidates as targeting ligands.[33] We functionalized antibodies with HyNic moieties and attached them covalently to 4FB modified polymersomes, similar to the method as described for polymersome-eYFP conjugates. In the first trial, HyNic-modified antibiotin IgG was attached to 4FB-modified polymersomes consisting of 3 wt % AB-NH and containing the fluorescent dye Alexa Fluor 647 maleimide (A647-M) encapsulated inside the polymersome cavity. The polymersome-antibody conjugates were incubated on a glass slide, which was previously patterned with biotinylated bovine serum albumin (BSA) by a microcontact printing process.[34] To avoid unspecific binding, the glass surface of the pattern interspaces was passivated with nonbiotinylated BSA. The surface was imaged by confocal laser scanning microscopy. As shown in Figure 18, the polymersome-antibody conjugates bonded specifically to the biotinylated pattern printed on the glass slide. As control experiments, polymersome-anti-RBC-IgG conjugates were synthesized and applied to patterned surfaces (Figure 18c). No specific binding of the polymersomes to biotinylated surface area was observed.

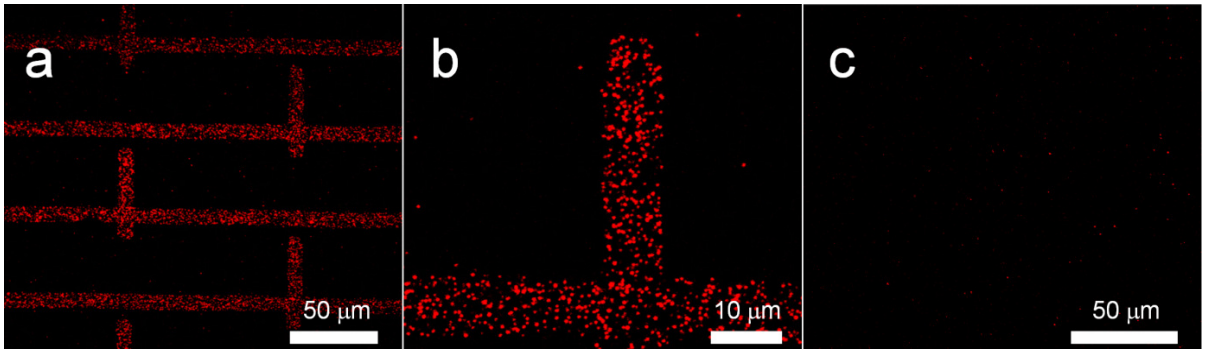

Figure 18. CLSM micrographs of a) A647-M containing polymersomes with covalently attached antibiotin IgG, immobilized on a biotin-BSA pattern; b) close-up view of a); and c) A647-M containing polymersomes with covalently attached anti-erythrocyte IgG conjugates.

The packing density of immobilized polymersomes in Figure 18a+b on the glass substrate was sufficiently low to be able to recognize dots that possibly represent single immobilized polymersomes. This is due to the fact that every antibody exhibits only three HyNic functionalities on average, which could also be positioned at the active antibody binding site.[35] Therefore, some antibodies might be covalently attached, with

their active binding site facing the polymersome surface, and thus might not be able to bind to the biotin-BSA pattern presented on the glass surface. Their specific antigen targeting properties and their high fluorescence intensities render polymersome-antibody conjugates ideal candidates for biosensor applications such as enzyme-linked immunosorbent assays (ELISA). When employing conventional antibody-dye conjugates, an optimum in labeling should be found between underconjugation, resulting in a fluorescence signal that is too low, and overconjugation, resulting in a change in antigen-binding characteristics and potentially inactivating the antibody completely with fluorophores.[36] In comparison to those conventional labeled antibodies, the sensitivity of ELISA should be increased several-fold by introducing polymersome-antibody conjugates, due to their high loading capacity with fluorescent molecules.

3.2.6. Targeted uptake of polymersome-trastuzumab conjugates

Targeted polymersomes have been shown to be ideal candidates to transport drugs specifically to diseased cells.[8] Because conjugates of trastuzumab with cytotoxic agents have been proven to specifically target HER2-positive breast cancer cells and considerably improve the therapeutic index,[37] we decided to use polymersome-trastuzumab conjugates for cell targeting. SKBR3 cells incubated for 2 h with sulforhodamine-B-containing polymersome-trastuzumab conjugates and sulforhodamine-B-containing polymersomes without trastuzumab, as the negative control, were analyzed for qualitative uptake with CLSM (Figure 19).

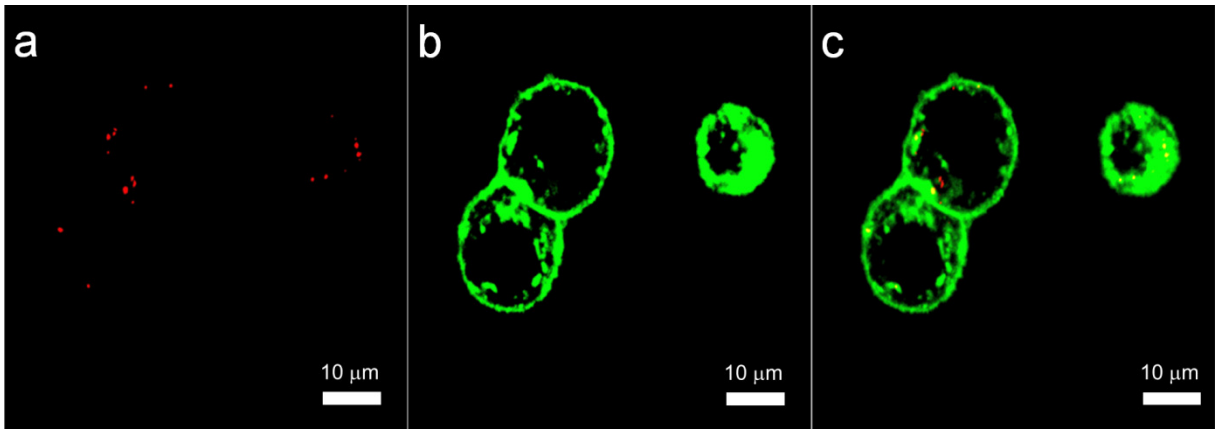

Figure 19. CLSM micrograph of SKBR3 cells after 2 h incubation with polymersome-trastuzumab conjugate, which encapsulated sulforhodamine B. a) Polymersome-trastuzumab located intracellularly and in the cell membrane, shown in the red channel; b) SKBR3 cell membrane stained with Deep Red, shown in the green channel; and c) overlay of the micrographs from the red and green channels.

To distinguish the extracellular and intracellular region of the cells, the cell membrane was stained with Deep Red. We observed polymersome-trastuzumab conjugates located intracellularly, and few were present in the cell membrane (Figure 19). Very low uptake of polymersomes without trastuzumab as compared to polymersome-trastuzumab conjugates was observed under similar conditions. This clearly indicates a fast and specific targeted uptake of polymersome-trastuzumab conjugates in SKBR3 cells. The targeting effect mediated by trastuzumab to HER2 receptors expressed on SKBR3 cell is significant at short incubation times, for example, 2 h. For a long incubation time (24 h),

the difference between polymersomes with and without trastuzumab was not distinguishable, due to the nonspecific uptake of polymersomes without trastuzumab.

The quantitative uptake of sulforhodamine B containing polymersome-trastuzumab conjugates in SKBR3 cells was analyzed with flow cytometry. The intensity of the fluorescence channel measured for cells after 1 h incubation with polymersome-trastuzumab conjugates was 8%, and it increased up to 13% after 2 h incubation, while for polymersomes without trastuzumab this was less than 3% even after 2 h. This supports the specific uptake of the polymersome-trastuzumab conjugates as being due to the presence of trastuzumab as the targeting ligand. By subtracting the auto fluorescence of cells, an uptake of polymersome-trastuzumab conjugates of approximately 10% was calculated for 2 h incubation (Figure 20).

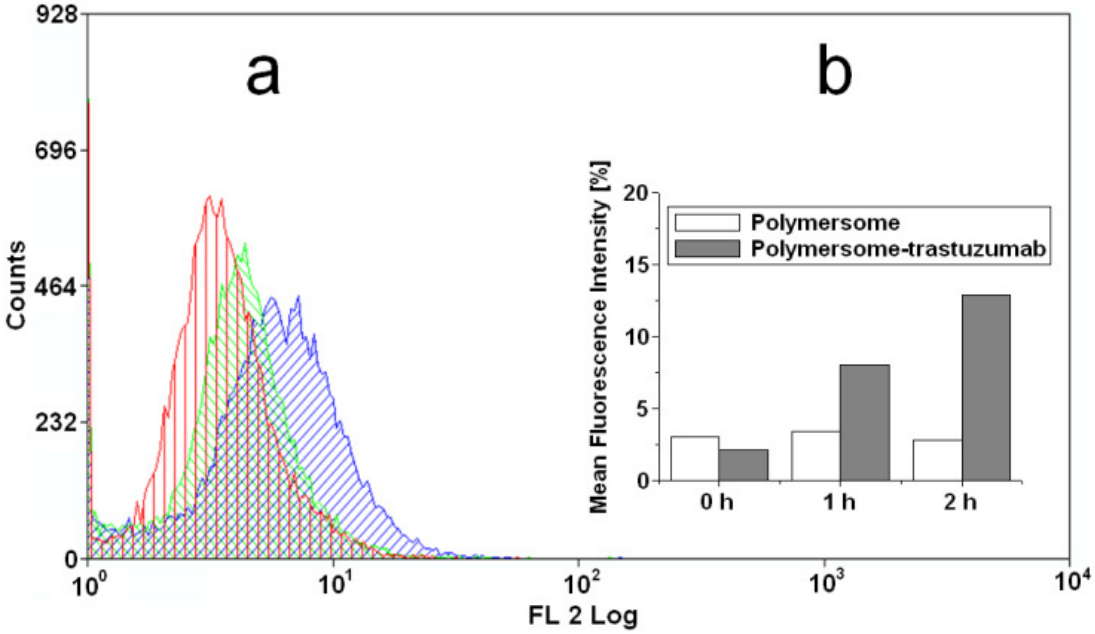

Figure 20. Flow cytometry analysis. (a) Histogram of SKBR3 cells (red), SKBR3 cells incubated 2 h with sulforhodamine-B-containing polymersomes (green), and SKBR3 cells incubated 2 h with sulforhodamine-B-containing polymersome-trastuzumab conjugate (blue); and (b) mean fluorescent intensity of SKBR3 cells, incubated with sulforhodamine-B-containing polymersomes with and without conjugated trastuzumab for 1 and 2 h.

As expected, uptake of polymersome-trastuzumab conjugates is significantly faster than that of polymersomes without trastuzumab, in agreement with other reported studies.[38] Besides, the uniform shift of the histogram in the fluorescent channel clearly indicates that the uptake is evenly distributed in the cells.

3.2.7. In vitro cell proliferation inhibition activity of polymersome-trastuzumab conjugates

Trastuzumab is known to inhibit proliferation of SKBR3 cells due to its specific binding to the HER2 receptor on the surface of the cells.[39] Therefore, the effect of polymersome-trastuzumab conjugates on cell proliferation was studied spectroscopically via the formation of a colored formazan product when MTS was biologically reduced by metabolically active cells.[40] After 24 h incubation, while polymersomes without trastuzumab induced an inhibition of 7-11%, polymersome-trastuzumab conjugates inhibited the proliferation in the range of 14-21% (Figure 21).

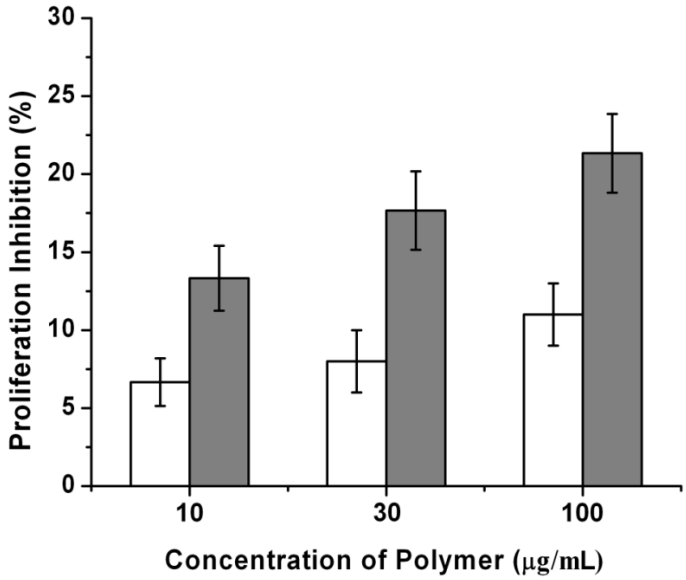

Figure 21. MTS assay. Proliferation inhibition effect on SKBR3 cells with different concentrations of polymersome with (gray) and without trastuzumab (white) after 24 h incubation.

Under similar conditions, polymersome-trastuzumab conjugates were able to inhibit proliferation of SKBR3 by a factor of almost 2. In addition, polymersome-trastuzumab conjugates inhibited cell proliferation in a dose-dependent manner (Figure 21). These findings allow us to consider that the conjugation to the polymersome did not affect the functionality of the antibody. The inhibiting effect of polymersome-trastuzumab conjugates as compared to polymersomes can be further improved by modulation of the

number of trastuzumab per polymersome, and in this respect further experiments are ongoing to optimize the system.

3.2.8. Conclusion

The goal of this work was to design and implement a simple, efficient, and universal method to covalently attach biological ligands, such as antibodies, to polymersomes to provide a platform for targeting experiments. New amphiphilic PDMS-*b*-PMOXA diblock copolymers comprising hydroxyl or amine functionalities at their hydrophilic ends were thereby synthesized and characterized. We were able to control covalent attachment of NHS-activated fluorescent dye to polymersomes in aqueous buffer by systematically varying the molar percentage of AB-NH in the polymersome. Polymersomes and ligands were modified with complementary functionalities (4FB and HyNic) to attach macromolecular ligands, such as eYFP or antibodies, to the polymersome surface. Successful conjugation of eYFP to polymersomes was proven by fluorescence diffusion measurements. In a subsequent step, we attached HyNic-modified antibodies to polymersomes that were subsequently used to target selected antigens.

With potential applications such as immunoassays (e.g. ELISA) in mind, polymersome antibiotin-IgG conjugates were shown to specifically target biotin-patterned glass surfaces with a virtual absence of nonspecific binding. In addition, polymersome-trastuzumab conjugates showed specific adherence to the HER2 receptor of SKBR3 breast cancer cells, as demonstrated by LSM imaging and FACS experiments. The effect of polymer concentration and incubation times on proliferation of cells was established via the MTS assay; polymersomes exhibited no significant toxicity. We do not expect any toxic effect due to the bis-aryl hydrazone bond, because it was shown elsewhere that PEGylated polyamidoamine dendrimers with bis-aryl hydrazone linkages induced no obvious cytotoxic response in HN12 tumor cells over a period of 48 h.[41] In contrast to, for example, copper-catalyzed alkyne-azide click chemistry, all procedures here, from polymersome formation to ligand attachment, can be carried out under mild, biocompatible conditions. This makes this system applicable to therapeutic application *in vivo*. However, further investigations on the influence of the packing density of bulky,

macromolecular ligands on the polymersome surface are ongoing. These should enhance our understanding of the polymersome-ligand conjugate attachment and uptake in cells, and thus lead to greater control.

In a nutshell, this polymersome-ligand platform, based on bis-aryl hydrazone conjugation chemistry that allows multifaceted and stable attachment of targeting ligands (e.g. antibodies), presents new opportunities to make immunoassays more sensitive and drug administration more effective.

3.3. References

[1] a) I. F. Uchegbu, *Expert Opin. Drug Delivery* **2006**, *3*, 629-640; b) V. Balasubramanian, O. Onaca, R. Enea, D. W. Hughes and C. G. Palivan, *Expert Opin. Drug Delivery* **2010**, *7*, 63-78.
[2] S. Litvinchuk, Z. Lu, P. Rigler, T. D. Hirt and W. Meier, *Pharm. Res.* **2009**, *26*, 1711-1717.
[3] F. Ahmed, R. I. Pakunlu, A. Brannan, F. Bates, T. Minko and D. E. Discher, *J. Controlled Release* **2006**, *116*, 150-158.
[4] P. Broz, N. Ben-Haim, M. Grzelakowski, S. Marsch, W. Meier and P. Hunziker, *J. Cardiovasc. Pharmacol.* **2008**, *51*, 246-252.
[5] a) D. E. Discher, P. Photos, F. Ahmed, R. Parthasrathy and F. S. Bates, *Biomedical Aspects of Drug Targeting* **2002**, pp. 459-471; b) D. H. Levine, P. P. Ghoroghchian, J. Freudenberg, G. Zhang, M. J. Therien, M. I. Greene, D. A. Hammer and R. Murali, *Methods (San Diego, CA, U. S.)* **2008**, *46*, 25-32; c) O. Onaca, R. Enea, D. W. Hughes and W. Meier, *Macromol. Biosci.* **2009**, *9*, 129-139.
[6] D. E. Discher and A. Eisenberg, *Science (Washington, DC, U. S.)* **2002**, *297*, 967-973.
[7] R. Konradi, B. Pidhatika, A. Muehlebach and M. Textor, *Langmuir* **2008**, *24*, 613-616.
[8] P. Broz, S. M. Benito, C. Saw, P. Burger, H. Heider, M. Pfisterer, S. Marsch, W. Meier and P. Hunziker, *J. Controlled Release* **2005**, *102*, 475-488.
[9] M. Kumar, M. Grzelakowski, J. Zilles, M. Clark and W. Meier, *Proc. Natl. Acad. Sci. U. S. A.* **2007**, *104*, 20719-20724.
[10] a) P. Rigler and W. Meier, *J. Am. Chem. Soc.* **2006**, *128*, 367-373; b) F. Axthelm, O. Casse, W. H. Koppenol, T. Nauser, W. Meier and C. G. Palivan, *J. Phys. Chem. B* **2008**, *112*, 8211-8217.
[11] a) N. Ben-Haim, P. Broz, S. Marsch, W. Meier and P. Hunziker, *Nano Lett.* **2008**, *8*, 1368-1373; b) J. J. Lin, P. P. Ghoroghchian, Y. Zhang and D. A. Hammer, *Langmuir* **2006**, *22*, 3975-3979; c) G. P. Robbins, R. L. Saunders, J. B. Haun, J. Rawson, M. J. Therien and D. A. Hammer, *Langmuir* **2010**, *26*, 14089-14096.
[12] a) J. A. Opsteen, R. P. Brinkhuis, R. L. M. Teeuwen, D. W. P. M. Loewik and J. C. M. van Hest, *Chem. Commun. (Cambridge, U. K.)* **2007**, 3136-3138; b) S. F. M. van Dongen, M. Nallani, J. J. L. M. Cornelissen, R. J. M. Nolte and J. C. M. van Hest, *Chem.--Eur. J.* **2009**, *15*, 1107-1114.
[13] a) N. Bruns, K. Pustelny, L. M. Bergeron, T. A. Whitehead and D. S. Clark, *Angew. Chem., Int. Ed.* **2009**, *48*, 5666-5669; b) D. M. Hartmann, M. Heller, S. C. Esener, D. Schwartz and G. Tu, *J. Mater. Res.* **2002**, *17*, 473-478; c) Y. Chen, J. Aveyard and R. Wilson, *Chem. Commun. (Cambridge, U. K.)* **2004**, 2804-2805; d) X.-b. Zhong, R. Reynolds, J. R. Kidd, K. K. Kidd, R. Jenison, R. A. Marlar and D. C. Ward, *Proc. Natl. Acad. Sci. U. S. A.* **2003**, *100*, 11559-11564; e) G. Steinberg-Tatman, M. Huynh, D. Barker and C. Zhao, *Bioconjugate Chem.* **2006**, *17*, 841-848.
[14] G. F. Walker, C. Fella, J. Pelisek, J. Fahrmeir, S. Boeckle, M. Ogris and E. Wagner, *Mol. Ther.* **2005**, *11*, 418-425.
[15] J. Baselga, *Eur. J. Cancer* **2001**, *37*, S18-S24.
[16] C. Nardin, T. Hirt, J. Leukel and W. Meier, *Langmuir* **2000**, *16*, 1035-1041.
[17] T. B. Bonne, K. Luedtke, R. Jordan, P. Stepanek and C. M. Papadakis, *Colloid Polym. Sci.* **2004**, *282*, 833-843.

[18] a) C. Nardin, M. Winterhalter and W. Meier, *Langmuir* **2000**, *16*, 7708-7712; b) K. Kita-Tokarczyk, F. Itel, M. Grzelakowski, S. Egli, P. Rossbach and W. Meier, *Langmuir* **2009**, *25*, 9847-9856.
[19] G. Battaglia and A. J. Ryan, *J. Phys. Chem. B* **2006**, *110*, 10272.
[20] A. J. Jin, D. Huster, K. Gawrisch and R. Nossal, *Eur. Biophys. J.* **1999**, *28*, 187-199.
[21] O. Stauch, R. Schubert, G. Savin and W. Burchard, *Biomacromolecules* **2002**, *3*, 565-578.
[22] K. Kita-Tokarczyk, J. Grumelard, T. Haefele and W. Meier, *Polymer* **2005**, *46*, 3540-3563.
[23] a) A. L. Martin, B. Li and E. R. Gillies, *J. Am. Chem. Soc.* **2009**, *131*, 734-741; b) R. Stahn and R. Zeisig, *Tumor Biol.* **2000**, *21*, 176-186.
[24] a) G. W. Cline and S. B. Hanna, *J. Am. Chem. Soc.* **1987**, *109*, 3087-3091; b) H. J. Gruber, G. Kada, B. Pragl, C. Riener, C. D. Hahn, G. S. Harms, W. Ahrer, T. G. Dax, K. Hohenthanner and H. G. Knaus, *Bioconjug Chem* **2000**, *11*, 161-166.
[25] Y. Nojima, K. Iguchi, Y. Suzuki and A. Sato, *Biol. Pharm. Bull.* **2009**, *32*, 523-526.
[26] D. A. Christian, A. Tian, W. G. Ellenbroek, I. Levental, K. Rajagopal, P. A. Janmey, A. J. Liu, T. Baumgart and D. E. Discher, *Nat. Mater.* **2009**, *8*, 843-849.
[27] G. Duportail, *Springer Ser. Fluoresc.* **2005**, *3*, 133-149.
[28] K. Starchev, J. Zhang and J. Buffle, *J. Colloid Interface Sci.* **1998**, *203*, 189-196.
[29] C. E. Evans and P. A. Lovell, *Chem. Commun. (Cambridge, U. K.)* **2009**, 2305-2307.
[30] I. A. Kozlov, P. C. Melnyk, K. E. Stromsborg, M. S. Chee, D. L. Barker and C. Zhao, *Biopolymers* **2004**, *73*, 621-630.
[31] T. D. Craggs, *Chem. Soc. Rev.* **2009**, *38*, 2865-2875.
[32] Z. Petrasek and P. Schwille, *Biophys. J.* **2008**, *94*, 1437-1448.
[33] R. P. Patel, G. Patel and N. A. Patel, *Pharma Rev.* **2008**, *6*, 144-146,148-149.
[34] E. Delamarche, *Chimia* **2007**, *61*, 126-132.
[35] A. A. Wakankar, M. B. Feeney, J. Rivera, Y. Chen, M. Kim, V. K. Sharma and Y. J. Wang, *Bioconjugate Chem.* **2010**, *21*, 1588-1595.
[36] S. Vira, E. Mekhedov, G. Humphrey and P. S. Blank, *Anal. Biochem.* **2010**, *402*, 146-150.
[37] B. Hughes, *Nat. Rev. Drug Discovery* **2010**, *9*, 665-667.
[38] S. C. Wuang, K. G. Neoh, E.-T. Kang, D. W. Pack and D. E. Leckband, *Biomaterials* **2008**, *29*, 2270-2279.
[39] K. E. Longva, N. M. Pedersen, C. Haslekas, E. Stang and I. H. Madshus, *Int. J. Cancer* **2005**, *116*, 359-367.
[40] G. Malich, B. Markovic and C. Winder, *Toxicology* **1997**, *124*, 179-192.
[41] Q. Yuan, W. A. Yeudall and H. Yang, *Biomacromolecules* **2010**, *11*, 1940-1947.

4. Cationic poly(dimethylsiloxane) vesicles

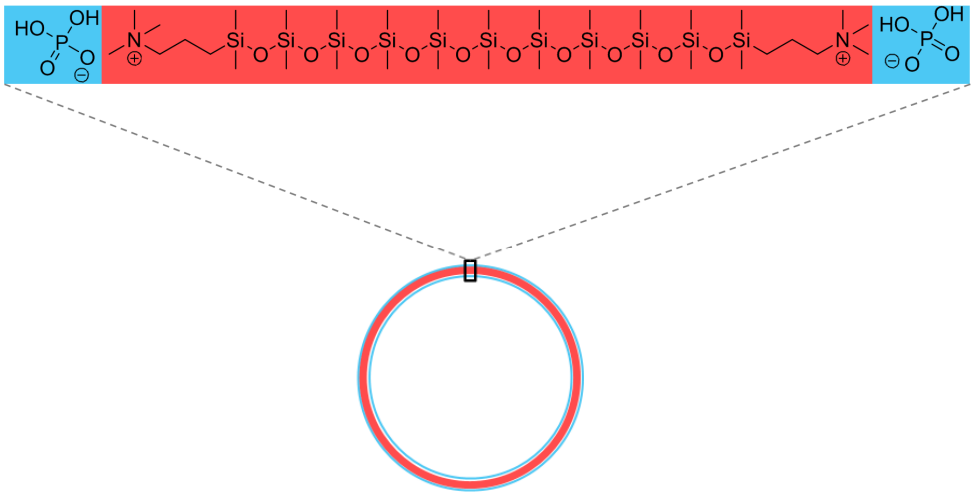

4.1. Introduction

The classical approach to predict amphiphilic properties in polymers is via the construction of block copolymers comprising hydrophilic and hydrophobic blocks.[1] In most reported cases, block copolymers have simple linear architectures.[1] By introducing branched or dendritic structures, by varying the length of the hydrophilic and the hydrophobic blocks or simply by using different kinds of polymers, one can influence the self-assembly in aqueous solution. It has been shown that vesicles based on flexible, hydrophobic poly(dimethylsiloxane) (PDMS) are almost impermeable to hydrophilic substances[2], what makes them interesting candidates for drug delivery purposes as well as for nanotechnology. In addition, by the reconstitution of membrane proteins in PMOXA-*b*-PDMS-*b*-PMOXA membranes, such polymers mimic natural lipid membranes and selectively transport hydrophilic substances.[3]

In contrast to polymers, lipids are built of short hydrophobic alkyl chains with hydrophilic charged or non-charged head groups. Additionally, they have well-defined chain lengths, whereas polymers, in general, have a certain molecular weight distribution, which impairs the reproducibility of the self-assembly. One drawback of lipid membranes is their low

stability and uncontrollable permeability. Presently, synthetic cationic phospholipids are the most widely used non-viral gene carriers.[4] They form stable complexes with polyanionic nucleic acids – so called lipoplexes – which have been proven to be good transfection agents.[5]

Special species that are related to lipids are bipolar amphiphiles, so called bolaform amphiphiles or bolaamphiphiles.[6] In most cases they consist of alkyl chains as hydrophobic part and two polar headgroups at both ends. Such lipids are found in archaebacteria and are supposed to contribute to their ability to survive in extreme environments. By varying structure and length of the hydrophobic part, their supramolecular self-assembly and lyotropic properties in aqueous solution have been studied extensively.[7]

Here we describe an approach on how to combine the advantages of short oligomers, as exhibited by lipids and bolaamphiphiles, with the properties of block copolymers. For the first time, a linear polydimethylsiloxane-based oligomer carrying positive charges on its ends was synthesized. In aqueous phosphate buffer solution this oligomer assembles exclusively in monolayer vesicles. We found that the morphology as well as the vesicle size is influenced by the nature and the concentration of the anion. In this respect, an effect on the vesicle size was observed when using the sterically demanding, hydrophilic glucose phosphate anion as compared to simple phosphate. By varying the molar ratio of phosphate salt to cationic PDMS (cPDMS) we further showed an anion concentration-dependent phase change of the self-assembly. From cryo-TEM investigations we proved the presence of monolayer vesicles that were agile and tubular at room temperature but tight and spherical at 37°C. Finally, we showed the ability of polyanionic siRNA to complex with the cPDMS.

4.2. Results and discussion

4.2.1. Polymer synthesis and characterization

The synthesis of the positively charged PDMS block was performed by a simple methylation reaction. As depicted in Scheme 7, an aminopropyl terminated bifunctional PDMS (DMS-A11) was reacted with iodomethane in THF in the presence of N,N-diisopropylethylamine, which acted as a proton scavenger, at room temperature for 72 hours. The product was dissolved in chloroform and extracted with potassium hydroxide solution in order to exchange iodine for hydroxide anions.

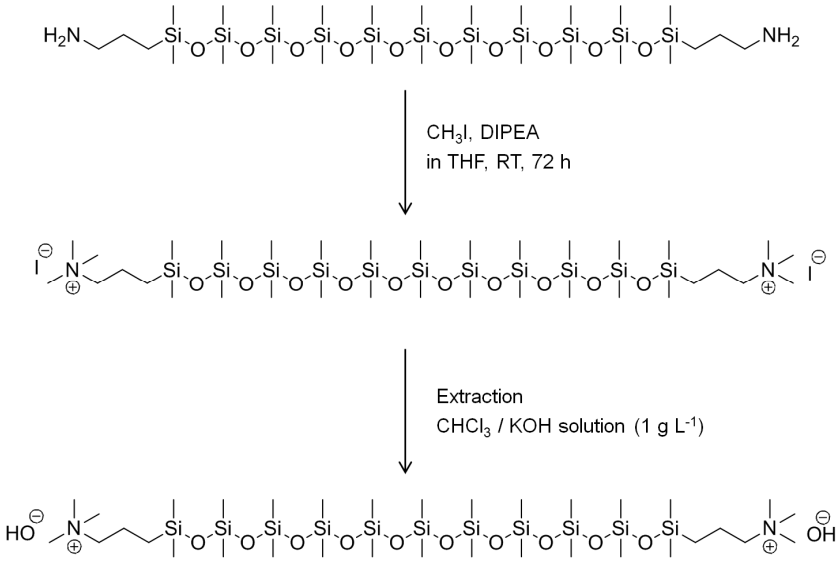

Scheme 7. Methylation followed by ion exchange of aminopropyl-terminated PDMS

The consistency of the PDMS completely changed upon methylation, as shown in Figure 22. Whereas the amine-functional PDMS is a low viscosity liquid, the product, which is a trimethylammonium salt, had a rubber-like consistency.

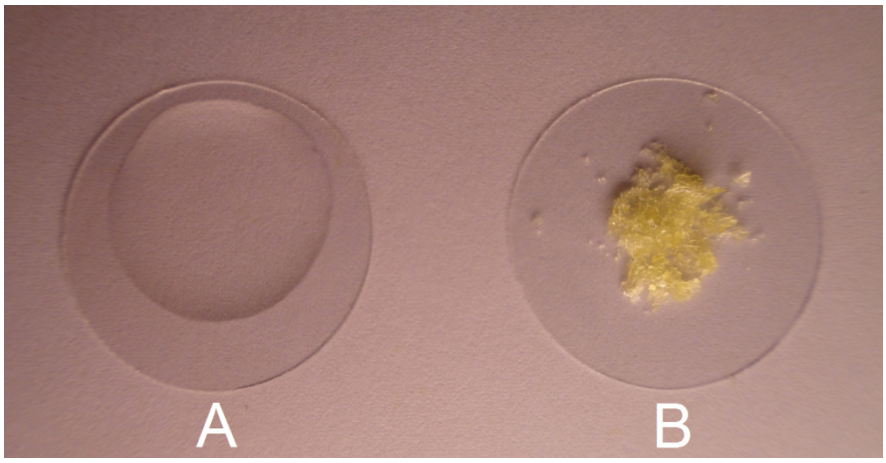

Figure 22. Aminopropyl-terminated PDMS before (A) and after (B) the methylation reaction.

Complete methylation was proven by ^{1}H NMR investigation (Figure 23). The resonance peak of the educt amine protons at 1.25 ppm disappeared upon methylation. In the product spectra, a new intense peak at 3.45 ppm appeared due to the ammonium methyl protons. From the integral values we calculated the molecular weight and could show that the methylation reaction was completed.

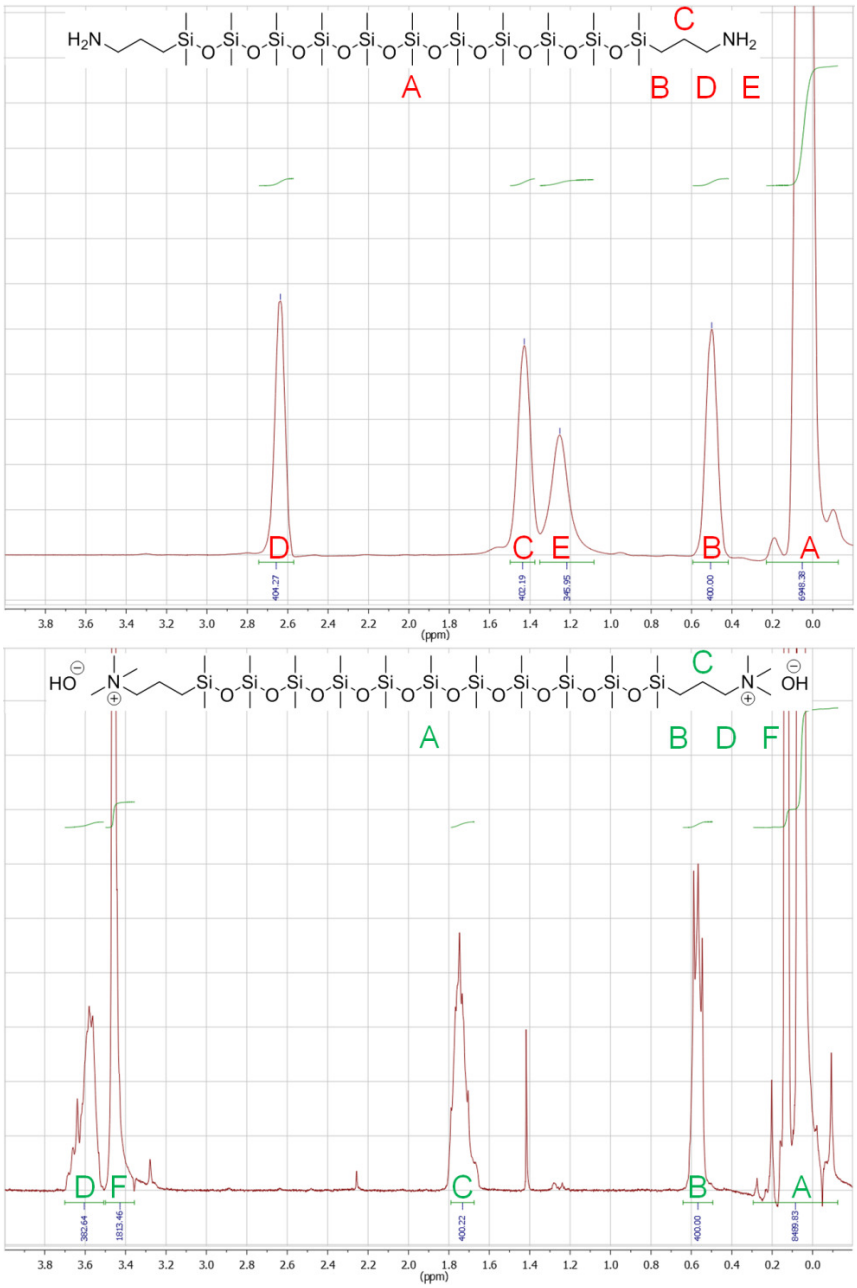

Figure 23. ^{1}H NMR spectra of the aminopropyl-terminated PDMS educt and the methylated product.

For the DMS-A11 we calculated an M_w of 956.9 g mol^{-1} and for the cPDMS an M_w of 1267.1 g mol^{-1} (assuming OH^- as counter ion). The difference between the M_w of the educt to the one of the product is higher than expected. This is explained by the loss of low molecular PDMS upon ion exchange extraction.

Further information on the composition and polydispersity of the PDMS was provided by matrix-assisted laser desorption / ionization time of flight mass spectrometry (MALDI-TOF-MS). As the matrix, we used dithranol, while the sample was prepared as described previously.[8] The MALDI spectra (Figure 24) shows dimethylsiloxane (Δ m/z = 74 g mol^{-1}) as well as $(CH_3)_3N^+(CH_2)_3(Si(CH_3)_2O)_3$ fragments (m/z = 323 g mol^{-1}).

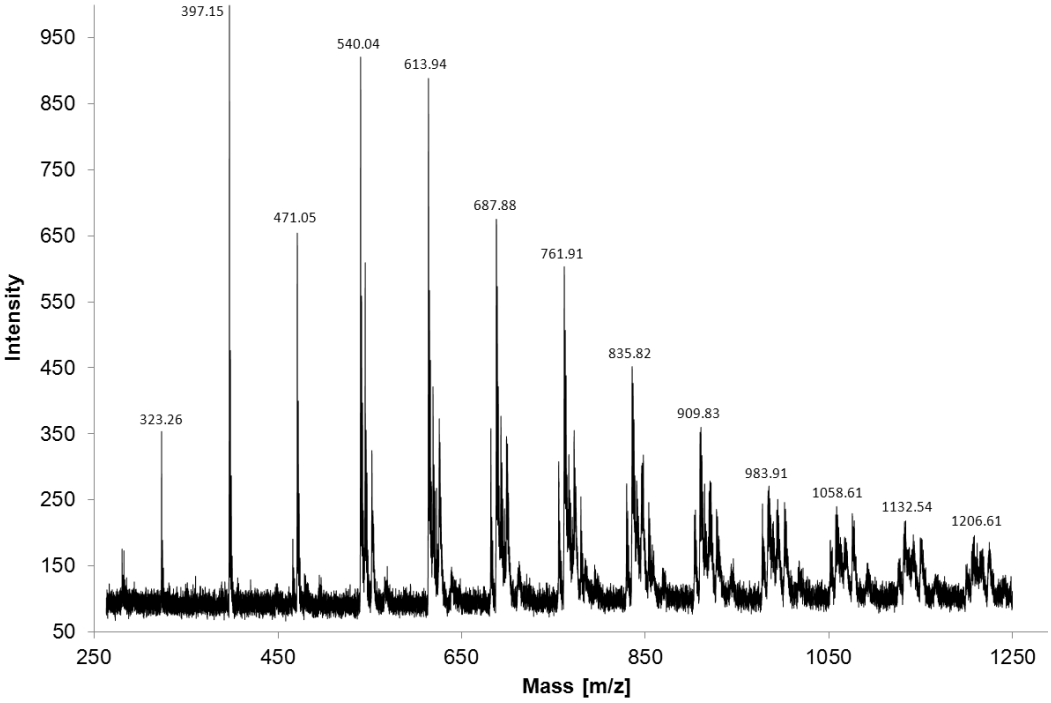

Figure 24. MALDI TOF mass spectra of cPDMS.

Using the Voyager-DE Pro Instrument software, we calculated molecular weights and PDI values for DMS-A11 and cPDMS, as shown in Table 6.

Table 6. Molecular weights and polydispersities as calculated from MALDI TOF MS

Sample	M_z [g mol^{-1}]	M_w [g mol^{-1}]	M_n [g mol^{-1}]	PDI [-]
DMS-A11	905.94	815.39	702.41	1.16
cPDMS	913.37	829.33	721.94	1.15

In contrast to ^{1}H NMR results, the differences between M_z, M_w and M_n of the educt and the product are lower than expected. We obtained clearly better signals for the cPDMS as compared to the DMS-A11, which is explained by the increased ionization / desorption properties of the cPDMS. The resulting low quality of the spectra of DMS-A11 has an influence on the calculated molecular weight values.

4.2.2. Self-assembly – varying the counter ion and its concentration

It has been reported that the aggregation of cationic, siloxane containing surfactants is a sensitive function of counteranion(s) present.[9] Accordingly, the relative concentrations of sodium salts required to favor vesicle formation were shown to follow the anion trend I < Br < Cl, whereas no vesicle formation was observed in concentrated NaF solution.

In order to show such an effect with the synthesized cPDMS, we performed experiments using potassium phosphate and potassium glucose phosphate solutions. By confocal laser scanning microscopy we investigated the morphologies of cPDMS in solution which was stained by the hydrophobic fluorophore BODIPY®630/650. Although the cPDMS itself contains hydroxyl anions, it was not possible to dissolve it in double distilled water. Furthermore, we observed that flocculation occurs upon dissolving cPDMS in a solution of K_2HPO_4, whereas in a solution of KH_2PO_4 few vesicle-like structures were observed, but more frequently aggregates (Figure 25a). An explanation for this finding is the obviously higher pH in a solution of K_2HPO_4 than in one of KH_2PO_4 and thus a higher concentration of OH^- ions, which are as well counter ions to the trimethylammonium groups and competitors to the phosphate.

In a solution of glucose phosphate with the same molar negative-to-positive charge ratio resulted in the formation of giant unilamellar vesicles (GUV) with diameters of 5 to 30 μm, as shown in Figure 25b. It is obvious that the size of the glucose phosphate anion has a significant impact on the curvature and diameter of the vesicles. Besides stabilization by the anionic phosphate, the glucose part is supposed to shield the vesicle membrane from other positively and negatively charged ions. This leads to the formation of large vesicles at comparably low glucose phosphate concentrations as well as to less vesicle-to-vesicle attachment.

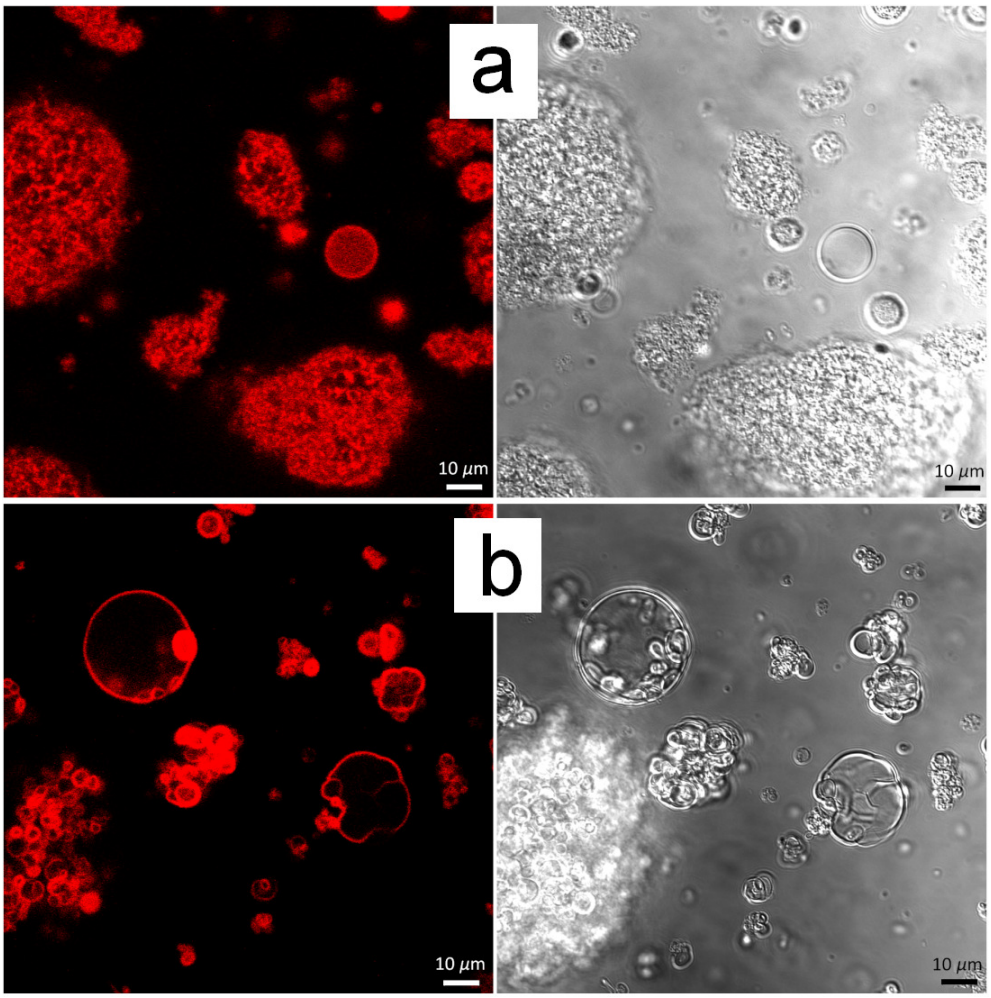

Figure 25. CLSM (left) and transmission (right) micrographs of cPDMS self-assemblies in (a) monobasic phosphate solution and (b) glucose phosphate solution. The molar ratio of the anions to the positively charged trimethylammonium groups at the cPDMS was 10.

In order to find out more about the influence of the anion concentration on the phase behavior, we made a series of samples in KH_2PO_4 solution with a varying molar ratio of phosphate anions to cPDMS. As shown in Figure 26, there is a clear trend from sponge-like aggregates (molar ratio 3 and 10) to multi-compartment vesicles (molar ratio 30) to vesicles (molar ratio 100 and 300). Also, we observed that vesicles at a molar ratio of 100 are larger than such of a molar ratio of 300.

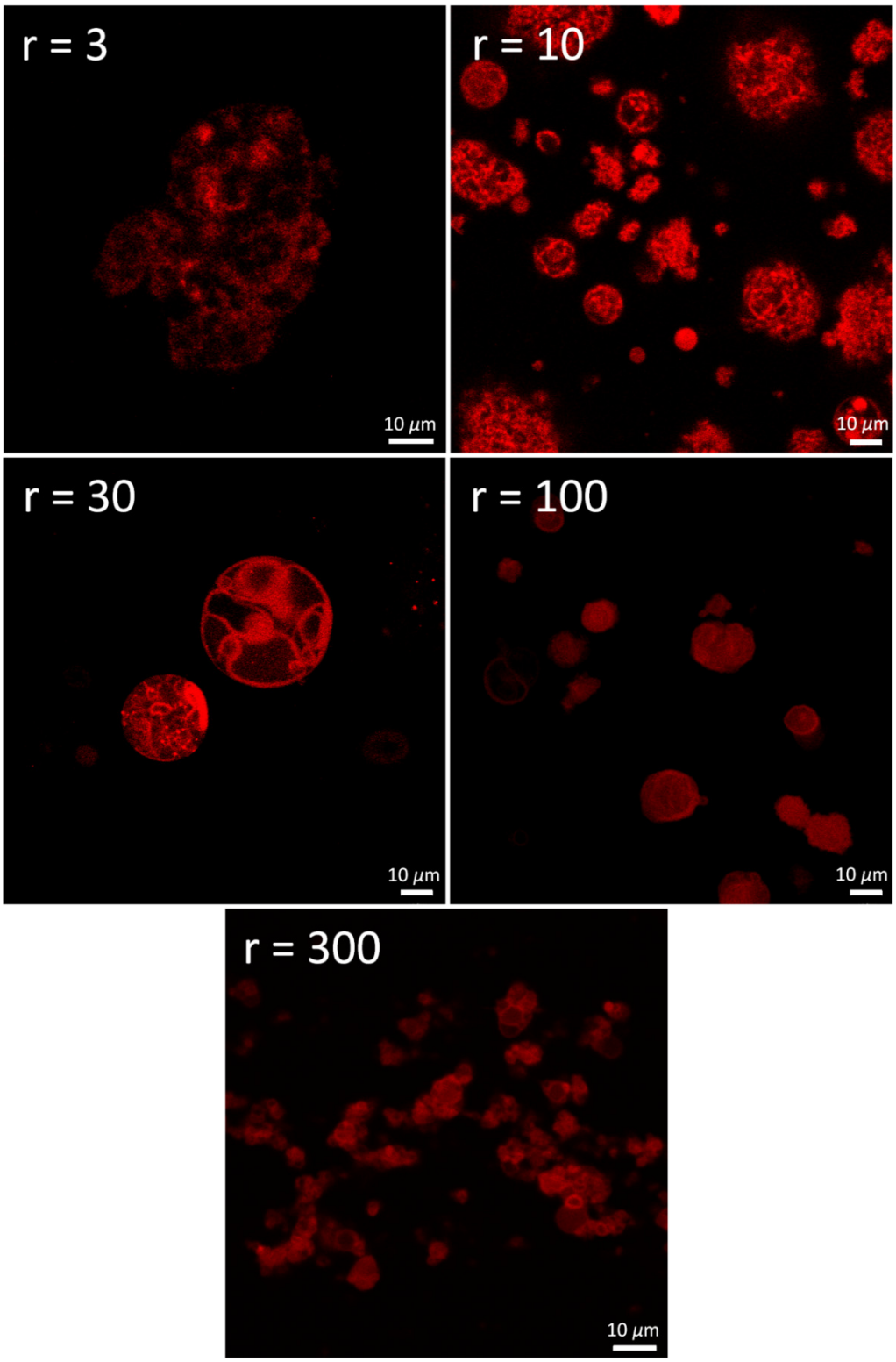

Figure 26. CLSM micrographs of cPDMS self-assemblies in aqueous KH_2PO_4 solution, stained with BodiPy 630/650. The molar ratio of $H_2PO_4^-$ ions to positively charged trimethylammonium groups is represented by "r" (λ_{ex} = 543 nm; concentration cPDMS = 1 mg mL^{-1}).

A general explanation of those observed morphologies is a crowding effect of the anions on the positively charged membrane surface. Whereas different membrane layers have to share a small number of anions at a low negative to positive ratio (sponge-like structures), at higher ratios the anions are densely packed on the membrane surface and thus force the formation of vesicles. At a too high ratio, lowering of the vesicle curvature occurs in order to increase the overall surface area. Another explanation is the differing ratio of phosphate anions to the original counter ion upon changing the phosphate concentration. While in this experiment the cPDMS and thus the cPDMS counter ion (OH^-) concentration stays constant, the phosphate concentration changes. At lower phosphate concentration the influence of the OH^- counter ion could be dominant and thus avoid the formation of vesicles. However, we cannot be sure about the mechanism that influences the vesicle formation, an anion concentration-dependent trend in self-assembly is clearly distinguishable.

Because for most medical and pharmaceutical applications physiological phosphate buffer solution is required, we investigated the self-assembly characteristics of cPDMS vesicles in phosphate buffered saline (PBS). After extrusion through a 0.2 μm track-etched membrane filter the solution was characterized by light scattering and cryo-TEM. Figure 27 shows a Guinier-plot with different concentrations of cPDMS from 0.1 to 1.0 mg mL^{-1}.

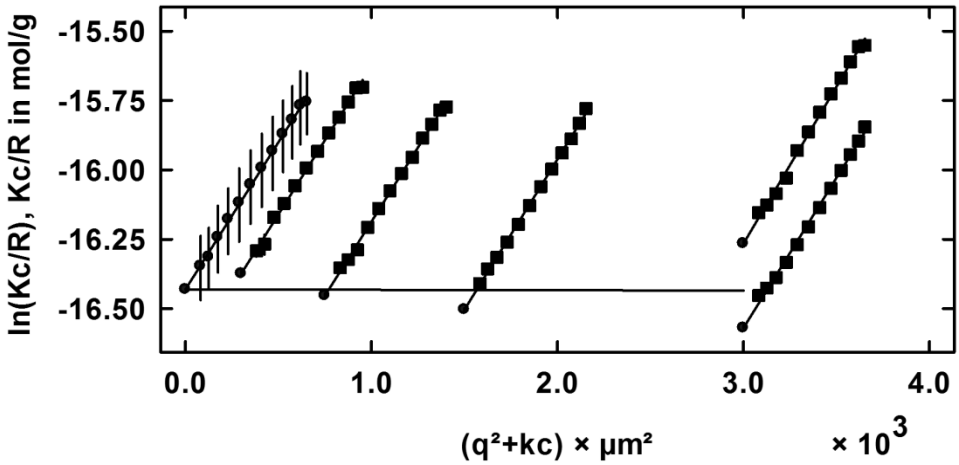

Figure 27. Gunier plot of polymersomes consisting of cationic PDMS in PBS

The resulting R_g was determined as 56.4 ± 0.4 nm and the average M_w of the vesicles as 13.7 ± 1.6 × 10^6 g mol^{-1}. For R_h we obtained a surprisingly low value of 14.1 ± 6.6 nm. From this we obtain a ρ-parameter of 4.0 ± 2.4, which is far away from the value to be expected

for vesicle morphologies. This result can be explained by the non-spherical, but rather ellipsoid shape of most of the vesicles, as shown by cryo-TEM (Figure 28). It was found for liposomes that the *ρ*-parameter for ellipsoids and other deformed spherical structures differs towards values larger than 1.0.[10] However, we could further show that the temperature of the PBS solution has an effect on vesicle shape. At ambient temperature vesicles are, as mentioned before, mainly ellipsoids (Figure 28A), whereas at 37°C most vesicles present a spherical shape (Figure 28B).

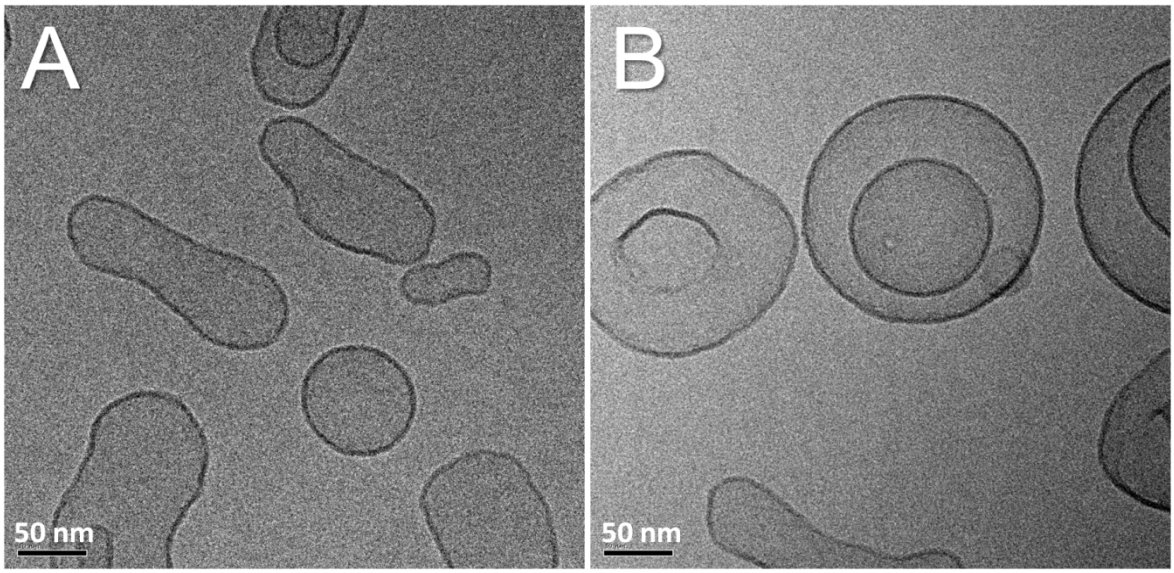

Figure 28. Cryo-TEM of cPDMS vesicles in PBS. (A) initial sample temperature 25°C; (B) initial sample temperature 37°C.

Therefore, we assume that the values obtained for light scattering at ambient temperature should be regarded with suspicion. However, more precise values could be obtained by small-angle X-ray scattering, which was not performed in the frame of this work. From the membrane thickness and the contrast characteristics shown in TEM images, we can assess that the membrane is a monolayer with a thickness of 3.0 ± 0.1 nm (value and standard deviation out of 50 measurements). The maximum theoretical thickness of the membrane is about 4.0 nm (considering the Si-O bond length to be 1.63 Å and the bond angle 130°). From those values we can assume that the PDMS molecules exhibit around 75% of their maximum length. Furthermore, no micelles could be found in TEM, which supports our concept of the cPDMS positive charges that force the system to form a membrane instead of the unfavorable micelles.

4.2.3. Complexes of siRNA with cationic PDMS in physiological buffer

Cationic lipids have been shown to be effective agents to complex and deliver nucleic acids into cells, both *in vitro* and *in vivo*.[11] In this respect, our aim was to show the potential of cPDMS to complex polyanionic nucleic acids. Cy^{TM}3 labeled GAPDH siRNA was mixed with cPDMS during and after vesicle formation. In the sample where siRNA was added after vesicle formation, we observed homogenously fluorescent vesicle membranes (Figure 29). From this finding we assume that siRNA uniformly coats the surface of PDMS vesicles, without rupturing their structure. When adding siRNA during vesicle formation, we observed single fluorescent spots evenly distributed throughout the sample. We assume that these are lamellar or helical complexes of cPDMS with siRNA.[12]

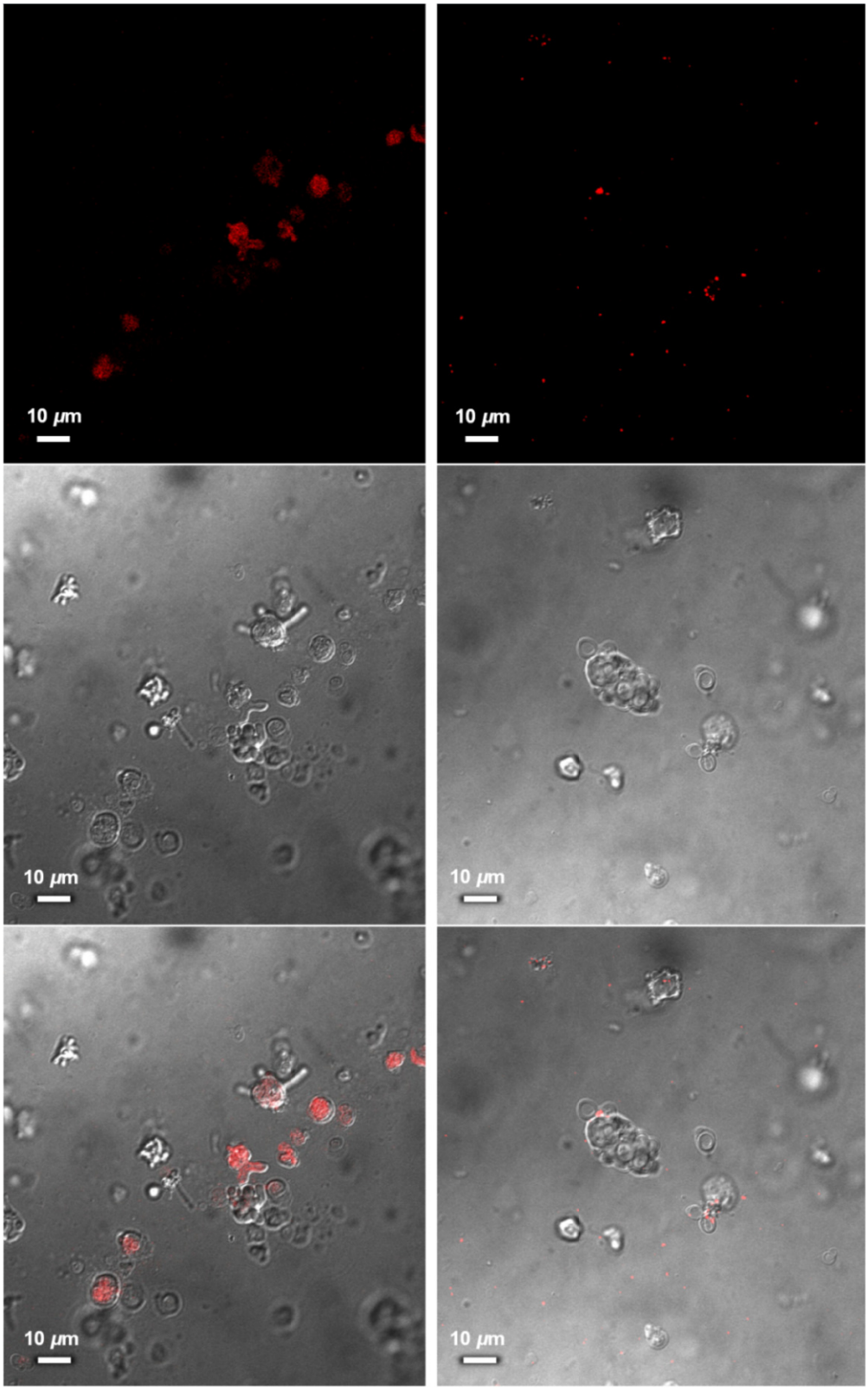

Figure 29. CLSM (top), transmission (middle) and merge (bottom) images of cationic PDMS vesicles and Cy3-labelled siRNA in PBS buffer. The siRNA was added after (left) and before (right) vesicle formation.

This assumption is supported by TEM images (Figure 30), where mesh-like structures are shown. We have not found similar structures in samples where the siRNA was added after vesicle formation or in samples lacking siRNA. Such mesh-like structures potentially originate from continued aggregation and growth of the siRNA-cPDMS complexes.[11]

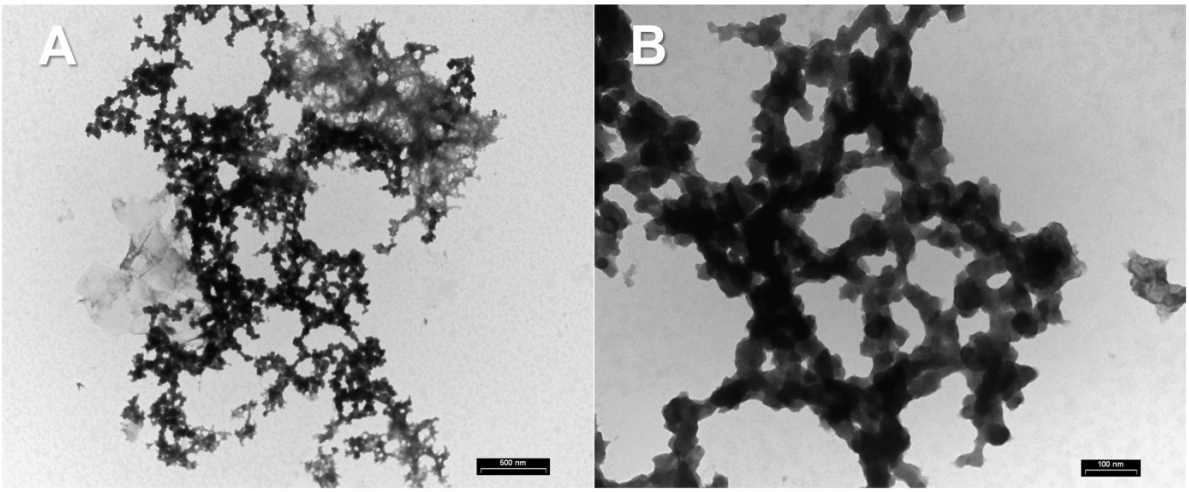

Figure 30. TEM image of a cPDMS sample where siRNA was added during vesicle formation

However, the results presented here only give a hint as to how cPDMS complexes with siRNA and related nucleic acids. More detailed and systematic experiments need to be performed. In particular, the effects of concentration and ionic strength on the cPDMS-siRNA complex should be investigated. In addition, the whole procedure on how to complex nucleic acids with cPDMS should be improved. As desirable result small rods or spheres with diameters of a few nanometers should be obtained. Such species are supposed to enable optimal transfection efficiency.[4]

4.3. Conclusion

We designed and synthesized a linear, bolaamphiphile-like cationic PDMS by a simple methylation reaction. It was shown that the assembly of this material in aqueous solution is strongly influenced by the nature and concentration of salts and especially of their anions. In this respect, glucose phosphate, which is a comparably bulky, hydrophilic anion, could induce the formation of large, well-separated vesicles at low glucose phosphate concentrations. In contrast, more than the 10-fold concentration of phosphate anions was necessary to induce the formation of small, agglomerated vesicles. In the frame of this work, the influence of the pH on the self-assembly of cPDMS was not investigated. This is definitively one of the points that should be considered for future experiments and which could help to control vesicle formation.

Few preliminary results on the complexation of cPDMS with siRNA were presented in the frame of this chapter. We could show the attachment of siRNA to the membrane of vesicles composed of cPDMS. However, important data on the stability as well as on the structure of those complexes could not be shown and should be investigated by fluorescence correlation spectroscopy and small-angle X-ray scattering. Finally, *in vitro* and *in vivo* experiments should proof the transfection efficiency of those complexes and being compared to the effect of established transfection agents (e.g. cationic lipids).

4.4. References

[1] D. E. Discher and A. Eisenberg, *Science (Washington, DC, U. S.)* **2002**, *297*, 967-973.
[2] S. Litvinchuk, Z. Lu, P. Rigler, T. D. Hirt and W. Meier, *Pharm. Res.* **2009**, *26*, 1711-1717.
[3] a) W. Meier, C. Nardin and M. Winterhalter, *Angew. Chem., Int. Ed.* **2000**, *39*, 4599-4602; b) C. Nardin, S. Thoeni, J. Widmer, M. Winterhalter and W. Meier, *Chem. Commun. (Cambridge)* **2000**, 1433-1434; c) A. Graff, M. Sauer, P. Van Gelder and W. Meier, *Proc. Natl. Acad. Sci. U. S. A.* **2002**, *99*, 5064-5068; d) M. Kumar, M. Grzelakowski, J. Zilles, M. Clark and W. Meier, *Proc. Natl. Acad. Sci. U. S. A.* **2007**, *104*, 20719-20724; e) M. Grzelakowski, O. Onaca, P. Rigler, M. Kumar and W. Meier, *Small* **2009**, *5*, 2545-2548.
[4] R. Koynova and B. Tenchov, *Soft Matter* **2009**, *5*, 3187-3200.
[5] P. L. Felgner and G. Rhodes, *Nature* **1991**, *349*, 351-352.
[6] A. Meister and A. Blume, *Curr. Opin. Colloid Interface Sci.* **2007**, *12*, 138-147.
[7] T. Benvegnu, M. Brard and D. Plusquellec, *Curr. Opin. Colloid Interface Sci.* **2004**, *8*, 469-479.
[8] X. M. Liu, E. P. Maziarz, D. J. Heiler and G. L. Grobe, *J. Am. Soc. Mass Spectrom.* **2003**, *14*, 195-202.
[9] Z. Lin, M. He, L. E. Scriven, H. T. Davis and S. A. Snow, *J. Phys. Chem.* **1993**, *97*, 3571-3578.
[10] a) A. J. Jin, D. Huster, K. Gawrisch and R. Nossal, *Eur. Biophys. J.* **1999**, *28*, 187-199; b) O. Stauch, R. Schubert, G. Savin and W. Burchard, *Biomacromolecules* **2002**, *3*, 565-578.
[11] M. T. Kennedy, E. V. Pozharski, V. A. Rakhmanova and R. C. MacDonald, *Biophys. J.* **2000**, *78*, 1620-1633.
[12] I. Koltover, T. Salditt, J. O. Radler and C. R. Safinya, *Science (Washington, D. C.)* **1998**, *281*, 78-81.

5. General conclusion and outlook

In this work we presented the synthesis and characterization of novel amphiphilic tri- and new diblock copolymers based on PDMS and PMOXA comprising different functional groups at their hydrophilic ends. Their self-assembled structures, in general vesicles, presenting the respective functionality on the surface, could be covalently coupled with biological ligands by copper catalyzed click chemistry or by the specific interaction of 4-formylbenzoate and 6-hydrazinonicotinate resulting in a stable bis-aryl hydrazone bond. In addition, cationic PDMS was synthesized, characterized and it's self-assembly, depending on the counter anion, was investigated. The main findings of this work are:

- ✓ Polymersomes assembled from ABA-1 (hydroxyl), ABA-2 (alkyne) and ABA-SRB were modified with azide-functional poly$(G)_{23}$ oligonucleotide strands by copper catalyzed click chemistry. We showed that such polymersomes were taken up by THP-1 cell lines in a time-dependent manner. Even though uptake of polymersomes by cells was shown, we could not directly proof the binding of the poly$(G)_{23}$ ligands to the polymersome surface. Due to the insufficient water solubility of some of the reagents involved, it was difficult to control this click reaction in aqueous solution.
- ✓ The sulforhodamine B functionalized triblock copolymer ABA-SRB has proven to be useful for the labeling of polymersomes for *in vitro* fluorescence imaging.
- ✓ For the first time, PDMS-*b*-PMOXA diblock copolymers were synthesized. They assembled to stable and water impermeable vesicles. Via the specific and biocompatible reaction of 4-formylbenzamide and 6-hydrazinonicotinamide functionalities, a stable and traceable bis-aryl hydrazone bond between the vesicles and biomolecules was obtained. We could show the specific cell targeting of polymersome-antibody conjugates without toxic effects.
- ✓ To a short amino-bifunctional silicone, cationic charged trimethylammonium groups were introduced via a simple methylation reaction. The rubber-like product was shown – depending on the nature and properties of the counter anion – to assemble to unilamellar vesicle structures in aqueous solution. They

could potentially find application as transfection agent.

Based on the results listed above, the following points are suggested for further investigation:

- ✓ The cationic ring opening polymerization of 2-methyl-2-oxazoline to the pre-activated PDMS is very sensitive to moisture and impurities. Furthermore, only few solvents are suitable for the resulting block copolymer, which is a limiting factor for e.g. the use of microwave-assisted synthesis of well-defined poly(2-methyloxazolines). Therefore, a more robust method for the synthesis of PDMS-*b*-PMOXA block copolymers is desirable.
- ✓ By mixing PDMS-*b*-PMOXA diblock copolymers being different in the PMOXA chain length, we foresee a higher degree of ligands exposed at the polymersome surface. In this respect, also dendron-like pending structures could help to improve the conjugation efficiency.
- ✓ The polymersome platform presented here has shown to be rather stable. A combination with a triggered release system would be beneficial in order to release the cargo at a specific site and finally to show a therapeutic effect *in vitro* and *in vivo*.
- ✓ In the course of this work, the cationic PDMS could not be examined in great detail. To expand the information obtained in this work and to obtain clear trends, systematic self-assembly experiments of the cationic PDMS in salt solutions differing in ion strength and anion size should be performed. Furthermore, the complexation of the cationic PDMS with siRNA or DNA should be further investigated by FCS and small-angle X-ray scattering and the applicability as transfection agent should be considered.

6. Experimental part

6.1. Experimental part

6.1.1. Materials

Reagents and materials were of the highest commercially available grade and were used without further purification, unless indicated. Monocarbinol-terminated polydimethylsiloxane (AB146681, M_{nGPC} = 5633 g mol^{-1}, M_{wGPC} = 6332 g mol^{-1}, M_w/M_n = 1.12, M_n ^{1}H-NMR = 5323 g mol^{-1}) was purchased from ABCR GmbH, Germany. 2-Methy-2-oxazoline, triethylamine, triflic anhydride and all solvents were purchased from Sigma Aldrich in highest quality. The crosslinkers succinimidyl-4-formyl benzoate (S-4FB) and succinimidyl 6-hydrazinonicotinate acetone hydrazone (S-HyNic) were purchased from Solulink. Anti-biotin-IgG antibodies were purchased from antibodies-online GmbH (Aachen, Germany), trastuzumab (Herceptin®) was provided by the University Hospital Pharmacy of Basel. SKBR3 cell culture was provided by the group of Nancy Hynes (Friedrich Miescher Institute, Basel). Dulbecco's Modified Eagle Medium (DMEM, GIBCO), fetal bovine serum (FBS), penicillin and streptomycin (Sigma Aldrich), phosphate-buffered saline (PBS) (Sigma-Aldrich) were used as received. Sulforhodamine B, Alexa Fluor® 647 maleimide, Alexa Fluor® 633 NHS and Cellmask™ Deep Red were purchased from Invitrogen.

6.1.2. Polymer synthesis

PDMS synthesis was performed by an acid-catalyzed polycondensation reaction of dimethoxydimethylsilane in the presence of aqueous hydrochloric acid and end-capper, resulting in butylhydroxy-terminated bifunctional PDMS. The detailed synthesis and purification procedure is described elsewhere.[1]

For the *synthesis of PMOXA-b-PDMS-b-PMOXA triblock copolymer* (ABA), PDMS was purified by vacuum stripping at 80°C and precipitation in an equal (by weight) water/methanol mixture. Purified PDMS was reacted with triflic acid anhydride in hexane at -10°C for 3 hours, resulting in triflate-PDMS bifunctional macroinitiator. The reaction mixture was then filtered under argon through a G4 filter. Hexane was evaporated under

vacuum and dry ethyl acetate was added as reaction solvent. Addition of dry 2-methyl-2-oxazoline resulted in symmetric ring-opening cationic polymerization of PMOXA blocks on the macroinitiator. The reaction was terminated by addition of either 0.1 M potassium hydroxide solution in methanol (to result in the hydroxyl endfunctional polymer ABA1) or by N-methylpropargylamine (to result in the alkyne endfunctional polymer ABA2). The polymers were purified by extensive ultrafiltration (UF) in a 1/1 water/ethanol mixture (MWCO 5000 g mol^{-1}).

The *sulforhodamine B labelled PMOXA-b-PDMS-b-PMOXA triblock copolymer* was synthesized by an esterification reaction. Hydroxyl endfunctionalized ABA polymer (1 equivalent) was dried under vacuum and dissolved in dry chloroform. After the solution was cooled to 8°C, triethylamine (TEA, 2 equivalent) and a concentrated solution of sulforhodamine B acid chloride (10 equivalent) in $CHCl_3$ was added dropwise and the reaction mixture was allowed to stir for 24 hours at 8°C. $CHCl_3$ was evaporated at 40°C and the dark red solid was dissolved in ethanol. Non-reacted free SRB and TEA were removed by extensive UF in pure ethanol (MWCO 5000 g mol^{-1}). After evaporation of ethanol we obtained a dark red solid product (reaction yield = 95%).

Synthesis of *PDMS-b-PMOXA-hydroxyl and PDMS-b-PMOXA-piperazinyl diblock copolymers*. All reaction steps were carried out under an inert argon atmosphere. The amounts used for the syntheses are listed in Table 7.

Table 7. Amounts of educts used for the synthesis. Monocarbinol terminated poly(dimethylsiloxane) (PDMS), 2-methyl-2-oxazoline (MOXA), triethylamine (TEA) and trifluoromethanesulfonic anhydride (TfSA)

Sample	PDMS [g; mmol]	MOXA [g; mmol]	TEA [g; mmol]	TfSA [g; mmol]
AB-OH	26.62; 5.0	8.68; 100	0.524; 5.2	1.47; 5.2
AB-NH	10.00; 2.0	5.61; 66	0.213; 2.1	0.60; 2.1

PDMS was put into a three-neck, round-bottomed flask and evacuated under stirring over night at 60 °C. Dry hexane was added under an argon atmosphere and the solution was dried for 24 h by reflux in a Soxleth apparatus containing a molecular sieve 4A (Chemie Uetikon AG, Switzerland).

After cooling to room temperature, triethylamine (dried over CaH2 and freshly distilled) was added. The solution was cooled to -10 °C and trifluoromethanesulfonic anhydride (TfSA) in 15 mL of dry hexane were added slowly over 30 minutes. After completion of the addition, the mixture was reacted for 3 h at 10 °C. Hexane was evaporated at room temperature in vacuum. The residual PDMS oil was redissolved in cold hexane and separated from triflate salt by filtration at 0 °C through a glass frit. The hexane was again evaporated, dry ethyl acetate and 2-methyl-2-oxazoline, previously dried and distilled over calcium hydride, were added. The reaction mixture was stirred for 60 h at 40 °C.

Finally, the solution was cooled to room temperature, 5 mL of 1.0 M potassium hydroxide solution in dry methanol (for AB-OH synthesis) and 20 mL of 1.0 M piperazine solution in dry methanol (for AB-NH synthesis) were added. After 1 h ethyl acetate was removed under vacuum to obtain the transparent, rubber-like raw product.

The raw product was suspended in bidistilled water and the pH was set to 7.0. The water was then removed by lyophilization. The polymer was dissolved in ethanol and centrifuged (4000 rpm for 40 minutes) to separate unreacted, non-ethanol soluble PDMS. Subsequently the ethanol solution was transferred into a solvent-resistant, stirred ultrafiltration device (Millipore, USA) equipped with a 3000 MWCO regenerated cellulose membrane (Millipore, USA) and extensively washed with ethanol. The ethanol solution was then evaporated. The resulting transparent, rubber-like diblock copolymer was characterized and stored under dry conditions. Yields and characterization data of the PDMS and the diblock copolymers are shown Table 8.

Table 8. Specification of the diblock copolymer products. M_w/M_n calculated from M_n^{GPC} and M_w^{GPC}.

Sample	M_n^{GPC} [g mol^{-1}]	M_w^{GPC} [g mol^{-1}]	M_w/M_n [-]	$M_n^{1H\text{-}NMR}$ [g mol^{-1}]	Yield [g; %]
AB-OH	5153	7785	1.51	6139	17.4; 56.7
AB-NH	4518	7506	1.66	6185	8.30; 67.1

The synthesis of *cationic PDMS* was carried out by a methylation reaction of aminopropyl terminated polydimethylsiloxane. 1.50 g (1.76 mmol) aminopropyl terminated polydimethylsiloxane DMS-A11 from ABCR GmbH & Co. was dissolved in 15 mL of dry tetrahydrofurane (THF). 3.04 g (21.2 mmol) iodomethane and 1.73 g (13.3 mmol) N,N-diisopropylethylamine were added and the mixture was stirred under argon atmosphere for 65 h at room temperature. The reaction mixture contained yellowish-white precipitate. After evaporation of THF at 40 °C under vacuum, the yellowish-white solid was dissolved in 30 mL of chloroform and extracted four times against 40 mL 1.0 g mL-1 potassium hydroxide solution. The organic phase was separated and chloroform was evaporated. The residual yellowish product had a soft-crystalline consistency. Yield = 1.62 g (1.51 mmol; 86 %).

6.1.3. Vesicle formation process

Polymer vesicles were formed using the film hydration method. Generally, 25 mg of polymer were dissolved in 5 mL ethanol in a 10 mL round-bottom flask. The ethanol was evaporated using a Rotavapor R216 (Büchi, Switzerland) at 100 mbar pressure, 40 °C and under rotation (90 rpm). Additionally, the polymer film was dried at 4×10^{-2} mbar at room temperature for 2 h. For hydration, 5 mL of aqueous solution (water, buffer or fluorescent dye solution) were added into the flask and stirred overnight using a magnetic stirrer. To homogenize the vesicle size, the vesicle solution was extruded using a LIPEX™ extruder (Northern Lipids Inc., Canada). Each solution was extruded twice through a nucleopore track-etch membrane with an average pore diameter of 0.4 μm, followed by 12 extrusion steps through a nucleopore track-etch membrane with an average pore diameter of 0.2 μm (Whatman, GE Healthcare, UK).

6.1.4. Characterization techniques

Nuclear magnetic resonance expermients were performed using Bruker spectrometers operating at 400 MHz or at 600.13 MHz proton frequency. All samples were dissolved in $CDCl_3$ as solvent and as lock substance. Self-diffusion measurements were performed on samples listed in Table 2 with the bipolar gradient pulse sequence using a Bruker Avance DRX NMR spectrometer operating 600.13 MHz proton frequency. The instrument was equipped with a 5-mm broadband inverse probe with a shielded z-gradient coil and a GAB gradient amplifier (10 Ampere, maximum gradient strength 52.5 G cm^{-1}). Measurements were performed at 298 K and the temperature was calibrated using a methanol standard showing accuracy within ± 0.2 K. The gradient strength was calibrated using a Shigemi tube filled with H_2O to a height of 4.0 mm and imaging this water cylinder. The resulting gradient calibration was validated by determining the diffusion coefficient of water at 310 K and reproduced the literature value within 5%.

The diffusion experiments were performed by varying the gradient strength between 2% and 95% of the maximum strength in typically 8 or 16 single experiments while keeping the diffusion times and gradient lengths constant. The entire experiment was then repeated with a different diffusion time (100 ms to 500 ms). The intensity decrease of the signal of interest was determined and fitted with a Bruker t1/t2 software package suitable for dosy experiments, which is included in the XWINNMR software.

Light scattering was carried out to determine the hydrodynamic (R_h) and the gyration (R_g) radius of assembled structures in solution. Dynamic (DLS) and static (SLS) light scattering experiments were performed on an ALV goniometer (ALV GmbH, Germany), equipped with an ALV He-Ne laser (λ = 632.8 nm). Light scattering measurements were performed in 10 mm cylindrical quartz cells at angles of 40 – 140° at 293 K. For DLS and SLS data processing we used the ALV static & dynamic fit and plot software (version 4.31 10/01). SLS data were processed according the Guinier-model.

Transmission electron microscopy (TEM). Vesicle solutions were negatively stained with 2% uranyl acetate solution and deposited on a carbon-coated copper grid. The samples were examined with a transmission electron microscope (Philips Morgagni 268D) operated at 80 kV.

Cryo-transmission electron microscopy (Cryo-TEM). A 4 μL aliquot of sample was adsorbed onto a holey carbon-coated grid (Quantifoil, Germany), blotted with Whatman 1 filter paper and vitrified into liquid ethane at -178 °C using a Vitrobot (FEI company, Netherlands). Frozen grids were transferred onto a Philips CM200-FEG electron microscope using a Gatan 626 cryo-holder. Electron micrographs were recorded at an accelerating voltage of 200 kV and a magnification of 20 000 x, using a low-dose system (10 e-/Å^2) while keeping the sample at -172 °C. Micrographs were recorded on a 2K x 2K CCD camera (Gatan, USA).

Laser scanning microscopy and fluorescence correlation spectroscopy. Laser scanning microscopy (LSM) and fluorescence correlation spectroscopy (FCS) were performed with an inverted confocal fluorescence laser scanning microscope LSM 510 META/Confocor2 (Zeiss, Germany) equipped with an argon laser (for 405, 458, 477, 488 and 514 nm), and two helium-neon lasers (543 and 633 nm) as excitation sources. For FCS, 15 μL of sample were applied to the glass surface of a cover glass (Huber & Co. AG, Switzerland) which was positioned on the xy-stage of the microscope. The excitation laser beam and the fluorescence emission passed through the same objective. The fluorescence signal was detected by highly sensitive avalanche photo diodes. Fluorescence intensity fluctuations were processed in terms of an autocorrelation function. Evaluation of FCS data was performed as described previously.[2]

Matrix-assisted laser desorption / ionization mass spectroscopy time of flight. Spectra were recorded on a Voyager-DE Pro instrument (Perseptive Biosystems). The irradiation source was a pulsed nitrogen laser with λ = 337 nm. The measurements were carried out using the following conditions: reflector operation mode; polarity-positive mode, mass-high (20 kV acceleration voltage), 200 pulses per spectrum. The delayed extraction technique was used applying the delay time of 200 ns. The matrix was dithranol and the measurements were performed using a gold plate.

6.1.5. Modification of polymersomes and ligands

Alexa Fluor 633 modification of polymer vesicles. 3.0 mL of vesicle solution with a polymer concentration of 0.5 mg mL^{-1} were produced in 0.1 M sodium bicarbonate buffer (pH 8.3). The polymer composition was varied from 0.3% AB-NH / 99.97% AB-OH to 100% AB-NH / 0% AB-OH. Detailed information on polymersome composition is shown in Table 9.

Table 9. Composition and volumes of polymer solutions in ethanol for preparation of polymersomes with varying molar percentages of AB-NH. The stock solutions used to prepare the polymer films were the following: (A) AB-OH, 0.3 mg mL^{-1}, (B) AB-NH, 60 μg mL^{-1} and (C) AB-NH, 0.3 mg mL^{-1}; solvent for all solutions was ethanol.

AB-OH [%]	(A) [mL]	AB-NH [%]	(B) [μL]	(C) [mL]
100	5	-	-	-
0	-	100	-	5
70	3.5	30	-	1.5
90	4.5	10	2500	-
97	4.85	3	750	-
99	4.95	1	250	-
99.7	4.985	0.3	75	-
99.9	4.995	0.1	25	-
99.97	4.999	0.03	7.5	-

To 1.0 mL of each solution, 10 μL of 50 μM Alexa633-NHS was added. After 2 h reaction time at room temperature, the vesicle solutions were transferred into dialysis membranes (MWCO 300 kDa, Spectrum Laboratories Inc., USA) and dialyzed extensively against a 0.1 M sodium chloride solution. Measurements were performed by FCS using a 633 nm He/Ne laser excitation source.

4-formylbenzoate modification of polymer vesicles. 3.0 mL polymersome solution with a polymer concentration of 1.5 g mL^{-1} was produced in 0.1 M sodium bicarbonate buffer (pH 8.3). The polymer composition was 3% AB-NH and 97% AB-OH. To 1.0 mL of

polymersome solution, 20 μL of 10 mg mL^{-1} (0.81 μmol) 4-formylbenzoate (S-4FB) in DMSO were added. After 2 h reaction time at room temperature, the vesicle solution was transferred into a dialysis membrane (MWCO: 300 kDa) and dialyzed extensively against 0.1M NaCl. In a last step, the solvent was exchanged by dialysis with conjugation buffer (0.1 M sodium phosphate buffer pH 6.0).

6-hydrazinonicotinate acetone hydrazone modification of enhanced yellow fluorescence protein (eYFP). eYFP was expressed in and purified from E. coli. The concentration of the protein was measured with a NanoDrop 2000c system (ThermoFisher Scientific, USA). eYFP was obtained in 0.1 M sodium phosphate buffer pH 6.0 at a concentration of 57.1 mg mL^{-1} (2.1 mM).

Primary amino groups of eYFP were modified with succinimidyl 6-hydrazinonicotinate acetone hydrazone (S-HyNic). For this, 80 μL 2.1 mM eYFP were incubated with 120 μL 5.8 mM (4.1 equivalents) HyNic in modification buffer pH 7.4 for 2.5 h under gentle stirring at room temperature. Non-reacted S-HyNic was separated from modified eYFP-HyNic conjugate by diafiltration three times using Amicon Ultra 30K centrifugal filters (regenerated cellulose, MWCO: 30 kDa, Millipore, USA) with conjugation buffer. After the last diafiltration step, the concentration of the eYFP was determined by UV/Vis to be 690 μM with a final volume of 200 μL.

6-hydrazinonicotinate acetone hydrazone modification of antibodies. Concentrations and volumes of antibodies after washing and quantities of NHS-HyNic solution used for modification, including the resulting molar substitution ratio (MSR), are shown in Table 10.

Table 10. Concentrations and volumes of antibodies after washing and quantities of S-HyNic solution used for modification and resulting MSR.

Sample	^{1}st washing [μM; μL]	S-HyNic [mM; µL]	^{2}nd washing [μM; μL]	MSR [-]
Anti-biotin IgG	7.0; 100	3.4; 4.1	1.9; 200	5.4
Trastuzumab IgG	16.7; 930	34.4; 2.5	21.5; 500	3.1

The lyophilized antibody was dissolved in and washed with PBS buffer pH 7.4 in Amicon Ultra 30 K centrifugal filters. Thereafter, we measured the antibody concentration and added S-HyNic solution in DMF. After 90 minutes reaction at room temperature, the IgG-HyNic solution was washed five times with Amicon Ultra centrifugal filters with 0.1 M sodium phosphate buffer pH 6.0. The concentration of IgG and the MSR of HyNic to IgG were measured by UV/Vis spectroscopy. For MSR determination, the IgG-HyNic solutions were reacted with 4-nitrobenzaldehyde (4-NB) and the specific absorbance was measured at 390 nm (Figure 31).

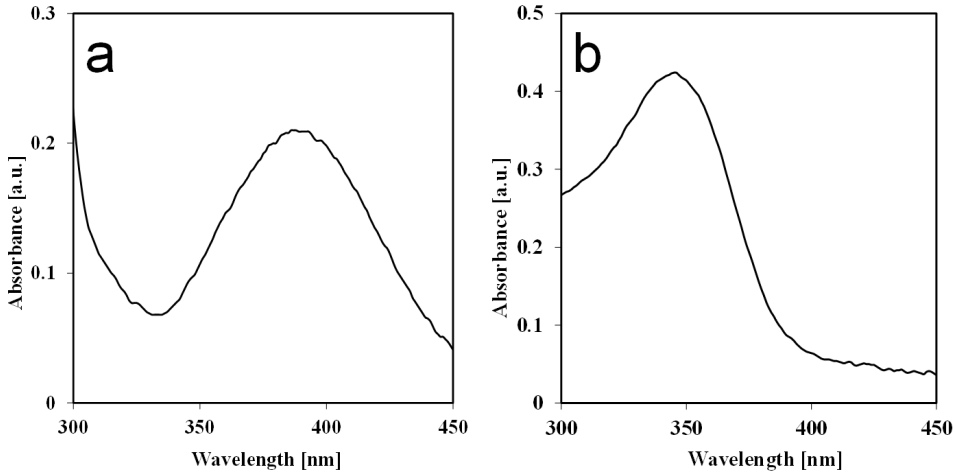

Figure 31. UV-Vis spectrograph of (a) 6-hydrazinonicotinate acetone hydrazone modified anti-biotin antibody reacted with 4-nitrobenzaldehyde (λmax 390 nm) and (b) 4-formylbenzoate modified polymersomes after dialysis reacted with 4-hydrazinonicotinate acetone hydrazone (λmax 350 nm).

PolyG_{23} modification of polymersomes by click-chemistry. ABA1, ABA2, and ABA-SRB were mixed in weight ratios of 16/3.7/1 and polymersome solutions with a final polymer concentration of 4 mg mL^{-1} were prepared. To 1.5 mL polymersome solution in bidistilled water, the azide-functional poly$(G)_{23}$ ligand, sodium ascorbate solution, $CuSO_4$ solution, and a Tris[(1-benzyl-1H-1,2,3-triazol-4-yl)methyl] amine (TBTA) solution at a volume ratio of: 25/120/2/1/1/1 using concentrations mentioned elsewhere.[3] As control sample, a polymersome solution without addition of azide-functional poly$(G)_{23}$ was used.

6.1.6. Microcontact printing

The microcontact printing of the biotin-bovine serum albumin pattern to the cover glass slide was performed according to a previously published protocol.[4] The polymersome-

anti-biotin-IgG conjugate solution (0.1 M sodium phosphate buffer pH 7.4) was incubated for 1 h on the patterned glass surface before washing three times with PBS buffer pH 7.4.

6.1.7. THP-1 cell experiments

Two days prior to imaging, THP-1 cells were activated with phorbol-12-myristate-13-acetate (PMA, 100 nM) to differentiate the monocytes into macrophages and approximately 500 000 cells/mL were seeded into each well of the tissue culture slide (Lab-tek, NUNC). Both Poly$(G)_{23}$-modified and control ABA nanocontainers (lacking the ligand) were added to the activated cells and incubated (37°C, 5% CO_2) for 1, 2, 4, and 24 hours, respectively. Confocal fluorescence imaging using the 543 nm laser line of a ZEISS LSM 510 microscope was used to determine the extent of specific cellular uptake.

6.1.8. SKBR3 cell experiments

Cell culture. SKBR3 cells were cultured in DMEM growth medium supplemented with 10% fetal bovine serum, 1% penicillin (10,000 units mL^{-1}), streptomycin (10,000 $\mu g\ mL^{-1}$), 2 mM L-glutamine and 1 mM pyruvate. Cells were grown in a humidified incubator (HERA Cell 150, Thermo Scientific, Germany) at 37 °C in a 5% CO_2 atmosphere. The medium was replenished every two day and the cells were subcultured by trypsinization.

Targeted uptake of polymersome-antibody conjugates. Cells were seeded at a density of 1 × 105 cells per well in a 6-well plate and incubated for 24 h to allow attachment of cells to the plate prior to the uptake experiments. SKBR3 cells were then incubated with sulforhodamine B containing polymersomes (1000 $\mu g\ mL^{-1}$) with and without conjugated trastuzumab for 1 h and 2 h at 37 °C in a humidified 5% CO_2 incubator. After harvesting by trypsinization, the resulting cells were washed with PBS to remove non-internalized polymersomes. The cells were analyzed for the uptake of polymersome with and without conjugated trastuzumab with confocal laser scanning microscopy and flow cytometry.

Cell imaging by laser scanning microscopy. SKBR3 cells pre-treated with sulforhodamine B containing polymersomes with and without conjugated trastuzumab were further incubated at 37 °C with freshly prepared Deep Red (Cellmask^{TM}) plasma membrane stain (5 $\mu g\ mL^{-1}$) for 5 min. They were then washed with PBS buffer and visualized with a confocal laser scanning microscope (Carl Zeiss LSM510) equipped with 63× water emulsion lens (Olympus). The measurements were performed in multi-track mode, and the intensity of each fluorescent dye was adjusted individually: sulforhodamine B excited at 543 nm in channel 3, Deep Red excited at 633 nm in channel 2. The images were processed using Carl Zeiss LSM software (version 3.99) and ImageJ (version 1.43u).

Flow cytometry. The uptake of polymersome-trastuzumab conjugates and polymersomes by SKBR3 cells was analyzed via flow cytometry (CYAN, Beckman Coulter, USA) based on the measurement of cellular-associated fluorescence of cells (1 × 105) and the mean fluorescence intensity of gated viable cells. A total of 20 000 events were analyzed for each condition.

In vitro cell proliferation inhibition activity of polymersome-trastuzumab conjugates. SKBR3 cells at a density of 1 × 104 cells per well were cultured in a 96-well plate and incubated with different concentrations of polymersomes and polymersome-trastuzumab conjugates (10, 30, 100, 300 μg mL^{-1} polymer concentration) for 24 h at 37 °C and 5% CO_2 atmosphere. The proliferation inhibition activity was determined by the MTS (3-(4,5-dimethylthiazol-2-yl)-5-(3-carboxymethoxyphenyl)-2-(4-sulfophenyl)-2H-tetrazolium) assay. This assay measures the dehydrogenase activity of viable cells by the reduction of MTS to a colored product, formazan. Subsequently, 20 μL of CellTiter 96 AQueous One Solution Cell Proliferation Assay (MTS) reagent (Promega) were added to each well and then incubated for 2 h. The absorbance of each well mixture was measured with a microplate reader (Spectramax M5, Molecular Devices, USA) at λ = 490 nm. The untreated control cells were considered as 100% viable and cell proliferation after treatment with polymersome and polymersome-trastuzumab conjugate was calculated from [A_{sample} / $A_{control}$] X 100. Errors are standard deviations of triplicate of samples.

6.1.9. Formation/complexation with cPDMS

For the *preparation of cPDMS-vesicle solutions*, lower polymer concentrations were required than for common block copolymer vesicle solutions. By the film hydration method we formed vesicle solutions of 1 mg mL^{-1}, using different salts or Dulbecco's Phosphate Buffered Saline. Before film formation, 2 µL of 10 µM BODIPY 630/650 in DMSO was added. The final volume of the aqueous vesicle solution was 2.0 mL. All solutions were investigated immediately after their preparation.

The *complexation of cPDMS with siRNA* was performed using Cy^{TM}3 labeled GAPDH siRNA (Applied Biosystems/Ambion, USA). Vesicles were prepared as described before, but exclusively in Dulbecco's Phosphate Buffered Saline. 10 µL of 5 nM siRNA solution was added to 40 µL of 0.1 mg mL^{-1} vesicle solution and slightly shaken for 5 min. For the experiment where siRNA was added before vesicle formation, 20 µL of 5 nM siRNA solution was added to 80 µL Dulbecco's Phosphate Buffered Saline before adding to a cPDMS film of 10 µg. The film was hydrated for 1 hour.

6.2. References

[1] M. Kumar, M. Grzelakowski, J. Zilles, M. Clark and W. Meier, *Proc. Natl. Acad. Sci. U. S. A.* **2007**, *104*, 20719-20724.
[2] P. Rigler and W. Meier, *J. Am. Chem. Soc.* **2006**, *128*, 367-373.
[3] J. A. Opsteen, R. P. Brinkhuis, R. L. M. Teeuwen, D. W. P. M. Loewik and J. C. M. van Hest, *Chem. Commun. (Cambridge, U. K.)* **2007**, 3136-3138.
[4] M. Grzelakowski, O. Onaca, P. Rigler, M. Kumar and W. Meier, *Small* **2009**, *5*, 2545-2548.

7. Curriculum Vitae, List of Contributions

PERSONAL INFORMATION

Stefan Egli

from Wald (ZH)

born on December 21st, 1981

ACADEMIC EDUCATION

10/2007-03/2011 ***Doctorate***

Ph. D. student at the Department of Chemistry, University of Basel, supervised by Prof. Wolfgang P. Meier

10/2006-07/2007 ***Master of Science in Chemistry***

University of Basel, Department of Chemistry

04/2005-08/2006 ***Master of Engineering***

University of Applied Science, Konstanz, Germany
Master thesis under the supervision of Prof. Dr. Thomas Graule and Dr. Markus Wegmann at the Laboratory for High Performance Ceramics, EMPA Dübendorf

10/2001-12/2004 ***Chemiker FH***

University of Applied Science, Winterthur, Switzerland

ORAL PRESENTATIONS

Functional Polymersomes for Biomedical Applications
Makromolekulares Kolloquium
February 25, **2011**; Universität Freiburg, Germany

Functionalized Polymer Vesicles for Drug Delivery Purposes
8th Snow Symposium, Organized by the the SCS Swiss Young Chemists' Association
February 19, **2010**, Parpan, Switzerland

Click-Conjugation of Specific Biologicall Ligands to Polymeric Nanocarriers
Europolymer Conference on "Click"-Methods in Polymer and Materials Science
June 2, **2009**; Gargnano, Italy

LIST OF PUBLICATIONS

Monolayer interactions between lipids and amphiphilic block copolymers
Kita-Tokarczyk, K., Itel, F., Grzelakowski, M., Egli, S., Rossbach, P. & Meier, W.
Langmuir **2009**, 25(17), 9847

Towards targeted drug delivery by covalent ligand-modified polymeric nanocontainers
Egli, S., Fischer, B., Hartmann, S., Hunziker, P., Meier, W. & Rigler, P.
Macromolecular Symposia **2010**, 296(1), 278

Functionalization of block copolymer vesicle surfaces
Egli, S., Schlaad, H., Bruns, N. & Meier, W.
Polymers **2011**, 3(1), 252

Biocompatible functionalization of polymersome surfaces: A new approach to surface immobilization and cell targeting using polymersomes
Egli, S., Nussbaumer, M.G., Balasubramanian, V., Chami, M., Bruns, N., Palivan, C. & Meier, W.
J. Am. Chem. Soc. **2011**, 133, 4476

Functional polymersomes for biomedical applications
Egli, S.; Balasubramanian, V.; Palivan, C.; Meier, W.
Macromolecular Rapid Communication **2011**, 32(2), F95

Polymeric nanoreactors as artificial organelles
Tanner, P.; Egli, S.; Balasubramanian, V.; Onaca, O.; Palivan, C.G.; Meier, W.,
FEBS letters **2011**, 585(11), 1699

LIST OF POSTER PRESENTATIONS

Functional Polymersomes for Biomedical Applications
Egli, S., Nussbaumer, M., Balasubramanian, V., Bruns, N., Palivan, C., Meier, W.
Makromolekulares Kolloquium, February 25, **2011**
Universität Freiburg, Deutschland

Covalent and Efficient Attachment of Ligands to Polymer Vesicles
Egli, S., Nussbaumer, M., Balasubramanian, V., Bruns, N., Meier, W.
Fall Meeting of the Swiss Chemical Society, September 16, **2010**
Swiss Federal Institute of Technology Zurich, Switzerland

Conjugation of Antibodies to Polymer Vesicles for Targeted Drug Delivery Purposes
Nussbaumer, M., Egli, S., Meier, W.
International Nanoscience Conference, August 22, **2010**; The Netherlands

Versatile Surface Functionalization of Polymer Vesicles

Egli, S., Nussbaumer, M., Meier, W.

MACRO2010, 43rd IUPAC Wolrd Polymer Congress, July 15, **2010**

SECC, Glasgow, United Kingdom

Nanoreactors for Biosensing

Onaca, O., Egli, S., Nussbaumer, M., Meier, W.

NCCR Nanoscale Science - 9th Site Visit of the Review Panel, April 27, **2010**

University of Basel, Switzerland

Targeted Delivery by Ligand Modified Polymersomes

Egli, S., Meier, W.

Spring Meeting of the Polymers and Colloids Division, Swiss Chemical Society; June 12, **2009**

Swiss Federal Institute of Technology Zurich, Switzerland

Polymeric Drug Delivery Devices

Egli, S., Rigler, P., Hunziker, P., Meier, W.

Polymers in Life Sciences, Swiss Chemical Society; September 4 - 5, **2008**

University of Basel, Switzerland

8. Appendix

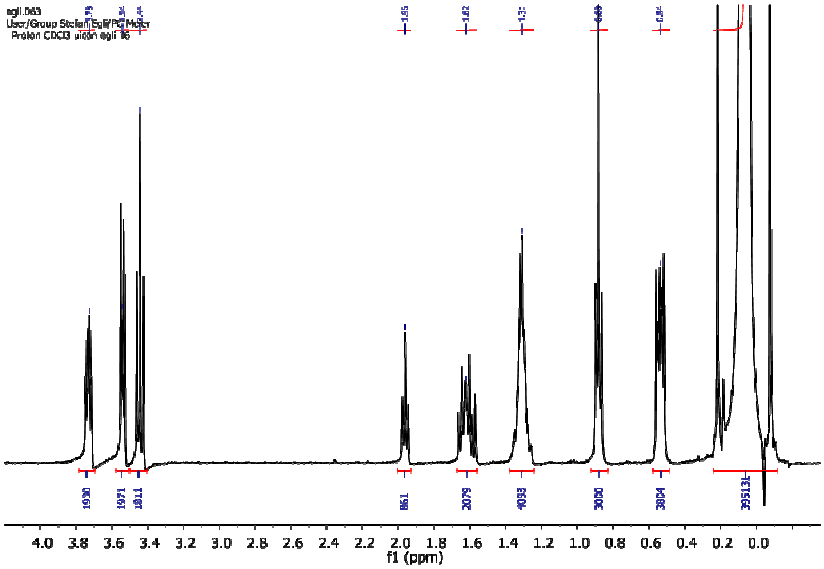

Figure 32 ^{1}H NMR spectrum of PDMS as received from ABCR GmbH

PDMS: ^{1}H NMR (600.1 MHz, CDCl3) δ/ppm = 3.80 – 3.70 (m, 2H), 3.60 – 3.50 (m, 2H), 3.5 – 3.4 (m, 2H), 1.96 (t, 1H), 1.70 – 1.55 (bm, 2H), 1.40 – 1.25 (m, 4H), 0.88 (t, 3H), 0.58 – 0.50 (m, 4H), 0.25 – -0.1 (bs, 3H)

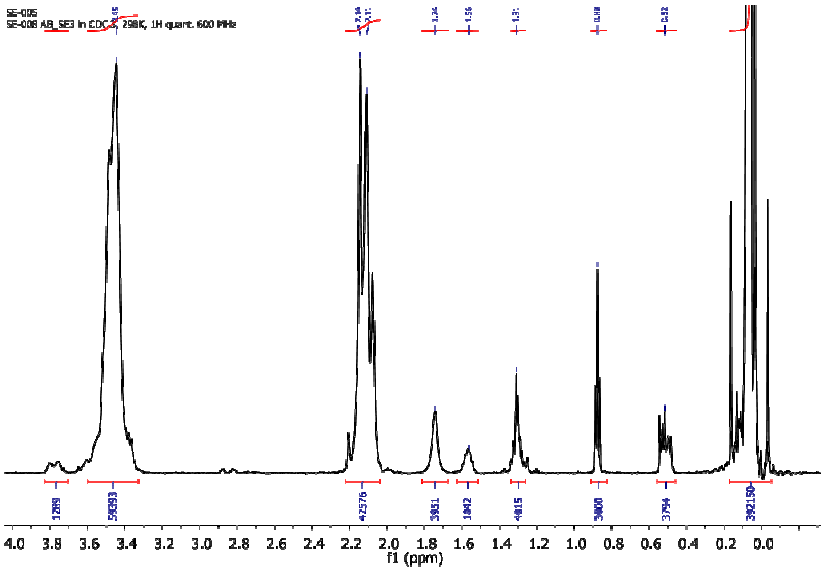

Figure 33 ^{1}H NMR spectrum of the PDMS-*b*-PMOXA AB-OH

AB-OH: ^{1}H NMR (600.1 MHz, $CDCl_3$) δ/ppm = 3.80 – 3.70 (m, 2H), 3.60 – 3.30 (bm, 8H), 2.25 – 2.05 (bm, 3H), 1.80 – 1.70 (m, 4H), 1.65 – 1.55 (bm, 2H), 1.40 – 1.25 (m, 4H), 0.88 (t, 3H), 0.58 – 0.50 (m, 4H), 0.25 – -0.1 (bs, 3H)

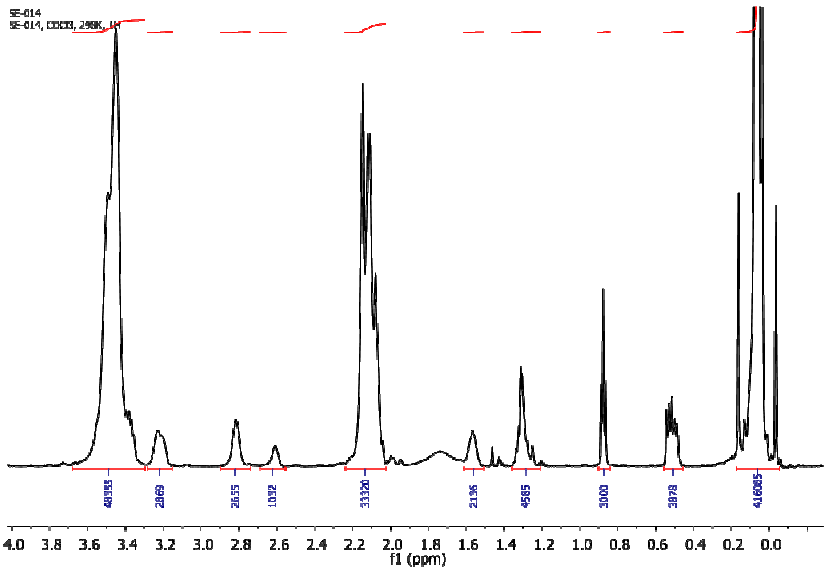

Figure 34 ^{1}H NMR spectrum of the PDMS-*b*-PMOXA AB-NH

AB-NH: ^{1}H NMR (600.1 MHz, $CDCl_3$) δ/ppm = 3.70 – 3.30 (bm, 10H), 3.30 – 3.15 (m, 2H), 2.85 – 2.75 (m, 2H), 2.65 – 2.55 (m, 2H), 2.25 – 2.05 (bm, 3H), 1.80 – 1.70 (bs, 1H), 1.60 – 1.50 (bm, 2H), 1.50 – 1.20 (m, 4H), 0.88 (t, 3H), 0.58 – 0.50 (m, 4H), 0.25 – -0.1 (bs, 3H)

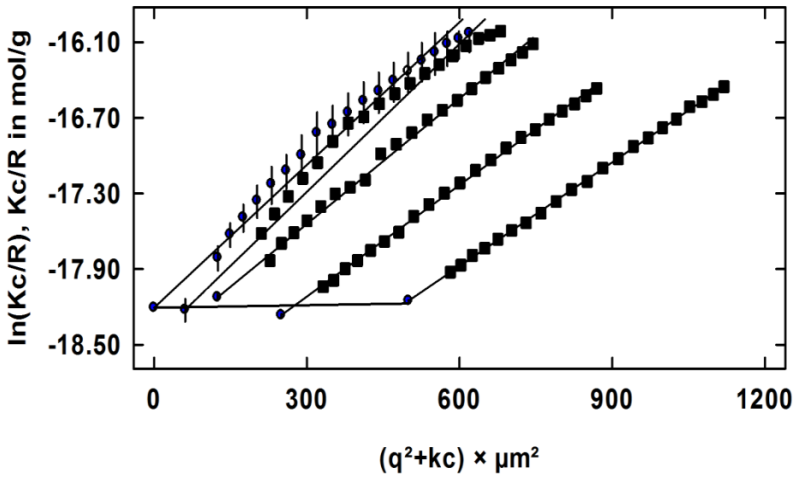

Figure 35. Gunier plot of polymersomes consisting of ABA-1 in water

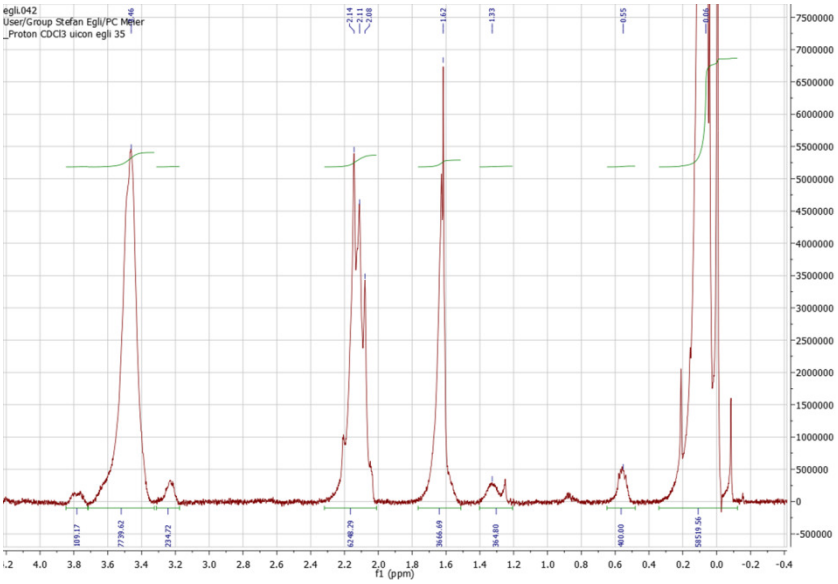

Figure 36. ^{1}H NMR spectrum of the PMOXA-*b*-PDMS-*b*-PMOXA ABA-1

ABA-1: ^{1}H NMR (400 MHz, $CDCl_3$) δ/ppm = 3.80 – 3.20 (bm, 12H), 2.25 – 2.05 (bm, 6H), 1.40 – 1.20 (bm, 4H), 0.58 – 0.50 (m, 4H), 0.30 – 0.0 (bs, 3H)

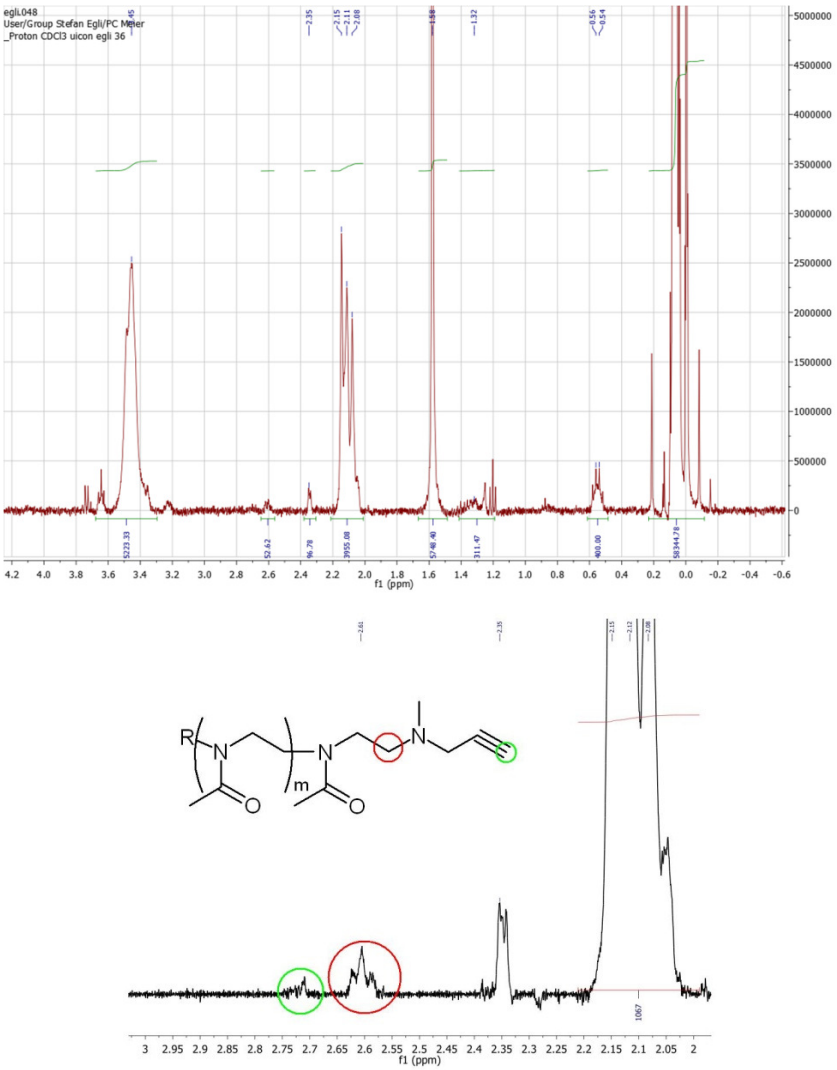

Figure 37. ^{1}H NMR spectrum of the PMOXA-*b*-PDMS-*b*-PMOXA ABA-2 (top); The proton shifts of the N-methylpropargylamine conjugated to the PMOXA is shown in the range between 2.5 and 3.0 ppm (bottom).

ABA-2: ^{1}H NMR (400 MHz, $CDCl_3$) δ/ppm = 3.70 – 3.20 (bm, 12H), 2.73 (d, 2H), 2.60 (m, 4H), 2.35 (m, 4H), 2.25 – 2.05 (bm, 6H), 1.40 – 1.20 (bm, 4H), 0.58 – 0.50 (m, 4H), 0.25 – 0.1 (bs, 3H)